

25 huge local eruption occurred. This episode drove the evolution of Lake Azul through six
26 distinct phases, commencing with a restart of ecological succession after tephra deposition
27 disrupted biogeochemical cycling. The alteration was so profound that the lake underwent
28 a state of oligotrophic conditions for approx. 650 yr. Nutrients were sourced by fish-induced
29 internal recycling and the overflow of the near Lake Verde during this period, rather than by
30 allochthonous nutrient inputs modulated by climate variability and/or vegetation cover
31 changes in the watershed after the official Portuguese colonization. It was only after recent
32 artificial fertilization when the system overcame the volcanic-induced long-term resilience.
33 This over-fertilization and a reduction in water turnover exacerbated the recent symptoms
34 of eutrophication after 1990 AD. Contrary to other studies, Lake Azul constitutes an
35 uncommon case of long-term resilience to trophic change induced by a cataclysmic volcanic
36 eruption. It brings new insights into the fate of lake ecosystems which might be affected by
37 similar events in the future.

38

39 **Keywords**

40 Eutrophication; oligotrophication; lake ontogeny; invasive species; volcanic eruptions;
41 regime shifts

42

43

44 **1. Introduction**

45 Oceanic islands have been particularly sensitive to the effects of anthropogenic impacts,
46 despite being subjected to relatively recent human colonization extending back to only the
47 last centuries. Human impacts usually have striking effects on their ecosystems because of
48 their isolated location and usually very small sizes. Forest clearance (Cañellas-Boltá et al.,
49 2013), exotic species introduction (Sax and Gaines, 2008) or local species extinctions
50 (Wood et al., 2017) are among the most prominent impacts exerted by human colonization
51 on oceanic islands. But whereas the effects of human colonization on terrestrial landscapes
52 are well known, the impacts exerted on aquatic ecosystems still remain to be more fully
53 understood.

54 The Azores archipelago (Macaronesian biogeographical region) lies in the middle of the
55 North Atlantic Ocean and it was officially colonized by the Portuguese in 1432 AD. Since
56 precolonization times to present, notable landscape changes occurred related to, first, pure
57 extractive activities, and, later, transformation by agricultural and livestock management
58 (Dias, 1996). Palynological paleoenvironmental reconstructions have shown that
59 anthropogenic impact in the Azores largely surpassed natural processes, such as volcanism
60 or climate change, as main drivers of landscape changes (Connor et al., 2012; Rull et al.,
61 2017). Less is known however on the human-driven impacts on the rich mosaic of lake
62 ecosystems of the archipelago. This knowledge is of particular importance since studies
63 have shown that insularity makes lakes from the Macaronesian region to be markedly
64 different to their continental counterparts from an ecological perspective (Hughes and
65 Malmqvist, 2005).

66 In the short-term, water quality deterioration due to cultural eutrophication has been
67 reported in the Azores lakes since the 1980's related to agricultural and farming activities
68 (Gonçalves, 2008; Cruz et al., 2015). Yet, the lack of detailed and regular limnological data

69 before water quality monitoring surveys started in 1992-1993 (Cruz et al., 2015) hinder any
70 evaluation of the response of the Azorean lakes to the long-term cultural eutrophication and
71 its potential causes, not exclusively related to recent artificial fertilization. It is known that
72 changes in the food webs are another mechanism which can profoundly alter the trophic
73 trajectory of any lake ecosystem (Smith, 2003). It is particularly relevant how the abundance
74 and structure of fish communities modify the interactions between zooplankton and
75 phytoplankton. Fishes can promote algal biomass both by predation on zooplankton (top-
76 down control) and by nutrient recycling when their activity at the lake bottom stir up the
77 sediments (bottom-up control) (Scheffer and Van Nes, 2007). This seems to have been the
78 case of the formerly fishless Azorean lakes Furnas and Fogo (São Miguel island), which
79 were not only very sensitive to artificial nutrient loading, but also to trophic web controls after
80 the introduction of detritivorous fishes which promoted eutrophication (Skov et al. 2010;
81 Buchaca et al., 2011). As it has been addressed elsewhere, cultural eutrophication is
82 therefore the result of cumulative actions, distant in time and space, which make it difficult
83 to disentangle past and present causes from the legacy of past anthropogenic activities
84 (Thornton et al., 2013; Le Moal et al., 2019).

85 Besides human direct actions on freshwater ecosystems, it is also necessary to assess
86 the relative importance of natural processes which can also induce increases in productivity,
87 as climate-related or volcanic factors. Volcanism in particular could be a potential significant
88 source of nutrient enrichment in the highly active volcanic Azorean context. Ash deposition
89 after volcanic eruptions can prompt significant phytoplankton growth by nutrient enrichment
90 and attenuation of excessive light intensities (Modenutti et al., 2013), but it can also have
91 the opposite effect interfering with nutrient balances which in turn can strongly reduce
92 productivity (e. g., Barker et al., 2000). Although the amount of volcanic-derived nutrients is
93 at present negligible in terms of changes in trophic state of the Azorean lakes (Cruz et al.,
94 2006), this might not have been the case in the past, when volcanic activity was much more

95 common (Queiroz et al., 2008). Yet, the very short time spans covered by studies in lakes
96 Fogo (approx. 150 yr; Skov et al., 2010) and Furnas (approx. 50 yr; Buchaca et al., 2011)
97 does not allow the determination of the precise role played by tephra deposition in the trophic
98 status of lakes in the archipelago.

99 Finally, any eutrophication effect on a collection of different lake systems, natural- or
100 human-induced, must take into account that each lake has own characteristics which makes
101 it unique regarding resistance, resilience and trajectory (Thornton et al., 2013; Le Moal et
102 al., 2019). For instance, for assessing the effects of exotic fish introductions it is necessary
103 to consider a large array of trophic conditions, since understanding the coupling between
104 zooplankton and phytoplankton is dependent on nutrient levels (Esler and Goldman, 1991).
105 Such array of trophic conditions can be found in lakes of the Azores with studied
106 paleorecords. The mentioned lakes Furnas and Fogo constitute examples of systems with
107 distinct trophic status, eutrophic-hypereutrophic and mesotrophic respectively (Skov et al.,
108 2010; Buchaca et al., 2011). Yet, the paleoenvironmental reconstructions from these lakes
109 do not show periods of extended oligotrophy. By contrast, historical accounts (Barrois, 1896;
110 Bohlin, 1901) and fossil chironomid data (Raposeiro et al., 2017) point to past persistent
111 oligotrophy in Lake Azul (São Miguel island), the largest lake of the Azorean archipelago.
112 This lake constitutes an excellent candidate to understand changes in trophic status due to
113 anthropogenic and natural forcings acting in an insular lotic system from a former
114 oligotrophic condition, particularly as the chironomids (Raposeiro et al., 2017) and pollen
115 (Rull et al., 2017) have been analyzed from the same Lake Azul core.

116 In this study we reconstruct the environmental history of Lake Azul since early human
117 colonization, focussing on its response to both natural (volcanism and climate-related drivers)
118 and anthropogenically-induced perturbations (i. e., changes in land use, exotic species
119 introduction, and over-fertilization). We aim to understand the resilience of Lake Azul to
120 different long-term causes of eutrophication, contrasting it with analogous lake systems in

121 the Azorean archipelago and elsewhere which had a different trophic status in the past or
122 present. Such a study on the long-term combined effects of different types of nutrient loading,
123 biological invasions and natural forcings, a key issue in contemporary ecology (Ellis, 2011),
124 has barely been addressed in insular lake systems and/or those affected by catastrophic
125 volcanism. Understanding the long-term changes in the trophic condition of Lake Azul
126 provide a much better insight into the process of recent eutrophication affecting this lake.

127

128 **2. Geological, climate and limnological settings of Lake Azul**

129 Lake Azul is located in Sete Cidades caldera (37°51'N – 25°46'W), which occupies the
130 westernmost part of São Miguel Island (eastern sector of Azores archipelago) (Fig. 1). Three
131 major eruptive phases, at approximately 36, 29 and 16 kyr BP, conditioned the caldera
132 formation (Queiroz et al., 2008). The subsequent explosive Holocene eruptions formed
133 secondary volcanoes inside the caldera, generating ash and lapilli volcanoclastic deposits
134 (Queiroz et al., 2008). At present, the bottom of some of these secondary volcano craters
135 are occupied by perched lakes. Tephra deposits from Holocene eruptions of secondary
136 volcanoes accumulated both inside and in source areas of the lakes. The most significant
137 and recent eruptive episode which accumulated tephra in lakes of Sete Cidades was the
138 P17 eruption, which occurred in the Caldeira Seca volcano in the last millennium (Queiroz
139 et al., 2008, Shotton and Williams, 1971; Fig. 1) and which consisted in three different
140 phases of lapilli deposition (phases L1, L2 and L3 according to Cole et al., 2008).

141 Lake Azul is located approximately 260 m above sea level (Pereira et al., 2014) and has an
142 irregular bottom topography, resulting from faults affecting the substrate (Queiroz, 1997). It
143 can be divided into three main physiographic zones, from south to north, in an increasing
144 depth gradient (Figs. 1D and 2): (1) a shallow platform or ramp (0 to ~12 m depth), (2) a rise
145 (~12 to ~24 m depth) related to an extensional fault slope, and (3) a deep offshore plain

146 (~24 to 27 m depth). The deep plain receives water and sediments from ephemeral streams
147 located at the north of the inner caldera wall and from a main river forming a delta system
148 at the east, close to the locality of Cerrado das Freiras (Fig. 1). Lake Azul is a part of a more
149 complex lacustrine system inside the Sete Cidades caldera which includes a second large
150 waterbody located at its southern side, Lake Verde, to which it is connected hydrologically
151 by an inundated isthmus. Yet, historical accounts show that the two lakes were separated
152 water bodies in the past, as deduced by descriptions of the 16th century (Frutuoso, 1977) or
153 by the cartographic representation which still shows the two lakes in isolation in 1844 AD
154 (Vidal, 1850). Hydrologic connection occurred in 1877 AD, according to local accounts
155 (Andrade, 2003) and a preserved pictorial engraving (Reclus, 1830-1905). Both lakes
156 together constitute at present the largest lacustrine system in the island. A temperate
157 oceanic climate is characteristic of the archipelago, with mild temperatures, a rainfall regime
158 with a strong seasonal cycle and large interannual variability, high relative air humidity, and
159 frequent strong winds (Hernández et al., 2016). Those conditions are driven by oceanic
160 (strength and position of the Azores Current) and atmospheric (semi-permanent high-
161 pressure Azores Anticyclone) factors (Volkov and Fu, 2010). Thus, when the anticyclone
162 migrates northerly or is weaker, generally during the autumn-winter period, the archipelago
163 may be crossed by the North Atlantic storm tracks resulting in heavy rainfalls over it.
164 Conversely, in the spring-summer period, the strengthened anticyclone blocks the
165 storminess path (Santos et al., 2004). New insights, focused on the large-scale climate
166 variability modes of the North Atlantic, revealed that the North Atlantic Oscillation (NAO) and
167 the Atlantic Multidecadal Oscillation (AMO) exert a strong influence on the Azorean climate
168 variability. Thus, seasonal and interannual variability is mainly due to the NAO influence
169 (Andrade et al., 2008; Cropper and Hanna, 2014; Hernández et al., 2016), but at decadal
170 and longer time scales, the AMO also becomes relevant (Yamamoto and Palter, 2016;
171 Hernández et al., 2017).

172 The main physiographic and limnological variables of Lake Azul and Lake Verde are
173 summarized in Table 1. A generalized process of eutrophication has been observed in Lake
174 Azul since 1987 (Cruz et al., 2015). Primary productivity at present is governed by
175 cyanobacteria and, secondarily, by diatoms and cryptophytes. Diatoms reach maximum
176 abundances during autumn-winter and spring, with *Asterionella formosa* Hassal,
177 *Aulacoseira ambigua* (Grunow) Simonsen, *A. granulata* (Ehrenberg) Simonsen, *Fragilaria*
178 *crotonensis* Kitton, *F. cf. tenera*, *Ulnaria ulna* (Nitzsch) Compère and *U. delicatissima* var.
179 *angustissima* (Grunow) Aboal and P. C. Silva as the main dominant taxa (Gonçalves, 2008;
180 Pereira et al., 2014). At present, hydrophyte communities are mainly composed of invasive
181 species such as *Egeria densa* Planch., *Elodea canadensis* Michaux. and *Nymphaea alba*
182 Linnaeus (Gonçalves et al., 2013). The originally fishless condition of the Azorean lakes was
183 modified in the late 18th century, when different taxa of cyprinids and salmonids were
184 introduced and stocked (Valois-Silva, 1886; Vicente, 1956; Flor de Lima, 1993; Raposeiro
185 et al., 2017).

186

187 **3. Materials and methods**

188 In September 2011, fifteen sediment cores (AZ11) were recovered in Lake Azul (Fig. 1)
189 using a UWITEC[®] corer (Ø 60 mm) installed in a UWITEC[®] platform raft following two
190 transects: SW-NE direction (transect A) and W-E direction (transect B). Cores were split
191 longitudinally into two halves and imaged using a high-resolution digital photographic
192 camera installed in the Avaatec XRF core scanner (University of Barcelona). A detailed
193 description of colors, textures and sedimentary structures was performed. Smear slides
194 were also prepared for cores AZ11-02 (37°52'20.6" N – 25°46'26.1" W), AZ11-03
195 (37°52'21.5" N – 25°46'26.4" W) and AZ11-10 (37°52'33,3" N – 25°46'57,0" W) at 5 cm
196 intervals and examined to define facies and lithostratigraphic units. The cores were

197 correlated using the defined sedimentary facies and key beds.

198 The core AZ11-02 (133 cm long) from transect B, sampled at the deep offshore plain
199 (25.1 m of water depth), was selected as representative of the hemipelagic sedimentation
200 environment and used for the study of diatom assemblages. To ensure that the upper
201 sediments were recovered, we checked diatom analysis on a short gravity core taken in
202 2006 in a location very close to the deep offshore plain of Lake Azul (AZ06 (37°52'16.05" N-
203 25°46'30.68" W), 62 cm long, Fig. 1; Gonçalves, 2008). Because clear comparable changes
204 in diatom relative abundance data occur in both cores, tie-in levels could be defined,
205 especially using the trends in the relative abundances of *Aulacoseira* spp. and
206 *Psammothidium abundans* f. *rosenstockii* (Lange-Bertalot) Bukhtiyarova (see the diatom
207 diagram in the Results section). The resulting stratigraphic correlation allowed the
208 construction of a composite record referred in the text hereafter as the composite column.
209 This correlation showed a lack of correspondence between the diatom assemblages found
210 at the top of cores AZ06 and AZ011-02, allowing us to estimate that the first ~30 cm of AZ11-
211 02 were not recovered in the field.

212 Total carbon (TC), total nitrogen (TN), and isotopic composition of bulk organic matter
213 ($\delta^{13}\text{C}_{\text{org}}$ and $\delta^{15}\text{N}_{\text{org}}$) determinations were performed in core AZ11-02 using a Finnigan delta
214 Plus EA-CF-IRMS spectrometer at Center Científics i Tecnològics of the Universitat de
215 Barcelona (CCiTUB). Previous analyses by X-ray diffraction showed negligible amounts of
216 carbonates in the samples; consequently, TC was considered to be equal to total organic
217 carbon (TOC) (Raposeiro et al., 2017). TOC and TN results are expressed as percent values
218 of the sediment dry weight. The atomic ratio of TOC/TN was calculated and corrected
219 according to Talbot (2001) to discriminate inorganically bound nitrogen content from TN.
220 From here on, the TOC/TN ratio is therefore referred to as $\text{TOC}/\text{TN}_{\text{corr}}$. Fluxes of TOC into
221 the sediments have also been estimated in the form of mass accumulation rate (MAR, mg
222 $\text{cm}^{-2}\text{yr}^{-1}$) by multiplying their concentrations by the sediment dry densities and sedimentation

223 rates at each depth. For the calculation of dry bulk densities, the samples were dried to
224 remove free water. The isotopic composition of sediment organic matter was determined,
225 and isotopic values are reported in the conventional delta-notation in per mil (‰) relative to
226 the Pee Dee Belemnite (PDB) carbon and atmospheric nitrogen (N₂) standards.

227 Diatom analysis was performed following standardized procedures (Renberg, 1990). Slides
228 were mounted with Naphrax[®] mountant, and at least 400 valves per sample were counted
229 at X1000 using a Nikon Eclipse 600 microscope with Nomarski differential interference
230 contrast optics. Identifications of taxa were based on standard sources (e.g., Krammer and
231 Lange-Bertalot, 1986-1991; Lange-Bertalot, 2000-2013), and contrasted with previous
232 studies made on the Azores archipelago (Gonçalves et al., 2010). Taxa were grouped,
233 according to their habitat preferences, as allochthonous (aerophilic) or autochthonous
234 (euplanktonic, facultatively planktonic or tycho planktonic, and benthic). Raw valve counts
235 were converted to percentage abundance data. Statistical analyses were carried out on a
236 diatom relative abundance matrix of those taxa attaining an abundance of more than > 5%
237 in at least one sample. Samples which had sum abundances of allochthonous taxa reaching
238 at least 5% were excluded from the analyses (n = 37). Diatom abundances from the
239 remaining 77 samples were transformed by square-root transformation prior statistical
240 analysis. The definition of the main Diatom Assemblage Zones (DAZs) was performed using
241 stratigraphically constrained cluster analysis based on squared Euclidean dissimilarity
242 (CONISS, Grimm, 1987), as implemented in Psimpoll 4.10 (Bennett, 2002). Zonations with
243 variances that exceeded the values generated by a broken-stick model of the distribution of
244 variance were considered to be statistically significant (Bennett, 1996; Supplementary
245 Material). A detrended correspondence analysis (DCA) was performed to measure the
246 length of the main environmental gradient, which recommended the use of a linear model of
247 ordination (principal component analysis; PCA) to determine the environmental drivers in
248 the composition of the diatom assemblages. Both DCA and PCA were performed with the

249 CANOCO 4.5 software (ter Braak and Smilauer, 1998).

250 A new age-depth model was constructed for the composite column (cores AZ-06 + AZ11-
251 02), updating the previously available model which was restricted to core AZ11-02
252 (Raposeiro et al., 2017; Rull et al., 2017), and taking into account the non-recovery of the
253 upper sediments of this core. This new model is based on linear interpolation of the available
254 ^{210}Pb profile for the AZ06 core (Gonçalves, 2008), the radiocarbon data from the AZ11 cores
255 (Table 2), and several independent tie-in points. All ^{14}C ages were calibrated to calendar
256 years (cal AD) using the CALIB 7.1 software (Stuiver and Reimer, 1993), and the latest
257 INTCAL13 curve (Reimer et al., 2013).

258

259 **4. Results**

260 ***4.1. Lithological units and sedimentary facies***

261 Facies analysis from cores retrieved in 2011 resulted in the definition of eleven facies and
262 eight sedimentary units for the entire basin (Fig. 2; definition also followed by Raposeiro et
263 al., 2011 and Rull et al., 2011). These facies have been differentiated by lithology, texture,
264 color, lamination characteristics, and shards content. Offshore sedimentary facies of the
265 composite column have been grouped in 4 lithological units as follows:

266 Unit 1 (base–132 cm) is composed of gray tephra deposits (ash and lapilli) (Facies VS)
267 from the P17 eruptive episode (Queiroz et al., 2008). These volcanoclastic deposits are
268 usually interbedded by some thin layers of gray lacustrine muds in the deep plain. Cores
269 taken during the 2011 survey indicate that this unit extends to the entire lake bottom area.

270 Unit 2 (132–114 cm) is deposited above Unit 1 in the deep plain and rise zones of the
271 lake. This unit is made up of banded-to-laminated gray muds (Facies E). These deposits

272 were transported to the lake by runoff eroding volcanic ashes deposited in the catchment
273 from the same eruptive episode that deposited Unit 1.

274 Unit 3 (114–90 cm) is recorded above Unit 2 and is mainly composed of
275 greenish/yellowish brown laminated to banded muds (Facies C) deposited by decantation
276 of fine-grained particles forming plumes of the surface and/or subaquatic nepheloid layers
277 in the lake during short-term regular rains. These deposits intercalate some brown mud
278 horizons enriched in shard particles (Facies B) that could be added to the suspended
279 material by ash fallout from minor or distal eruptive episodes. Moreover, this unit intercalates
280 dark brown mud layers rich in terrestrial plant remains, but poor in diatoms (Facies D). The
281 composition and short lateral extent of layers of facies D indicate that they correspond to
282 subaquatic lobes deposited by flood events, likely during heavy rain episodes.

283 Unit 4 (90 cm–top) is deposited above Unit 3 and it is mainly composed of brown massive
284 to poor laminated mud (Facies A) transported and deposited in a process similar to facies
285 C. These muds also intercalate dark brown mud layers rich in terrestrial plant remains
286 corresponding to lobular deposits (Facies D).

287

288 **4.2. Chronology**

289 Available ^{210}Pb data from core AZ06 (Gonçalves, 2008) and non post-bomb radiocarbon
290 ages of the AZ11 cores (table 2, Fig. 3, Supplementary Materials) were used to construct
291 the age-depth model of the composite column which best fitted with events of independently
292 known age. The radiocarbon age at the bottom of the sequence was obtained immediately
293 above the basal tephra, yielding 690 ± 30 yr BP, almost exactly fitting with the age previously
294 estimated for the P17 eruptive episode of 663 ± 105 14C yr BP (Shotton and Williams,
295 1971). By contrast, the basal flood layer of Unit 4 yielded a ca. 100 yr difference when dated

296 in cores AZ11-02 (c. 1770 AD) and AZ11-03 (c. 1870 AD) (Fig. 3, Supplementary Materials).
297 Comparison of the estimated and known dates for the first appearances in the pollen record
298 of AZ11-02 (Rull et al., 2017) of the exotic *Cryptomeria japonica* and *Pinus* spp., resulted in
299 a much closer fit of the flood event dated to 1870 AD in core AZ11-03 rather than 1770 AD
300 dated in core AZ11-02 (Fig. 3), so the former was preferred for the final age model.
301 Chronology for the upper sediments is based on the ^{210}Pb data from core AZ06 because of
302 the more reliable use of ^{137}Cs tie-in points (Gonçalves, 2008), instead of using a single post-
303 bomb radiocarbon age of core AZ11-02 (table 2).

304 In conclusion, the new age model therefore differs from the previously published
305 (Raposeiro et al., 2017; Rull et al., 2017) in a) the use of new ^{210}Pb dates of core AZ06 which
306 provide a chronology for the non-recovered history in core AZ11-02, and b) a reassessment
307 of the age of the basal flood event of Unit 4. Comparison of chironomid (Raposeiro et al.,
308 2017), pollen (Rull et al., 2017), and diatom (this work) zones using the old and definite age
309 models is shown in the Supplementary Materials.

310

311 **4.3. Diatom assemblages**

312 Diatom taxa with abundances higher than 5% in at least one sampling level were plotted
313 in stratigraphic order for the composite column (Fig. 4). Except for the lacustrine muds
314 corresponding to the facies VS at the base of the core (Unit 1), benthic diatoms dominated
315 the assemblages from approx. 140 to 40 cm. ~~At this time~~Above 40 cm, planktonic diatoms
316 (mainly *Aulacoseira* spp. and also, ~~more recently~~higher up, *Asterionella*~~A.~~ *formosa* and *F.*
317 *crotonensis*) began their dominance. Those levels close to or coincident with flood events
318 (facies D) had a remarkably lower total valve content due to the massive short-term
319 deposition of terrestrial sediments. Furthermore, these levels were characterized by high
320 relative abundances of aerophilic diatoms, mainly from the genera *Diademsis* and *Diploneis*

321 (Fig. 4), indicating that any lacustrine signal given by the autochthonous taxa would be
322 masked by the effects of both the sedimentary dilution and by the incorporation of
323 allochthonous valves during the flood events. To avoid interferences in the lacustrine signal,
324 data from all the volcanic levels in Unit 1 (base–132 cm), as well as those with high
325 TOC/TN_{corr} values (see geochemical results below) and/or sum abundances of aerophilic
326 diatoms >5%, were excluded from any further statistical analyses.

327 The resulting broken-stick model of the distribution of variance allowed us to identify four
328 statistically significant DAZs (AZU-1 to AZU-4) based on CONISS (Table 3 and Fig. 4). DAZ
329 AZU-2 was also divided into two subzones.

330 DCA results indicated a linear response of the diatom assemblages to the environmental
331 gradients, since the longest gradient was 2.7 SD units (Leps and Smilauer, 2003), and a
332 PCA was therefore performed to interpret the underlying environmental variables explaining
333 the composition of the diatom assemblages.

334 The first two axes of the PCA explained 66.1% of the total variance (Fig. 5). The first axis
335 (PC1, 42.4% of the variance), places benthic diatoms (mostly epipellic and motile), such as
336 *Navicula notha* J. H. Wallace, *Eolimna* sp1, *Nitzschia* spp. aff. *pseudofonticola*, *N. lacuum*
337 Lange-Bertalot or *N. perminuta* (Grunow) M. Peragallo, on the positive side of the plot. The
338 negative side is occupied by some euplanktonic and eutrophic taxa as *A. ambigua*, *F.*
339 *crotonensis* and *A. Asterionella formosa*. The second axis (PC2, 23.7% of the variance),
340 shows the highest negative values for the euplanktonic. *A. ambigua*, *AsterionellaA. formosa*,
341 and *F. crotonensis*, whereas periphytic diatoms, mainly *Stauroforma exiguiformis* (Lange-
342 Bertalot) R.J. Flower, V.J. Jones & Round, *Encyonopsis* sp. aff. *cesatii*, *Adlafia minuscula*
343 var. *muralis* (Grunow) Lange-Bertalot, *Pseudostaurosira brevistriata* (Grunow) D.M.
344 Williams & Round, *P. abundans* f. *rosenstockii*, and the *Fragilaria capucina* group, exhibit
345 positive scores. The resulting biplot of PC1 vs. PC2 shows three main groups of samples

346 corresponding to the DAZs a) AZU-1, b) AZU-2 and c) AZU-3 + AZU4 (Fig. 5).

347 Variations in the two first principal components through the sedimentary sequence were
348 plotted on the stratigraphic chart (Fig. 6). PC1 shows a progressive decrease from AZU-1
349 to AZU-4, stabilizing at approx. 27 cm until the top of the core. PC2 shows an increasing
350 trend from the immediately post-eruptive phase at approx. 140 cm (~~ca. 1290 AD~~) until 70
351 cm (~~ca. 1870 AD~~), decreasing thereafter.

352

353 **4.4. Geochemical proxy data**

354 Very low percentages of TOC and TN characterize Units 1 to 3, with values ranging
355 between 0.18 to 1.13% and 0.05 to 0.12%, respectively (Fig. 6). Both proxies exhibit a net
356 increase in Unit 4 from 90 cm (~~ca. 1460 AD~~) to 40 cm (~~ca. 1940 AD~~) with values ranging
357 from 0.81 to 3.53% and 0.08 to 0.34% for TOC and TN, respectively. TOC MAR oscillate
358 between 0.21 and 14.86 mg C cm⁻²yr⁻¹ from the base to 29 cm (~~ca. 1960 AD~~), respectively.
359 TOC and TOC MAR exhibit a similar pattern from the base of the core to 64 cm depth (~~ca.~~
360 ~~1880 AD~~).

361 TOC and TN percent values show a high linear correlation ($r = 0.94$, $p < 0.01$), and
362 because of this, the correction suggested by Talbot (2001) was used to discriminate the
363 fraction of TN not attributable to TOC. Thus, the TOC/TN_{corr} atomic ratio allowed us to
364 separate those levels with allochthonous organic matter (Facies D) more efficiently. Facies
365 A, B and C show values of TOC/TN_{corr} between 8 and 13, a range that is typical of organic
366 matter of mixed but mainly lacustrine origin (Meyers and Teranes, 2001). Facies D shows
367 values ranging between 14 and 25, characteristic of the larger influence of C3 land plants,
368 which is consistent with the flood event origin of these sediments.

369 The $\delta^{13}\text{C}_{\text{org}}$ curve shows, in general, an inverse correspondence with the TOC/TN_{corr}

370 curve (Fig. 6). This is more clearly manifested in facies D deposits, where TOC/TN_{corr} values
371 are always higher than 14. Units 1, 2, 3, and the bottom half of Unit 4, when the last flood
372 event was recorded between 69–75 cm (~~ca. 1870 AD~~), show $\delta^{13}\text{C}_{\text{org}}$ values ranging between
373 -27.5 and -22.5‰. A significant rise is observed between 68 and cm (~~ca. 1870 AD~~) and 40
374 cm (~~ca. 1940 AD~~), when values oscillate between -26.4 and -22.4‰. From here to 29 cm
375 (~~ca. 1960 AD~~), the range shortens from -25.9 to -23.2‰. Despite the lack of correspondence
376 between TOC and $\delta^{13}\text{C}_{\text{org}}$ throughout most of the core, trends exhibited from 68 cm (~~ca.~~
377 ~~1870 AD~~) are quite similar, and remarkably decreasing in the uppermost values in both
378 proxies.

379 The $\delta^{15}\text{N}_{\text{org}}$ values range between -0.02‰ and 3.09‰, showing lower values (close to 0)
380 in Facies D terrestrial sediments or levels close to these facies. The lacustrine levels of Units
381 1, 2, 3, and the bottom half of Unit 4 to 68 cm (~~ca. 1870 AD~~) are characterized by oscillating
382 values ranging from 0.21 to 2.84‰. A slight upwards decreasing trend to values close to 0
383 is recorded towards the top of the core AZ11-02.

384

385 5. Discussion

386 5.1. Environmental gradients explaining diatom assemblage composition

387 Results of PCA indicate the two main environmental components driving the long-term
388 changes in diatom composition in Lake Azul. The negative scores exhibited along PC1 by
389 the eutrophic and euplanktonic species *A. ambigua*, *F. crotonensis* or *AsterionellaA-*
390 *formosa* (e. g., Reynolds et al., 2002) versus the high positive values of benthic species
391 such as *N. notha*, *N. lacuum* or *N. perminuta*, of predominantly oligotrophic affinities (e. g.
392 Krammer and Lange-Bertalot, 1986-1991), suggest that this main axis is related with a
393 trophic gradient (Fig. 5). The plot of samples on the space defined by the PC1 vs. PC2 (Fig.

394 5) shows two extremes represented by the oligotrophic conditions and exclusive benthic
395 production of DAZ AZU-1 (1290-1475 AD) vs. the meso- to eutrophy characteristic of the
396 pelagic production of DAZs AZU-3 and AZU-4 (1930-2006 AD).

397 The biplot of PC1 vs. PC2 (Fig. 5) also shows on the positive side of PC2 diatoms
398 performing a large array of life form strategies, ranging from purely euplanktonic (e. g., *A.*
399 *granulata*), tychoplanktonic (e. g., *Pseudostaurosira elliptica* (Schumann) Edlund, Morales
400 and Spaulding, *P. brevistriata*), epiphytic (e. g., *P. abundans* f. *rosenstockii*), to sediment
401 dwelling (e. g. *A. minuscula* var. *muralis*, *E. sp. aff. cesatii*). Most of the positive sample
402 scores correspond to DAZ AZU-2, an assemblage interpreted as related with an increase in
403 the relative extension of shallow littoral vs. deep lacustrine habitats (table 3). By contrast,
404 the negative side of the plot shows diatoms behaving only as euplanktonic (*A. ambigua*, *F.*
405 *crotonensis*, *Asterionella* ~~*A.*~~ *formosa*) or sediment dwelling (*Eolimna* sp1, *N. notha*, *N.*
406 *lacuum* and *N. perminuta*). PC2 is therefore understood as reflecting a gradient in
407 microhabitat availability, whose maximum would be reached in DAZ AZU-2 (1475-1930 AD).

408

409 **5.2. Main ecological phases in Lake Azul**

410 The multidisciplinary study of the recent sedimentary record of Lake Azul reveals the
411 complex overlapping of natural and anthropogenic forcings that drove the evolution of this
412 system in the last ca. 720 yr. According to the obtained multiproxy information the lake went
413 through six different environmental phases, as described below.

414 **5.2.1 Phase I. Basal zone – Eruptive phase (P-17 eruption)**

415 The recent history of Lake Azul begins with a volcanic catastrophic event indicated by the
416 deposition of a thick tephra layer (facies VS), recorded in Unit 1. This event corresponds to
417 the Caldeira Seca P17 volcano eruption, which accumulated tephra deposits ~~up to 10 m~~

418 ~~thick~~ in extensive areas of the Sete Cidades caldera (Cole et al., 2008). Although some
419 exceptional fallout of diatoms transported into the volcanic eruption plume cannot completely
420 be disregarded (Van Eaton et al., 2013), high abundances of the euplanktonic and eutrophic
421 *A. granulata* in muddy lacustrine sediments interbedded between volcanic deposits (facies
422 VS) (Fig. 4) are more easily explained by sedimentation *in situ* around the time of the
423 eruption. They would correspond to the most recent phase of the eruption (phase L3
424 according to Cole et al., 2008), which would have accumulated 4-20 m of lapilli in the lake's
425 bottom surface. -Diatoms of the genus *Aulacoseira* are characteristic of well-mixed waters
426 necessary to maintain their buoyancy and relatively high nutrient conditions (Hall and Smol,
427 2010). The species *A. granulata* is accompanied during this phase by *Nitzschia valdestriata*
428 Aleem and Hustedt, a benthic diatom which has been reported as aerophilic (e.g., Robinson,
429 2004); thus, its presence in Unit 1 can indicate transport from the emerged zones in the
430 margins to the innermost areas of the lake. The diatom assemblage found in this unit (Fig.
431 4) would therefore represent the existence of a moderately deep, well mixed, and meso to
432 eutrophic lake, approx. at the time of ash deposition, with a significant contribution of
433 allochthonous materials. This interpretation is reinforced by moderate TOC/TN_{corr} values of
434 approximately 15, along with low values of $\delta^{13}\text{C}_{\text{org}}$, which are indicative of isotopically light
435 terrestrial organic matter (Meyers and Teranes, 2001). Whereas the dominance of
436 *Aulacoseira* has been found as typical of the mid-depth zone across lake water-depth
437 gradients elsewhere (e. g. Kingsbury et al., 2012), the study of pollen and non-pollen
438 palynomorphs (NPPs) in Lake Azul suggested shallower water conditions (Rull et al., 2017).
439 This circumstance might imply that the lake was subjected to short-term fluctuations in water
440 levels at this time.

441 The main ecological consequence of the major phase of the P17 volcanic eruption was
442 the replacement of a diatom community that included *A. granulata* and *N. valdestriata* by a
443 new one controlled by benthic attached life forms, mainly *Achnantheidium minutissimum*

444 (Kützing) Czarnecki. Tephra deposition can involve a disruption in the internal recycling of
445 P, which is more significant in lakes with small catchment areas relative to the total lake area
446 (Barker et al., 2000; Telford et al., 2004), such as Lake Azul, with a total lake area of 3.59
447 km² vs. a lake drainage area of 15.35 km² (Fig. 1; table 1). This, plus a significant increase
448 in Si loading associated with the deposition of tephras, would have greatly altered the Si:P
449 ratio, prompting the replacement of the previous diatom communities by new opportunistic
450 species (Kilham et al., 1986). The species *A. minutissimum* has been documented as a
451 pioneering *r*-strategist on disturbed aquatic environments (Peterson, 1992; Stevenson, 1996;
452 Leira et al., 2015) with a strong affinity for waters with a high Si content and usually attaching
453 to unspecific substrates (Stenger-Kovács, 2006). Moreover, this taxon is referred as a good
454 indicator of low organic content in the water column (Potapova, 2007). High abundances of
455 *A. minutissimum* would therefore indicate that, after tephra fallout, the lapilli and ash sterile
456 materials which covered the lake bottom were colonized by a new diatom community that
457 restarted ecological succession. This situation was also accompanied by low values of TOC
458 and TN in the sediments, as well as of TOC MAR, which are maintained in the following
459 phase, suggesting an oligotrophication event.

460 5.2.2. Phase II: Moderately shallow oligotrophic lake (ca. 1290–1480 AD)

461 During this phase, which is coincident with DAZ AZU-1 (125-90 cm), coarse-grained
462 tephra sediments of Unit 1 were replaced by fine-grained muddy sediments from Units 2
463 (Facies E) and 3 (Facies B and C). The reduction in grain size induced a change to an
464 epipellic-dominated diatom assemblage characterized by high abundances of *Eolimna* sp1,
465 together with *Navicula* s. l. and *Nitzschia* spp. (AZU-1, Fig. 4). Extensive growth of epipellic
466 diatom communities after tephra deposition, when the sediment grain-size of the lake bottom
467 surface is adequate, has also been reported elsewhere (e. g., Harper et al., 1986; Telford et
468 al., 2004), indicating the progression of the ecological succession. The referred taxa are
469 also typical of both shallow and mid-depth zones of lakes where light can reach the bottom

470 (Wang et al., 2012). These characteristics, and the minor role of euplanktonic and
471 tychoplanktonic taxa during this phase, would be indicative of a moderately shallow water
472 environment (Wolin and Stone, 2010), which according to the pollen and NPPs-based water
473 level reconstruction (Rull et al., 2017) should be below 15 m. Maximum PC1 values are
474 recorded during this phase, suggesting that oligotrophic conditions were maintained over
475 the approximately 200 yr of this phase, according also with the low values of TOC and TOC
476 MAR. Maximum percent abundances of *Nitzschia* spp. are also recorded during this phase,
477 almost disappearing thereafter. This genus is reported to be good at growing at low P supply
478 (Kilham et al., 1986), and many species are facultative or obligate nitrogen heterotrophs
479 (Werner, 1977; Kilham et al., 1986). This observation suggests that although tephra
480 deposition inhibited complete P recycling the lake was probably not N-limited.

481

482 5.2.3. Phase III: Deep oligotrophic lake (ca. 1480-1870 AD)

483 The most significant feature of this phase, corresponding to sedimentation of the lower
484 part of Unit 4 (DAZ AZU-2a, 90-75 cm), is the flooding of the platform ramp associated with
485 a water level increase, which allowed a large relative increase in littoral vs. pelagic
486 environments (Fig. 1). Chronostratigraphical, historical and diatom data support this
487 hypothesis. The stratigraphical chart shows the first appearance of lacustrine sediments in
488 the ramp environment radiocarbon dated in core AZ11-07 to ca. 1545 AD (Fig. 2). This
489 position is located at approximately 500 m from the limit between the ramp and the slope
490 (Fig. 2), pointing to an earlier flooding of the ramp. According to the available chronicles of
491 Gaspar Frutuoso (1522-1591), the lake had, at the time, a maximum depth of 7–8 fathoms
492 (Frutuoso, 1977), that would equal ~15–17 m. The lake bathymetric map shows an extensive
493 area of the ramp that would be subaereally exposed (Fig. 1), and this agrees with the
494 description of a large “beach” made up of “sterile sands” (Frutuoso, 1977). Flooding of the

495 ramp brought a sharp change in the diatom communities. Fragilarioid taxa (mainly *P.*
496 *brevistriata* and *P. elliptica*) became clearly dominant (DAZ AZU-2a, Fig. 4). These taxa are
497 early colonizers characteristic of the shallow-water littoral zone of a wide variety of water
498 bodies under conditions of environmental instability (Reed et al., 1999). Although their
499 appearance in Lake Azul could be related to a deeper water column due to their
500 tychoplanktonic character, increased availability of shallow littoral habitats when the flooding
501 occurred was probably a decisive contributing factor for their expansion (Stone and Fritz,
502 2004; Wigdhal et al., 2014). Their rise is also coincident with the increase of *Myriophyllum*
503 *alterniflorum* (Rull et al., 2017), a submerged macrophyte characterized by a high number
504 of thin leaves that largely increase the colonizable area for periphytic microalgae (Cattaneo
505 and Kalff, 1980). A complex permanent periphytic community was therefore established in
506 the lake littoral zone for the first time. (Fig. 6). Compared to Phase II, when both oligotrophy
507 and a steeper lake bottom resulted in a low diversification of the diatom assemblages, the
508 flooding of the platform ramp in Phase III resulted in an increased area of benthic vs.
509 planktonic habitats. As a result, life-form strategies adopted by diatoms diversified in Phase
510 III, as indicated by the high recorded values of PC2.

511 Both regular flood events from the lake catchment and the effects of deforestation during
512 this period (Rull et al., 2017), probably also brought episodic high nutrient concentrations
513 that allowed the short-term growth of eutrophic euplanktonic diatoms (*A. ambigua* and *A.*
514 *granulata*), which appear for the first time since the reset of the lake after the P17 volcanic
515 episode. Both the increase in the TOC/TN ratio and negative excursions of $\delta^{13}\text{C}_{\text{org}}$,
516 associated with the floods, point to a significant delivery of terrestrial organic matter to the
517 lake (Meyers and Teranes, 2001). The *Nitzschia* spp. sharp decline during this phase
518 suggests that this increased nutrient availability altered the dynamics of the P and N cycles
519 within the lake, decreasing the N:P ratio. Although TOC and TOC MAR values increased
520 compared to the previous phase, they still remained low, suggesting that oligotrophic

521 conditions persisted during this stage, as indicated also by the high values of PC1.

522

523 *5.2.4. Phase IV: Deep oligotrophic lake and transition to a new trophic state (ca. 1870–*
524 *1940 AD)*

525 During the sedimentation of mid-to-upper part of Unit 4 (DAZ AZU-2b, 75-41 cm), TOC
526 and TN follow the steady uprising trend since the ecological reset after the Caldeira Seca
527 P17 eruption, which suggests an increase in productivity. Most of the organic matter
528 produced has an algal origin, according to the TOC/TN_{corr} values (Meyers and Teranes,
529 2001). Moreover, the still low values of TOC and TOC MAR, suggests that the water column,
530 despite the increase in productivity, remained oligotrophic. This would be in accordance with
531 the large light availability at the time (19th century), indicated by the high abundances of the
532 charophytes *Chara fragilis* Desvaux and *Nitella tenuissima* (Desvaux) Kützing (Trelease,
533 1897; Cunha, 1939), the presence of the typical oligotrophic chrysophycean *Dinobryon*
534 *sertularia* Ehrenberg (Barrois, 1896), and the recorded high abundances of desmids (Bohlin,
535 1901).

536 Despite the lake still being oligotrophic, the proxy data suggest that during this phase, a
537 long-lasting ecological change commenced, indicated by heavier $\delta^{13}\text{C}_{\text{org}}$ values and the
538 reduction in TOC/TN_{corr} associated with a lesser flood events occurrence, with the exception
539 of the ca. 1870 AD event recorded at the start of this phase. Additionally, the
540 correspondence found during this phase between the TOC and $\delta^{13}\text{C}_{\text{org}}$ curves, which up to
541 this time were uncoupled, points to a change in carbon fractionation compared to the
542 previous phases. This change co-occurs with the remarkable landscape reconfiguration due
543 to the massive introduction of the exotic arboreal taxa *C. japonica* and *Pinus* spp. in the
544 catchment after 1850 AD (Rull et al., 2017). Restricted delivery of terrestrial organic matter
545 to the lake due to the increase in tree cover in the catchment would induce heavier $\delta^{13}\text{C}_{\text{org}}$

546 values and a reduction in the TOC/TN_{corr} ratio (Meyers and Teranes, 2001).

547 However, not only a more restricted delivery of terrestrial organic matter to the lake could
548 induce heavier $\delta^{13}\text{C}_{\text{org}}$ values but also the increase of in-lake productivity (Meyers and
549 Teranes, 2001), which is also indicated by the net rise in TOC values (Fig. 6) and by the
550 regular presence of the euplanktonic and meso- to eutrophic diatoms of the genus
551 *Aulacoseira* (Fig. 4). The necessary nutrient enrichment that triggered this increase in
552 productivity and the presence of *Aulacoseira* could not be due to the delivery of materials
553 from the catchment, as indicated by the decrease in the TOC/TN_{corr} ratio. Two alternative
554 mechanisms can be invoked to explain nutrient enrichment. First, fish introductions which
555 started in the late 18th century in this formerly fishless lake could intensify internal nutrient
556 release in the lake, especially the stockings of cyprinids, such as Goldfish *Carassius auratus*
557 Linnaeus introduced in 1792 AD (Valois-Silva, 1886), and Carp *Cyprinus carpio carpio*
558 Linnaeus, introduced in 1890 (Vicente, 1956). Their feeding activity is known to have a
559 strong effect on the release of nutrients to the water by sediment resuspension (e.g.,
560 Richardson et al., 1995). This concentration effect was probably enhanced by the
561 development at this time of an oxygen-depleted deep hypolimnion on a ~~stational~~seasonal
562 basis, according to the chironomid data (Raposeiro et al., 2017), which would highly enrich
563 the bottom waters with P (Cohen, 2003). The primary role that internal nutrient recycling
564 induced by fish stockings could have played is in accordance with the known fact that the
565 major driver of eutrophication in this lake is, at present, internal P-loading (Cruz et al., 2015).
566 A second mechanism could be nutrient injection from Lake Verde overflow which probably
567 increased total nutrient concentration in Lake Azul after the connection between the two
568 lakes in 1877 AD (Andrade, 2003).

569 The multiproxy data suggest a long-term gradual process of eutrophication to a new trophic
570 state during this phase, mainly induced by sediment disturbance after fish introductions and
571 nutrient inputs from Lake Verde overflow after its connection in 1877 AD.

572 *5.2.5. Phase V: Deep mesotrophic lake (ca. 1940–1995 AD)*

573 In the upper part of Unit 4 (DAZ AZU-3, 41-11 cm), all proxies reveal a major and sudden
574 change in the ecosystem. From ca. 1940 to 1995 AD, there is a sharp shift in the diatom
575 assemblages, which now become dominated by the euplanktonic and eutrophic *A. ambigua*
576 (AZU-3, Fig. 4). Although tychoplanktonic diatoms subdominate the assemblages, benthic
577 taxa significantly decrease. Lighter values of $\delta^{13}\text{C}_{\text{org}}$, not related with flood events, also
578 support the hypothesis of a larger pelagic production compared to the previous phase, since
579 periphyton is usually enriched in ^{13}C compared to phytoplankton due to a higher CO_2
580 limitation of primary producers in the littoral zone (France, 1995). In addition, organic carbon
581 MARs attain maximum values, indicating increased productivity. The lack of correspondence
582 between the TOC MAR and TOC, which decrease during this phase, reflects the increased
583 relative importance of biogenic silica in the sediments associated with larger biosiliceous
584 productivity. The excess of nutrient loads from intensive fertilization and livestock manure,
585 especially since the 1960s (Gonçalves, 2008; Cruz et al., 2015), constitutes the main factor
586 responsible for the detected environmental change. They not only led to increased
587 eutrophication, but probably also prompted the shift from a benthic to pelagic-dominated
588 environment because of the shading effect of phytoplankton over benthic algae also
589 recorded in other Azorean lakes (Buchaca et al., 2011). This change is accompanied by the
590 significant decline in *Myriophyllum alterniflorum*, which already started in the previous phase
591 (Rull et al., 2017), a macrophyte sensitive to eutrophication and turbidity (Kohler and Labus,
592 1983).

593 *5.2.6. Phase VI: Deep meso-eutrophic stratified lake (ca. 1995–2006 AD)*

594 Although dominant pelagic production still characterizes this phase recognized at the
595 uppermost part of Unit 4 (DAZ AZU-4, 11-0 cm), there is an important reduction in *A.*
596 *ambigua*, which now co-dominates the diatom assemblages with *AsterionellaA. formosa* and

597 *Fragilaria* cf. *tenera*. There is also a peak of the euplanktonic *F. crotonensis* during this
598 phase. This assemblage of *A. ambigua*, *AsterionellaA. formosa* and *F. crotonensis* has been
599 reported elsewhere as typical of eutrophic light-limited conditions (Reynolds et al., 2002;
600 Saros and Anderson, 2015). Both *AsterionellaA. formosa* and *F. crotonensis* have similar
601 resource requirements (Hobbs et al., 2011), being indicative of modest eutrophication by P
602 enrichment in temperate lakes (Saros et al., 2005). Changes in the TN:TP ratios can explain
603 the shifts in the diatom assemblages and the recent dominance of cyanobacteria in the lake
604 (Gonçalves, 2008; Cruz et al., 2015), but the response of phytoplankton communities to
605 changes in water chemistry are many times site-specific (e.g., Saros et al., 2005). Moreover,
606 both P and N enrichment have been demonstrated to favor the development of
607 cyanobacterial blooms in Lake Azul (Cruz et al., 2015). Alternatively, changes in thermal
608 structure rather than changes in stoichiometric ratios can be behind significant shifts in the
609 composition of phytoplankton in modern lakes (Mantzouki et al., 2018). Enhanced water
610 column stratification associated with warmer temperatures could explain the decline in
611 heavy diatom taxa such as *Aulacoseira*, which need well-mixed waters to thrive (Margalef,
612 1978). Water stratification would favor the development of *F. crotonensis* (Wolin and Stone,
613 2010), and the known dominance of cyanobacteria in the phytoplankton over diatoms for 10
614 months a year (Gonçalves, 2008) would put very fast-growing species such as *AsterionellaA.*
615 *formosa* in the advantage (Reynolds, 2006). The data suggest that eutrophication increased
616 during this phase, transforming lake's condition into a meso-eutrophic state, and that
617 changes in the TN:TP ratio and/or enhanced stratification due to temperature increase were
618 the main factors responsible of this change.

619

620 **5.3. Main long-term drivers of trophic status changes**

621 Paleoenvironmental reconstruction of Lake Azul for the approx. last 700 yr allowed the

622 identification of different potential natural (volcanism and climate) and human-induced
623 drivers of change in its trophic status: a) eruptive volcanism, b) external nutrient loads from
624 the watershed, c) changes in morphometry associated to lake-level rise, d) bottom-up and
625 top-down trophic controls, e) changes in the water column mixing regime, and f) artificial
626 fertilization derived from agricultural and farming activities.

627 The recorded ca. 700 yr history of Lake Azul begins with the extreme Caldeira Seca P17
628 volcanic eruption of ca. 1290 AD (phase I) whose ashes deposited with a diatom
629 assemblage of meso to eutrophic affinities. Although this sin-eruptive process makes
630 unclear the existence of a pre-eruptive meso to eutrophic lake, the post-eruptive record
631 shows the abrupt replacement of this diatom assemblage by another characteristic of
632 oligotrophic conditions. This sharp shift in the diatom assemblages in Lake Azul points to a
633 likely reset of the lake ecosystem due to the sedimentation of thick tephra deposits. This
634 oligotrophication mediated by P limitation resembles that of Lake Massoko (Tanzania)
635 following the deposition of a few centimeters-thick tephra (Barker et al., 2000). Although the
636 magnitude of this event would be insignificant compared to the sedimentation of the several-
637 meters-thick tephra layer P17 in Lake Azul, both cases seem to have experienced a similar
638 process. Contrary to enhanced productivity after tephra deposition found elsewhere (e. g.
639 Modenutti et al., 2013), the catastrophic nature of the Caldeira Seca P17 eruption implied
640 settling of new pioneering biological communities which restarted ecological succession.
641 The dominant benthic algal community also played a prominent role in maintaining
642 oligotrophy in the following 200 yr (1290-1480 AD, phase II), irrespective of several flood
643 episodes (Facies D) that could potentially intensify allochthonous nutrient inputs. Despite
644 their similar requirements, planktonic algae obtain nutrients exclusively from water, while
645 periphytic algae, typical of the shallow water conditions during this period, can assimilate
646 nutrients from both water and the sediment pool (Hansson, 1992). The dominance of
647 periphytic communities during this phase would therefore have prevented the release of

648 nutrients to support euplanktonic diatoms, maintaining oligotrophy in the lake, more severe
649 in the pelagic environment. Moreover, the enhanced precipitation regime in São Miguel
650 Island for this period (Hernández et al., 2017) and the probable denudation of the watershed
651 by the eruption, which would favor large nutrient inputs to the lake, had no effect on aquatic
652 primary productivity at the studied temporal resolution.

653 The period 1480-1870 AD (phase III) encompasses the extractive and transformative
654 phases of human colonization which implied extensive deforestation in the archipelago
655 (Connor et al., 2012; Rull et al., 2017). Despite geochemical and diatom data which indicate
656 persistent allochthonous inputs due to forest clearance in the watershed, during approx. 400
657 yr the lake did not significantly alter its oligotrophic condition. Although precipitation events
658 might have contributed to very short-term flood events (Facies D, Figs. 3, 4 and 5), nutrient
659 delivery was not sufficient for a sustained development of the eutrophic *Aulacoseira* spp.
660 flora, which needs a more constant concentration of nutrients in the water column, as
661 reported by Hall and Smol (2010). It was also during this period when a net water level rise,
662 following regional more humid conditions (Hernández et al. 2017), flooded the platform ramp
663 (Fig. 2), increasing the area of the epilimnion sediments with respect to the total volume of
664 the epilimnion. Under these circumstances, recirculation of nutrients from the sediments to
665 the epilimnion should be increased (Fee, 1979), prompting eutrophication. Yet, this
666 ultimately natural eutrophication process did not significantly move Lake Azul from its
667 oligotrophic condition during 400 yr, acting at a much slower pace compared to meso- to
668 eutrophic paleo-lake systems, where significant changes in the area of the epilimnion
669 sediments with respect to the total volume of the epilimnion also occurred (e.g., Bao et al.,
670 2015). Oligotrophy was therefore maintained irrespective of the combined effect of man-
671 induced allochthonous nutrient inputs associated to deforestation and the natural infilling
672 with water which could have brought a situation of morphometric eutrophy as described by
673 Rawson (1955).

674 Another morphometric threshold would be represented by the connection between Lake
675 Azul and Lake Verde in 1877 AD, which is probably ~~coetaneous~~ contemporary with the flood
676 event of 1870 AD. It can be hypothesized that the much smaller water volume in Lake Verde
677 would have favored higher nutrient concentrations, as at present (table 1), and that
678 connection of both lakes could induce a significant nutrient transfer to Lake Azul. Exotic
679 species introduction in the lake is another factor which could have prompted any significant
680 change in trophic conditions via top-down and bottom-up controls of the food web (McQueen
681 et al., 1989). Data from Lake Azul indicate that the increase in productivity during the period
682 1870-1940 AD (phase IV), coincident with local drier and colder conditions (Hernández et
683 al., 2017) that would diminish the delivery of nutrients from the catchment, as it is also
684 indicated by the TOC/TN data, was likely due to both nutrient delivery from Lake Verde after
685 connection took place and by internal nutrient recycling. Fish disturbance action favoring
686 sediment resuspension was the most probable cause for the latter. Additionally, grazing
687 activity by planktivore fishes, such as carp, imply an intensification of predation pressure on
688 zooplankton, whose reduction, besides the mentioned intensified nutrient release from the
689 bottom, results in increased phytoplankton biomass and productivity (Vanni, 2002). But
690 these bottom-up (by sediment resuspension) and top-down (predation over zooplankton)
691 effects by fish activity, as well as nutrient load from Lake Verde, had a quite limited action in
692 Lake Azul. Compared to the major role that fish introductions had on the long-term pelagic
693 nutrient enrichment of other Azorean lakes (Skov et al., 2010; Buchaca et al., 2011), the
694 effects in Lake Azul were quite attenuated. Paleoenvironmental data from Lake Azul suggest
695 that both fish introductions and Lake Verde overflow induced a gradual process of
696 transformation, instead of a sudden non-linear ecological change ascribable to an ecological
697 regime shift, as described by Lees et al. (2006). The oligotrophic inertia of the system was
698 maintained for another 70 yr because, either nutrient delivery from Lake Verde was low, or
699 fish introduction did not induce enough return of P from the sediments. This is in accordance

700 with the suggestion that in oligotrophic lakes productivity is more limited by nutrient supply
701 rather than by changes in trophic interactions (Schindler et al., 2001). It is not possible from
702 our data to disentangle the relative importance of increased nutrient inputs from Lake Verde
703 versus enhanced nutrient recycling by fish activity in this gradual process of eutrophication.

704 The most significant trophic event since the likely reset of the P17 eruption (ca. 1290 AD)
705 occurred after 1940 AD to the present (phases V and VI), when the oligotrophic inertia of
706 the lake was interrupted. The observed changes, mainly the sudden maximum increase of
707 euplanktonic eutrophic diatoms, the reduction of hydrophytes in the recent pollen record
708 (Rull et al., 2017), and, more recently, the dominance of cyanobacteria in the lake
709 (Gonçalves, 2008; Cruz et al., 2015), indicate that the present-day status as a meso-
710 eutrophic lake was reached during this period. Although eutrophication due to increased
711 artificial nutrient input from the watershed was the main responsible for this major
712 environmental change, other intervening factors need also be considered. It cannot be
713 completely disregarded that part of the N enrichment influencing present-day phytoplankton
714 composition in Lake Azul had an atmospheric origin (sensu Elser et al., 2009), but this is
715 difficult to disentangle from the confounding effect of N loading from the catchment by
716 human activities (as reported by Catalan et al., 2013). Likewise, increased thermal
717 stratification could explain the shifts in phytoplankton composition, such as the decline in
718 *Aulacoseira* species (e.g., Rühland et al., 2008), and the concurrent increase of other
719 components, such as cyanobacteria (e.g., Mantzouki et al., 2018). The synergetic effect of,
720 first, excess nutrient load and, second, reduced water turnover, could be behind the
721 exacerbation of the symptoms of eutrophication (Jeppesen et al., 2014; Le Moal et al., 2019).
722 This can be the reason why, despite some remediation measures such as surface runoff
723 diversion, both monitoring (Cruz et al., 2015) and the paleolimnological (this study) data
724 show that the lake is not experiencing at present a significant change in its trophic status.

725 Our results indicate that cataclysmic volcanism was the main driver in configuring Lake

726 Azul ecology in the last ca. 700 yr. Previous studies on the long-term effects of deposition
727 of thin distal tephra on biological communities have shown that these are usually short-lived
728 (100-150 yr, Telford et al., 2004). Recovery can sometimes be very rapid, such as the case
729 of oligotrophic Lake Galletué (Chile) after the deposition of a few cm thick tephra in 1957
730 AD which took just approx. 5 yr (Cruces et al., 2006) or the meso to eutrophic Lake Holzmaar
731 (Germany) which lasted 10-20 yr maximum after the deposition of approx. 8 cm thick tephra
732 (Lotter et al., 1995). Even catastrophic eruptions such as that of Mt. St. Helene (United
733 States) in 1980 AD, which brought the virtual elimination of algae population in Lake Spirit,
734 implied the quasi-recovery to the pre-eruptive conditions of this oligotrophic lake in approx.
735 30 yr (Larson et al., 2006; Gawel et al., 2018). Although it has been hypothesized that the
736 long-term disruption of lake ecosystems can occur when biogeochemical cycling is
737 interrupted after catastrophic volcanic events (Telford et al., 2004), few examples have been
738 demonstrated in the literature (e. g., Barker et al., 2000). Lake Azul constitutes an example
739 of such a disruption and of the gradual reestablishment of its pre-eruptive meso to eutrophic
740 condition throughout 650 yr only after artificial fertilization accelerated this process in the
741 last decades.

742 A consequence of this primary role of volcanism as a driver in the ecological trajectory of
743 Lake Azul is the potential ability or not of its diatom and bulk organic matter content to
744 reconstruct paleoclimates in the region. Comparison with the paleoclimate data obtained
745 from Lake Empadadas, located just 6 km away in São Miguel island (Hernández et al., 2017),
746 shows the minor role of changes in nutrient delivery associated to precipitation variability in
747 changing the trophic status in Lake Azul. Besides noteworthy differences in the size and
748 morphometric characteristics of both basins which make Lake Empadadas more sensitive
749 to any subtle precipitation regime change, the effects of the P17 eruption were irrelevant in
750 this lake compared to Lake Azul. Contrary to the effects of the deposition of thin tephra
751 layers which do not override the long-term changes due to climate change (e. g., Lotter et

752 al., 1995; Telford et al., 2004; Egan et al., 2019), any climatic signature on productivity in
753 Lake Azul has been largely obscured by the massive tephra deposition of 1290 AD. Any
754 paleoclimatic reconstruction based on the study of the diatom and bulk organic matter
755 records in Lake Azul would therefore be largely biased by the overprinting of the volcanic
756 signature after the cataclysmic eruptive episode of 1290 AD, so using alternative proxy data
757 should consequently be preferred instead.

758

759 **6. Conclusions**

760 Artificial fertilization and, secondarily, fish stockings and connectivity with Lake Verde,
761 were the main factors responsible of changes in trophic status in Lake Azul. A vast eruptive
762 episode which implied the deposition of several meters of tephra in the lake ca. 1290 AD
763 determined a state of oligotrophic inertia during approx. 650 yr. Since this event the lake
764 experienced a net long-term increase in productivity, but showed a high resilience to change
765 from an oligotrophic to a mesotrophic condition, the latter only being achieved when artificial
766 fertilization and livestock manure practices were intensively implemented in the island in the
767 period 1940-1995 AD. Bottom-up and top-down food web controls by fish stocking in this
768 formerly fishless lake, which started in the 18th century, or nutrient injection from Lake Verde
769 overflow in the late 19th century, had a secondary role in lake's trophism. Compared to the
770 mesotrophic Lake Fogo and the eutrophic Furnas, Lake Azul did not significantly change its
771 trophic condition, confirming that the volcanic-induced oligotrophy of the lake, and not
772 trophic interactions, was the main factor explaining the trophic status of the lake during most
773 of its recent history. Other processes, such as natural morphometric eutrophy, or increased
774 delivery of nutrients due to man-induced deforestation and climate variability had a negligible
775 role in reverting the oligotrophic inertia of the lake. By contrast, despite several interventions
776 to avoid the excess nutrient load which drove recent eutrophication, more persistent water

777 stratification seem to maintain or even exacerbate the effects of eutrophication. Lake Azul
778 constitutes an uncommon case in the literature of complete ecosystem restructuring and
779 long-term resilience to trophic change induced by a catastrophic volcanic eruption.

780

781 **Acknowledgments**

782 This research was funded by the Spanish Ministry of Economy and Competitiveness
783 projects PaleoNAO, RapidNAO and PaleoModes (CGL2010-15767, CGL2013-40608-R and
784 CGL2016-75281-C2, respectively) and by the Fundação para a Ciência e Tecnologia
785 (PTDC/CTA-AMB/28511/2017). David Vázquez-Loureiro, Armand Hernández, María Jesús
786 Rubio and Pedro Raposeiro benefited with grants from the Xunta de Galicia (I2C
787 Programme co-funded with the European Social Fund), Generalitat de Catalunya (Beatriu
788 de Pinós - Marie Curie cofund programme), Spanish Ministry of Economy and
789 Competitiveness (Programa de Formación de Personal Investigador, FPI), and Fundação
790 para a Ciência e Tecnologia (SFRH/BPD/99461/2014), respectively. We thank Olga
791 Margalef and Guiomar Sánchez-López for field assistance.

792

793 **References**

- 794 Andrade, C., Trigo, R.M., Freitas, M.C., Gallego, M.C., Borges, P., Ramos, A.M., 2008. Comparing historic
795 records of storm frequency and the North Atlantic Oscillation (NAO) chronology for the Azores region.
796 *Holocene* 18, 745-754.
- 797 Andrade, J. (2003). *Concelho de Ponta Delgada: 500 anos de história : cronologia de figuras e factos, 1499-*
798 *1999*. [Ponta Delgada, Azores]: Câmara Municipal, 648 pp.
- 799 Bao, R., Hernández, A., Sáez, A., Giral, S., Prego, R., Pueyo, J.J., Moreno, A., Valero-Garcés, B.L., 2015.
800 Climatic and lacustrine morphometric controls of diatom paleoproductivity in a tropical Andean lake.
801 *Quaternary Sci.Rev.* 129, 96-110. <http://dx.doi.org/10.1016/j.quascirev.2015.09.019>
- 802 Barker, P., Telford, R., Merdaci, O., Williamson, D., Taieb, M., Vincens, A., Gibert, E., 2000. The sensitivity

803 of a Tanzanian crater lake to catastrophic tephra input and four millennia of climate change. *Holocene*
804 10(3), 303 – 310. <http://dx.doi.org/10.1191/095968300672848582>

805 Barrois, T., 1896. Recherches sur la faune des eaux douce des Açores. Mémoires de la Société des
806 Sciences de l'Agriculture et des Artes de Lille, Série V, Fasc. 6. Société des Sciences de l'Agriculture et
807 des Artes de Lille, Paris.

808 Bennett, K.D., 1996. Determination of the number of zones in a biostratigraphical sequence. *New Phytol.*
809 132, 155-170. <http://dx.doi.org/10.1111/j.1469-8137.1996.tb04521.x>

810 Bennett, K.D., 2002. Documentation for Psimpoll 4.10 and Pscomb 1.03, C Programs for Plotting Pollen
811 Diagrams and Analising Pollen Data. Uppsala University.

812 Bohlin, K., 1901. Étude sur la flore algologique d'eau douce des Açores. Bihang till Kongl. Svenska
813 Vetenskaps-Akademiens 27, 1-85.

814 Buchaca, T., Skov, T., Amsinck, S., Gonçalves, V., Azevedo, J., Andersen, T., Jeppesen, E., 2011. Rapid
815 Ecological Shift Following Piscivorous Fish Introduction to Increasingly Eutrophic and Warmer Lake
816 Furnas (Azores Archipelago, Portugal): A Paleoecological Approach. *Ecosystems* 1–20.
817 <https://doi.org/10.1007/s10021-011-9423-0>

818 Cañellas-Boltá, N., Rull, V., Sáez, A., Margalef, O., Bao, R., Pla-Rabes, S., Blaauw, M., Valero-Garcés, B.,
819 Giral, S., 2013. Vegetation changes and human settlement of Easter Island during the last millennia: a
820 multiproxy study of the Lake Raraku sediments. *Quaternary Sci. Rev.* 72, 36–48.
821 <http://dx.doi.org/10.1016/j.quascirev.2013.04.004>

822 Catalan, J., Pla-Rabés, S., Wolfe, A., Smol, J., Rühland, K., Anderson, N.J., Kopáček, J., Stuchlík, E.,
823 Schmidt, R., Koinig, K., Camarero, L., Flower, R., Heiri, O., Kamenik, C., Korhola, A., Leavitt, P.,
824 Psenner, R., Renberg, I., 2013. Global change revealed by palaeolimnological records from remote
825 lakes: a review. *J.Paleolimnol.* 49, 513-535. <https://doi.org/10.1007/s10933-013-9681-2>

826 Cattaneo, A., Kalff J., 1980. The relative contribution of aquatic macrophytes and their epiphytes to the
827 production of macrophyte beds. *Limnol. Oceanogr.* 25(2), 280-289.
828 <http://dx.doi.org/10.4319/lo.1980.25.2.0280>

829 Cohen, A.S., 2003. *Paleolimnology*. Oxford University Press, Oxford.

830 Cole, P.D., Pacheco, J.M., Gunasekera, R., Queiroz, G., Gonçalves, P., Gaspar, J.L., 2008. Contrasting
831 styles of explosive eruption at Sete Cidades, São Miguel, Azores, in the last 5000 years: Hazard
832 implications from modelling. *J. Volcanol. Geoth. Res.* 178 (3), 574-591.
833 <http://dx.doi.org/10.1016/j.jvolgeores.2008.01.008>

834 Connor, S.E., van Leeuwen, J.F.N., Rittenour, T.M., van der Knaap, W.O., Ammann, B., Björck, S., 2012.

835 The ecological impact of oceanic island colonization – a palaeoecological perspective from the Azores.
836 J. Biogeogr. 39, 1007–1023. <https://doi.org/10.1111/j.1365-2699.2011.02671.x>

837 Cropper, T.E., Hanna, E., 2014. An analysis of the climate of Macaronesia, 1865–2012. Int. J. Climatol. 34,
838 604–622. <http://dx.doi.org/10.1002/joc.3710>

839 Cruces, F., Urrutia, R., Parra, O., Araneda, A., Treutler, H., Bertrand, S., Fagel, N., Torres, L., Barra, R.,
840 Chirinos, L., 2006. Changes in diatom assemblages in an Andean lake in response to a recent volcanic
841 event. Arch. für Hydrobiol. 165, 23–35.

842 Cruz, J.V., Pacheco, D., Porteiro, J., Cymbron, R., Mendes, S., Malcata, A., Andrade, C., 2015. Sete
843 Cidades and Furnas lake eutrophication (São Miguel, Azores): Analysis of long-term monitoring data
844 and remediation measures. Sci. Total Environ. 520, 168-186.
845 <http://dx.doi.org/10.1016/j.scitotenv.2015.03.052>

846 Cunha, A. G. 1939. Sur la flore charologique des îles Açoréennes. *Bulletin de la Société Portugaise des*
847 *Sciences Naturelles* , 13 (13): 67-70

848 Dias, E., 2007. Açores e Madeira: A Floresta das Ilhas. Fundação Luso Americana, Lisboa.

849 Egan, J., Allott, T.E.H., Blackford, J.J., 2019. Diatom-inferred aquatic impacts of the mid-Holocene eruption
850 of Mount Mazama, Oregon, USA. Quat. Res. 91, 163–178. <https://doi.org/10.1017/qua.2018.73>

851 Ellis, B.K., Stanford, J.A., Goodman, D., Stafford, C.P., Gustafson, D.L., Beauchamp, D.A., Chess, D.W.,
852 Craft, J.A., Deleray, M.A., Hansen, B.S., 2011. Long-term effects of a trophic cascade in a large lake
853 ecosystem. Proc. Natl. Acad. Sci., 108: 1070-1075. <https://doi.org/10.1073/pnas.1013006108>

854 Elser, J.J., Andersen, T., Baron, J.S., Bergstrom, A.-K., Jansson, M., Kyle, M., Nydick, K.R., Steger, L.,
855 Hessen, D.O., 2009. Shifts in Lake N:P Stoichiometry and Nutrient Limitation Driven by Atmospheric
856 Nitrogen Deposition. Science 326, 835-837. <http://dx.doi.org/10.1126/science.1176199>

857 Elser, J.J., Goldman, C.R., 1991. Zooplankton effects on phytoplankton in lakes of contrasting trophic status.
858 Limnol. Oceanogr. 36, 64–90. <https://doi.org/10.4319/lo.1991.36.1.0064>

859 Fee, E.J., 1979. A relation between lake morphometry and primary productivity and its use in interpreting
860 whole-lake eutrophication experiments. Limnol. Oceanogr. 24(3), 401-416.
861 <http://dx.doi.org/10.4319/lo.1979.24.3.0401>

862 Flor de Lima, H.M.Q., 1993. Contribuição para o estudo ictiológico das lagoas das Furnas e Sete Cidades.
863 Estudos, Experimentação e Divulgação. p. 99., Ponta Delgada.

864 France, R.L., 1995. Differentiation between littoral and pelagic food webs in lakes using stable carbon
865 isotopes. Limnol. Oceanogr. 40, 1310-1313. <http://dx.doi.org/10.4319/lo.1995.40.7.131>

866 Frutuoso, G., 1977. Livro Quarto das Saudades da Terra. Instituto Cultural de PontaDelgada, Ponta Delgada,

867 1593 pp.

868 Gawel, J.E., Crisafulli, C.M., Miller, R., 2018. The New Spirit Lake: Changes to Hydrology, Nutrient Cycling,
869 and Biological Productivity, in: Crisafulli, C.M., Dale, V.H. (Eds.), *Ecological Responses at Mount St.*
870 *Helens: Revisited 35 Years after the 1980 Eruption*. Springer New York, New York, NY, pp. 71–95.
871 https://doi.org/10.1007/978-1-4939-7451-1_4

872 Gonçalves, V., 2008. Contribuição para o estudo da qualidade ecológica das lagoas dos Açores.
873 Fitoplâncton e diatomáceas bentónicas. PhD. Dissertation, Universidade dos Açores, Ponta Delgada,
874 343 pp.

875 Gonçalves, V., Marques, H., Fonseca, A., 2010. Lista das Diatomáceas (Bacillariophyta), in: Borges, P.A.V.,
876 Bried, J., Costa, A., Cunha, R., Gabriel, R., Gonçalves, V., Martins, A.F., Melo, I., Parente, M.,
877 Raposeiro, P., Rodrigues, P., Santos, R.S., Silva, L., Vieira, P., Vieira, V. (Eds.), *Listagem dos*
878 *Organismos Terrestres e Marinhos dos Açores*. Princípia, Cascais, pp. 81-97.

879 Gonçalves V., Costa A.C., Raposeiro P.M., Marques H.S., Cunha A., Ramos J., Cruz A.M., Pereira C.L.,
880 Vilaverde J., 2013. Monitorização das Massas de Água Interiores da Região Hidrográfica Açores.
881 Relatório Anual de 2012 (R5/2012). CIBIO Açores, Departamento de Biologia, Universidade dos
882 Açores, Ponta Delgada, 261 pp.

883 Grimm, E.C., 1987. CONISS: a Fortran 77 program for stratigraphically constrained cluster analysis by the
884 method of incremental sum of squares. *Comput. Geosci.* 13, 13-35. [http://dx.doi.org/10.1016/0098-](http://dx.doi.org/10.1016/0098-3004(87)90022-7)
885 [3004\(87\)90022-7](http://dx.doi.org/10.1016/0098-3004(87)90022-7)

886 Hall, R.I., Smol, J.P., 2010. Diatoms as indicators of lake eutrophication, in: Smol, J.P., Stoermer, E.F.
887 (Eds.), *The Diatoms: Applications for the Environmental and Earth Sciences*. Cambridge University
888 Press, Cambridge, pp. 122-151.

889 Harper, M.A., Howorth, R., McLeod, M., 1986. Late Holocene diatoms in Lake Poukawa: Effects of airfall
890 tephra and changes in depth. *New Zeal. J. Mar. Fres.* 20(1), 107-118.
891 <http://dx.doi.org/10.1080/00288330.1986.9516135>

892 Hansson, L. A., 1992. Factors regulating periphytic algal biomass. *Limnol. Oceanogr.* 37(2), 322-328.
893 <http://dx.doi.org/10.4319/lo.1992.37.2.0322>

894 Hernández, A., Kutiel, H., Trigo, R.M., Valente, M.A., Sigró, J., Cropper, T., Santo, F.E., 2016. New Azores
895 archipelago daily precipitation dataset and its links with large-scale modes of climate variability. *Int. J.*
896 *Climatol.* 36, 4439-4454. <http://dx.doi.org/10.1002/joc.4642>

897 Hernández, A., Sáez, A., Bao, R., Raposeiro, P.M., Trigo, R.M., Doolittle, S., Masqué, P., Rull, V.,
898 Gonçalves, V., Vázquez-Loureiro, D., Rubio-Inglés, M.J., Sánchez-López, G., Giral, S., 2017. The

899 influences of the AMO and NAO on the sedimentary infill in an Azores Archipelago lake since ca. 1350
900 CE. *Global Planet. Change* 154, 61-74. <https://doi.org/10.1016/j.gloplacha.2017.05.007>

901 Hobbs, W.O., Fritz, S.C., Stone, J.R., Donovan, J.J., Grimm, E.C., Almendinger, J.E., 2011. Environmental
902 history of a closed-basin lake in the US Great Plains: Diatom response to variations in groundwater flow
903 regimes over the last 8500 cal. yr BP. *Holocene* 21, 1203-1216.
904 <https://doi.org/10.1177/0959683611405242>

905 Hughes, S.J., Malmqvist, B., 2005. Atlantic Island freshwater ecosystems: challenges and considerations
906 following the EU Water Framework Directive. *Hydrobiologia* 544, 289–297.
907 <https://doi.org/10.1007/s10750-005-1695-y>

908 Jeppesen, E., Meerhoff, M., Davidson, T., Trolle, D., Søndergaard, M., Lauridsen, T., Beklioglu, M., Brucet,
909 S., Volta, P., González-Bergonzoni, I., Nielsen, A., 2014. Climate change impacts on lakes: An
910 integrated ecological perspective based on a multi-faceted approach, with special focus on shallow
911 lakes. *J. Limnol.* 73, 88–111. <https://doi.org/10.4081/jlimnol.2014.844>

912 Kilham P., Kilham S.S., Hecky R.E., 1986. Hypothesized resource relationships among African planktonic
913 diatoms. *Limnol. Oceanogr.* 6: 1169-181. <http://dx.doi.org/10.4319/lo.1986.31.6.1169>

914 Kingsbury, M. V, Laird, K.R., Cumming, B.F., 2012. Consistent patterns in diatom assemblages and diversity
915 measures across water-depth gradients from eight Boreal lakes from north-western Ontario (Canada).
916 *Freshw. Biol.* 57, 1151–1165. <https://doi.org/10.1111/j.1365-2427.2012.02781.x>

917 Kohler, A., Labus, B.C., 1983. Eutrophication processes and pollution of freshwater ecosystems including
918 waste heat, in: Lange, O.L., Nobel, P.S., Osmond, C.B., Ziegler, H. (Eds.), *Physiological plant ecology*
919 IV. Ecosystem processes: mineral cycling, productivity and man's influence. Springer, Berlin, pp. 413-
920 464.

921 Krammer, K., Lange-Bertalot, H., 1986-1991. Bacillariophyceae. Volumes 1-4, in: Ettl, H., Gerloff, J., Heynig,
922 H., Mollenhauer, D. (Eds.), *Süßwasserflora von Mitteleuropa*. Fischer-Verlag, Stuttgart.

923 Lange-Bertalot, H., 2000-2013. *Diatoms of the European Inland Waters and Comparable Habitats*. Volumes
924 1-7. A. R. G. Gantner Verlag, Ruggell, Liechtenstein.

925 Larson, D.W., Sweet, J., Petersen, R.R., Crisafulli, C.M., 2006. Posteruption Response of Phytoplankton and
926 Zooplankton Communities in Spirit Lake, Mount St. Helens, Washington. *Lake Reserv. Manag.* 22, 273–
927 292. <https://doi.org/10.1080/07438140609354362>

928 Le Moal, M., Gascuel-Oudou, C., Ménesguen, A., Souchon, Y., Étrillard, C., Levain, A., Moatar, F., Pannard,
929 A., Souchu, P., Lefebvre, A., Pinay, G., 2019. Eutrophication: A new wine in an old bottle?. *Sci. Total*
930 *Environ.* 651, 1–11. <https://doi.org/10.1016/j.scitotenv.2018.09.139>

931 Lees, K., Pitois, S., Scott, C., Frid, C., Mackinson, S., 2006. Characterizing regime shifts in the marine
932 environment. *Fish Fish.* 7, 104-127. <https://doi.org/10.1111/j.1467-2979.2006.00215.x>

933 Leira, M., Filippi, M.L., Cantonati, M., 2015. Diatom community response to extreme water-level fluctuations
934 in two Alpine lakes: a core case study. *J. Paleolimnol.* 53, 289-307. [http://dx.doi.org/10.1007/s10933-](http://dx.doi.org/10.1007/s10933-015-9825-7)
935 [015-9825-7](http://dx.doi.org/10.1007/s10933-015-9825-7)

936 Leps, J., Smilauer, P., 2003. *Multivariate analysis of ecological data using CANOCO*. Cambridge University
937 Press, Cambridge, 268 pp.

938 Lotter, A.F., Birks, H.J.B., Zolitschka, B., 1995. Late-glacial pollen and diatom changes in response to two
939 different environmental perturbations: volcanic eruption and Younger Dryas cooling. *J. Paleolimnol.* 14,
940 23–47.

941 Mantzouki, E., Lüring, M., Fastner, J., de Senerpont Domis, L., Wilk-Woźniak, E., et al., 2018. Temperature
942 Effects Explain Continental Scale Distribution of Cyanobacterial Toxins. *Toxins (Basel)*. 10, e156.

943 Margalef, R., 1978. Life forms of phytoplankton as survival alternatives in an unstable environment. *Oceanol.*
944 *Acta* 1(4), 493-509.

945 McQueen, D.J., Johannes, M.R.S., Post, J.R., Stewart, T.J., Lean, D.R.S., 1989. Bottom-Up and Top-Down
946 Impacts on Freshwater Pelagic Community Structure. *Ecol. Monogr.* 59, 289–309.
947 <https://doi.org/10.2307/1942603>

948 Meyers, P.A., Teranes, J.L., 2001. Sediment organic matter, in: Smol, J.P., Birks, H.J.B., Last, W.M. (Eds.),
949 *Tracking Environmental Change Using Lake Sediments. Volume 2: Physical and Geochemical Methods*.
950 Kluwer Academic Publishers, Dordrecht, pp. 239-269.

951 Modenutti, B.E., Balseiro, E.G., Elser, J.J., Navarro, M.B., Cuassolo, F., Laspoumaderes, C., Souza, M.S.,
952 Villanueva, V.D., 2013. Effect of volcanic eruption on nutrients, light, and phytoplankton in oligotrophic
953 lakes. *Limnol. Oceanogr.* 58, 1165–1175. <https://doi.org/10.4319/lo.2013.58.4.1165>

954 Pereira, C.L., Raposeiro, P.M., Costa, A.C., Bao, R., Giral, S., Gonçalves, V., 2014. Biogeography and lake
955 morphometry drive diatom and chironomid assemblages' composition in lacustrine surface sediments of
956 oceanic islands. *Hydrobiologia* 730, 93-112. <http://dx.doi.org/10.1007/s10750-014-1824-6>

957 Peterson, C., Stevenson, R., 1992. Resistance and resilience of lotic algal communities: Importance of
958 disturbance timing and current. *Ecology* 73(4), 1445-1461. <http://dx.doi.org/10.2307/1940689>

959 Potapova, M., Hamilton, P.B., 2007. Morphological and ecological variation within the *Achnantheidium*
960 *minutissimum* (Bacillariophyceae) species complex. *J. Phycol.* 43, 561-575.

961 Queiroz, G. 1997. *Vulcao das Sete Cidades (S. Miguel, Açores). Historia eruptiva e Avaliaçao do Hazrd.*
962 *PhD Thesis. Azores University, 226 pp.*

963 Queiroz, G., Pacheco, J.M., Gaspar, J.L., Aspinall, W.P., Guest, J.E., Ferreira, T., 2008. The last 5000 years
964 of activity at Sete Cidades volcano (São Miguel Island, Azores): Implications for hazard assessment. J.
965 Volcanol. Geoth. Res. 178: 562-573. <http://dx.doi.org/10.1016/j.jvolgeores.2008.03.001>

966 Raposeiro, P.M., Rubio, M.J., González, A., Hernández, A., Sánchez-López, G., Vázquez-Loureiro, D., Rull,
967 V., Bao, R., Costa, A.C., Gonçalves, V., Sáez, A., Giralt, S., 2017. Impact of the historical introduction of
968 exotic fishes on the chironomid community of Lake Azul (Azores Islands). Palaeogeogr. Palaeocl. 466,
969 77-88. <http://dx.doi.org/10.1016/j.palaeo.2016.11.015>

970 Rawson, D.S., 1955. Morphometry as a dominant factor in the productivity of large lakes. Int. Vereinigung
971 fuer Theor. und Angew. Limnol. Verhandlungen 12, 164–175.

972 Reclus, E., 1830-1905. Africa and its inhabitants. Volume 2. J. S. Virtue, London.

973 Reed, J., Roberts, N., Leng, M., 1999. An evaluation of the diatom response to Late Quaternary
974 environmental change in two lakes in the Konya Basin, Turkey, by comparison with stable isotope data.
975 Quat. Sci. Rev. 18, 631-646. [http://dx.doi.org/10.1016/S0277-3791\(98\)00101-2](http://dx.doi.org/10.1016/S0277-3791(98)00101-2)

976 Reimer, P.J., Bard, E., Bayliss, A., Beck, J.W., Blackwell, P.G., Ramsey, C.B., Buck, C.E., Cheng, H.,
977 Edwards, R.L., Friedrich, M., Grootes, P.M., Guilderson, T.P., Hafliðason, H., Hajdas, I., Hatté, C.,
978 Heaton, T.J., Hoffmann, D.L., Hogg, A.G., Hughen, K.A., Kaiser, K.F., Kromer, B., Manning, S.W., Niu,
979 M., Reimer, R.W., Richards, D.A., Scott, E.M., Southon, J.R., Staff, R.A., Turney, C.S.M., van der Plicht,
980 J., 2016. IntCal13 and Marine13 Radiocarbon Age Calibration Curves 0–50,000 Years cal BP.
981 Radiocarbon 55, 1869-1887. http://dx.doi.org/10.2458/azu_js_rc.55.16947

982 Renberg, I., 1990. A procedure for preparing large sets of diatom slides from sediment cores. J. Paleolimnol.
983 4, 87-90. <http://dx.doi.org/10.1007/BF00208301>

984 Reynolds, C.S., 2006. The Ecology of Phytoplankton. Cambridge University Press, Cambridge.

985 Reynolds, C.S., Huszar, V., Kruk, C., Naselli-Flores, L., Melo, S., 2002. Towards a functional classification of
986 the freshwater phytoplankton. J. Plankton Res. 24, 417-428. <https://doi.org/10.1093/plankt/24.5.417>

987 Richardson, M.J., Whoriskey, F.G., Roy, L.H., 1995. Turbidity generation and biological impacts of an exotic
988 fish *Carassius auratus*, introduced into shallow seasonally anoxic ponds. J. Fish Biol. 47:576–585.
989 <http://dx.doi.org/10.1111/j.1095-8649.1995.tb01924.x>

990 Robinson, M., 2004. A Late glacial and Holocene diatom record from Clettnadal, Shetland Islands, northern
991 Scotland. J. Paleolimnol. 31, 295-319. <http://dx.doi.org/10.1023/B:JOPL.0000021716.49552.da>

992 Rühland, K., Paterson, A.M., Smol, J.P., 2008. Hemispheric-scale patterns of climate-related shifts in
993 planktonic diatoms from North American and European lakes. Glob. Change Biol. 14, 2740-2754.
994 <http://dx.doi.org/10.1111/j.1365-2486.2008.01670.x>

995 Rull, V., Lara, A., Rubio-Inglés, M.J., Giral, S., Gonçalves, V., Raposeiro, P., Hernández, A., Sánchez-
996 López, G., Vázquez-Loureiro, D., Bao, R., Masqué, P., Sáez, A., 2017. Vegetation and landscape
997 dynamics under natural and anthropogenic forcing on the Azores Islands: A 700-year pollen record from
998 the São Miguel Island. *Quat. Sci. Rev.* 159, 155-168. <https://doi.org/10.1016/j.quascirev.2017.01.021>

999 Santos, F.D., Valente, M.A., Miranda, P.M.A., Aguiar, A., Azevedo, E.B., Tome, A.R., Coelho, F., 2004.
1000 Climate change scenarios in the Azores and Madeira Islands. *World Resour. Rev.* 16, 473–491.

1001 Saros, J.E., Anderson, N.J., 2015. The ecology of the planktonic diatom *Cyclotella* and its implications for
1002 global environmental change studies. *Biol. Rev.* 90, 522-541. <http://dx.doi.org/10.1111/brv.12120>

1003 Saros, J.E., Michel, T.J., Interlandi, S.J., Wolfe, A.P., 2005. Resource requirements of *Asterionella formosa*
1004 and *Fragilaria crotonensis* in oligotrophic alpine lakes: implications for recent phytoplankton community
1005 reorganizations. *Can. J. Fish. Aquat. Sci.* 62, 1681-1689. <https://doi.org/10.1139/f05-077>

1006 Sax, D.F., Gaines, S.D., 2008. Species invasions and extinction: The future of native biodiversity on islands.
1007 *Proc. Natl. Acad. Sci.* 105, 11490–11497. <https://doi.org/10.1073/pnas.0802290105>

1008 Scheffer, M., van Nes, E., 2007. Shallow lakes theory revisited: various alternative regimes driven by climate,
1009 nutrients, depth and lake size. *Hydrobiologia* 584, 455–466. <https://doi.org/10.1007/s10750-007-0616-7>

1010 Schindler, E.D., Knapp, A.R., Leavitt, R.P., 2001. Alteration of nutrient cycles and algal production resulting
1011 from fish introductions into mountain lakes. *Ecosystems* 4, 308-321. [http://dx.doi.org/10.1007/s10021-](http://dx.doi.org/10.1007/s10021-001-0013-4)
1012 [001-0013-4](http://dx.doi.org/10.1007/s10021-001-0013-4)

1013 Shotton, F.W., Williams, R.E.G., 1971. Birmingham University Radiocarbon dates V. *Radiocarbon* 11, 141-
1014 156. <https://doi.org/10.1017/S0033822200008419>

1015 Skov, T., Buchaca, T., Amsinck, S., Landkildehus, F., Odgaard, B., Azevedo, J., Gonçalves, V., Raposeiro,
1016 P., Andersen, T., Jeppesen, E., 2010. Using invertebrate remains and pigments in the sediment to infer
1017 changes in trophic structure after fish introduction in Lake Fogo: a crater lake in the Azores.
1018 *Hydrobiologia* 654, 13-25. <http://dx.doi.org/10.1007/s10750-010-0325-5>

1019 Stenger-Kovács, C., Padisák, J., Bíró, P., 2006. Temporal variability of *Achnanthydium minutissimum*
1020 (Kützing) Czarnecki and its relationships to chemical and hydrological features of the Torna-stream,
1021 Hungary. Program, abstracts & extended abstracts: 6th International Symposium on Use of Algae for
1022 monitoring Rivers. Magyar Algológiai Társaság, Göd, pp. 133-138. ISBN 963 06 0497 3

1023 Stevenson, R.J., Bothwell, M.L., Lowe, R.L., 1996. *Algal Ecology*. Academic Press, San Diego, p. 759.

1024 Stone, J.R., Fritz, S.C., 2004. Three-dimensional modeling of lacustrine diatom habitat areas: Improving
1025 paleolimnological interpretation of planktic : benthic ratios. *Limnol. Oceanogr.* 49, 1540-1548.
1026 <http://dx.doi.org/10.1371/journal.pone.0108936>

- 1027 Stuver, M., Reimer, P.J., 1993. Extended ¹⁴C data base and revised CALIB 3.0 ¹⁴C age calibration
1028 program. Radiocarbon 35, 215-230. <https://doi.org/10.1017/S0033822200013904>
- 1029 Talbot, M.R., 2001. Nitrogen isotopes in paleolimnology, in: Smol, J.P., Birks, H.J.B., Last, W.M. (Eds.),
1030 Tracking Environmental Change Using Lake Sediments. Volume 2: Physical and Geochemical Methods.
1031 Kluwer Academic Publishers, Dordrecht, pp. 401-439.
- 1032 Telford, R.J., Barker, P., Metcalfe, S.E., Newton, A., 2004. Lacustrine responses to tephra deposition:
1033 examples from Mexico. Quat. Sci. Rev. 23, 2337-2353.
1034 <http://dx.doi.org/10.1016/j.quascirev.2004.03.014>
- 1035 ter Braak, C.J.F., Smilauer, P., 1998. CANOCO Reference Manual and User's Guide to CANOCO for
1036 Windows: Software for Canonical Community Ordination (Version 4). Microcomputer Power, Ithaca,
1037 New York.
- 1038 Thornton, J.A., Harding, W.R., Dent, M., Hart, R.C., Lin, H., Rast, C.L., Rast, W., Ryding, S.-O., Slawski,
1039 T.M., 2013. Eutrophication as a 'wicked' problem. Lakes Reserv. Sci. Policy Manag. Sustain. Use 18,
1040 298–316. <https://doi.org/10.1111/lre.12044>
- 1041 Trelease, W., 1897. Botanical Observations on the Azores. Missouri Bot. Gard. Annu. Rep. 1897, 77–220.
1042 <https://doi.org/10.2307/2992160>
- 1043 Valois-Silva, F., 1886. Descrição das águas minerais das Furnas na ilha de São Miguel, Archivo dos Açores.
1044 Vol. 8. Typografia do arquivo dos Açores. (Ponta Delgada). pp. 437–446.
- 1045 Van Eaton, A.R., Harper, M.A., Wilson, C.J.N., 2013. High-flying diatoms: Widespread dispersal of
1046 microorganisms in an explosive volcanic eruption. Geology 41, 1187-1190.
1047 <http://dx.doi.org/10.1130/G34829.1>
- 1048 Vanni, M., 2002. Nutrient Cycling by Animals in Freshwater Ecosystems. Annu. Rev. Ecol. Syst. 33, 341-370.
1049 <http://dx.doi.org/10.1146/annurev.ecolsys.33.010802.150519>
- 1050 Vicente, A., 1956. Introdução de peixes de água doce nas lagoas de S. Miguel. Açoreana 5.
- 1051 Vidal, A.T.E., Hydrographic Office, R.U., Walker, J.& C.C.N.-C.C. 166 A.. C.C. 166 A., 1850. San Miguel.
1052 Hydrographic Office, London.
- 1053 Volkov, D.L., Fu, L.-L., 2010. On the reasons for the formation and variability of the
1054 Azores current. J. Phys. Oceanogr. 40, 2197–2220. [http://dx.doi.org/10.1175/](http://dx.doi.org/10.1175/2010JPO4326.1)
1055 2010JPO4326.1.
- 1056 Wang, Q., Yang, X., Hamilton, P., Zhang, E., 2012. Linking spatial distributions of sediment diatom
1057 assemblages with hydrological depth profiles in a plateau deep-water lake system of subtropical China.
1058 Fottea 12, 59-73. <http://dx.doi.org/10.5507/fot.2012.005>

1059 Werner, D., 1977. *The Biology of Diatoms*. University of California Press, Berkely and Los Angeles, 498 pp.

1060 Wigdahl, C.R., Saros, J.E., Fritz, S.C., Stone, J.R., Engstrom, D.R., 2014. The influence of basin
1061 morphometry on the regional coherence of patterns of diatom-inferred salinity in lakes of the northern
1062 Great Plains (USA). *Holocene* 24, 603-613. <http://dx.doi.org/10.1177/0959683614523154>

1063 Wolin, J.A., Stone, J.R., 2010. Diatoms as indicators of water-level change in freshwater lakes, in: Smol,
1064 J.P., Stoermer, E.F. (Eds.), *The Diatoms: Applications for the Environmental and Earth Sciences*.
1065 Cambridge University Press, Cambridge, pp. 174-185.

1066 Wood, J.R., Alcover, J.A., Blackburn, T.I.M.M., Bover, P., Duncan, R.P., Hume, J.P., Louys, J., Meijer,
1067 H.J.M., Rando, J.C., Wilmhurst, J.M., 2017. Island extinctions: processes, patterns, and potential for
1068 ecosystem restoration. *Environ. Conserv.* 44, 348–358. <https://doi.org/10.1017/S037689291700039X>

1069 Yamamoto, A., Palter, J.B., 2016. The absence of an Atlantic imprint on the multidecadal
1070 variability of wintertime European temperature. *Nat. Commun.* 7. <http://dx.doi.org/10.1038/ncomms10930>
1071

1072

1073

1074 **Table captions**

1075

1076 **Table 1.** Environmental variables of Lake Azul and Verde, obtained from Pereira *et al.*
1077 (2014) and Gonçalves (2008).

1078 **Table 2.** Radiocarbon and calibrated dates from AZ11 core samples. (*) Used in the
1079 construction of the age model (see explanation in the text).

1080 **Table 3.** Summarized description of diatom assemblage zones from Lake Azul.

1081

1082 **Figure captions**

1083 **Figure 1.** A and B. Location of Azores archipelago and São Miguel island. C. Location of
1084 Sete Cidades crater caldera on São Miguel island with lakes Azul (rectangle) and
1085 Verde on caldera floor. D. Bathymetric map of Lake Azul showing transects A
1086 and B and cores recovered. Coring sites studied in this work (AZ06 and AZ11)
1087 are indicated with red circles.

1088 **Figure 2.** NE-SW cross section of Lake Azul showing lithological units, coring sites, and
1089 main sedimentary subenvironments. Thickness of lacustrine units not to scale.

1090 **Figure 3.-** Updated age-depth model (black line) based on the ^{210}Pb activity-depth profile of
1091 core AZ06 (Gonçalves, 2008) and the AMS ^{14}C dates of core AZ11-02. The
1092 expected age was calculated using linear interpolation and compared with
1093 palynological data studied in the same core (Rull *et al.*, 2017). Plot of the previous
1094 age model (grey line) for core AZ11-02 (Raposeiro *et al.*, 2017; Rull *et al.*, 2017)

1095 is also shown for comparison purposes. Corresponding sedimentary units are
1096 indicated.

1097 **Figure 4.-** Diatom percentage diagram for selected taxa ($\geq 5\%$ abundance in at least one
1098 sample) of Lake Azul cores: AZ11-02 (filled curves) and AZ06 (discontinued lines).
1099 Composite column on the left is based on the biostratigraphical correlation of both
1100 cores (see text). Notice comparison of the *Aulacoseira* spp. and *Psammothidium*
1101 *abundans* f. *rosenstockii*, among other taxa, percent abundance curves used for
1102 stratigraphic correlation of cores AZ11-02 and AZ06. Diatoms are grouped
1103 according to their habitat preferences. Diatom Assemblage Zones generated by a
1104 broken-stick model of the distribution of variance (Bennett, 1996) are represented
1105 by discontinued lines. Main lithological units and sedimentary facies are also
1106 shown.

1107 **Figure 5.-** Principal Component Analysis (PCA) ordination biplot of samples (numbers) and
1108 diatom taxa (acronyms) in Lake Azul. Achmin=*Achnantheidium minutissimum*,
1109 Adlmin=*Adlafia minuscula* var. *muralis*, Astfor=*Asterionella formosa*,
1110 Aulamb=*Aulacoseira ambigua*, Aulgra=*Aulacoseira granulata*, Diswol=*Discostella*
1111 *woltereckii*, Encces=*Encyonopsis* sp. aff. *cesatii*, Eolsp1=*Eolimna* sp1,
1112 Eolsp2=*Eolimna* sp2, Eunimp=*Eunotia implicata*, Fracap=*Fragilaria capucina*,
1113 Fracro=*Fragilaria crotonensis*, Fraten=*Fragilaria tenera* Navnot=*Navicula notha*,
1114 Nitgra=*Nitzschia gracilis*, Nitlac=*Nitzschia lacuum*, Nitper=*Nitzschia perminuta*,
1115 Nitpse=*Nitzschia* spp. aff. *pseudofonticola*, Pladau=*Planothidium dau*, Psaros=
1116 *Psammnothidium abundans* f. *rosenstockii*, Psebre=*Pseudostaurosira brevistriata*,
1117 Pseell=*Pseudostaurosira elliptica*, Rospus=*Rosithidium pusillum*,
1118 Stfexi=*Stauroforma exiguiiformis*, Stamut=*Staurosira mutabilis*, Stapse=*Staurosira*
1119 *pseudoconstruens*, Tabflo=*Tabellaria flocculosa*. Shadings correspond to the two
1120 main groups of samples reflecting differences in trophic status.

1121 **Figure 6.-** Geochemical and diatom proxy data for Lake Azul. Proxies include: percent total
1122 organic carbon (%TOC), TOC mass accumulation rates (MARs), percent total
1123 nitrogen (%TN), TOC/TN (black line) and TOC/TN_{corr} (gray line) ratio (following
1124 Talbot, 2001), carbon and nitrogen isotopes of organic matter ($\delta^{13}\text{C}_{\text{org}}$, $\delta^{15}\text{N}_{\text{org}}$), and
1125 sample scores for axis 1 (PC1) and axis 2 (PC2) of Principal Component Analysis
1126 on the diatom assemblages. All data are plotted against age (cal yr AD).

1127

1128 **Supplementary material captions**

1129 Supplementary material I: Diatom abundance data

1130 Supplementary material II: Bulk organic matter elemental and isotopic composition

1131 Supplementary material III: Synthetic correlation diagram of chironomid biozones
1132 (core AZ11-02; Raposeiro et al., 2017), pollen zones (core AZ11-02; Rull et al.,
1133 2017), and diatom assemblage zones (composite column AZ06+AZ11-02; this
1134 work), showing the preliminary and updated age-depth models.

1135

Highlights

- Trophic history of Lake Azul (Azores archipelago) since 1290 AD
- Atypical long-lasting (650 yr) catastrophic volcanic-induced oligotrophy
- Portuguese colonizers and fish introduction had a minor effect on eutrophication
- Change to meso-eutrophic conditions only after recent human fertilization
- Climate signature on diatom and organic matter records overridden by eruption

25 huge local eruption occurred. This episode drove the evolution of Lake Azul through six
26 distinct phases, commencing with a restart of ecological succession after tephra deposition
27 disrupted biogeochemical cycling. The alteration was so profound that the lake underwent
28 a state of oligotrophic conditions for approx. 650 yr. Nutrients were sourced by fish-induced
29 internal recycling and the overflow of the near Lake Verde during this period, rather than by
30 allochthonous nutrient inputs modulated by climate variability and/or vegetation cover
31 changes in the watershed after the official Portuguese colonization. It was only after recent
32 artificial fertilization when the system overcame the volcanic-induced long-term resilience.
33 This over-fertilization and a reduction in water turnover exacerbated the recent symptoms
34 of eutrophication after 1990 AD. Contrary to other studies, Lake Azul constitutes an
35 uncommon case of long-term resilience to trophic change induced by a cataclysmic volcanic
36 eruption. It brings new insights into the fate of lake ecosystems which might be affected by
37 similar events in the future.

38

39 **Keywords**

40 Eutrophication; oligotrophication; lake ontogeny; invasive species; volcanic eruptions;
41 regime shifts

42

43

44 **1. Introduction**

45 Oceanic islands have been particularly sensitive to the effects of anthropogenic impacts,
46 despite being subjected to relatively recent human colonization extending back to only the
47 last centuries. Human impacts usually have striking effects on their ecosystems because of
48 their isolated location and usually very small sizes. Forest clearance (Cañellas-Boltá et al.,
49 2013), exotic species introduction (Sax and Gaines, 2008) or local species extinctions
50 (Wood et al., 2017) are among the most prominent impacts exerted by human colonization
51 on oceanic islands. But whereas the effects of human colonization on terrestrial landscapes
52 are well known, the impacts exerted on aquatic ecosystems still remain to be more fully
53 understood.

54 The Azores archipelago (Macaronesian biogeographical region) lies in the middle of the
55 North Atlantic Ocean and it was officially colonized by the Portuguese in 1432 AD. Since
56 precolonization times to present, notable landscape changes occurred related to, first, pure
57 extractive activities, and, later, transformation by agricultural and livestock management
58 (Dias, 1996). Palynological paleoenvironmental reconstructions have shown that
59 anthropogenic impact in the Azores largely surpassed natural processes, such as volcanism
60 or climate change, as main drivers of landscape changes (Connor et al., 2012; Rull et al.,
61 2017). Less is known however on the human-driven impacts on the rich mosaic of lake
62 ecosystems of the archipelago. This knowledge is of particular importance since studies
63 have shown that insularity makes lakes from the Macaronesian region to be markedly
64 different to their continental counterparts from an ecological perspective (Hughes and
65 Malmqvist, 2005).

66 In the short-term, water quality deterioration due to cultural eutrophication has been
67 reported in the Azores lakes since the 1980's related to agricultural and farming activities
68 (Gonçalves, 2008; Cruz et al., 2015). Yet, the lack of detailed and regular limnological data

69 before water quality monitoring surveys started in 1992-1993 (Cruz et al., 2015) hinder any
70 evaluation of the response of the Azorean lakes to the long-term cultural eutrophication and
71 its potential causes, not exclusively related to recent artificial fertilization. It is known that
72 changes in the food webs are another mechanism which can profoundly alter the trophic
73 trajectory of any lake ecosystem (Smith, 2003). It is particularly relevant how the abundance
74 and structure of fish communities modify the interactions between zooplankton and
75 phytoplankton. Fishes can promote algal biomass both by predation on zooplankton (top-
76 down control) and by nutrient recycling when their activity at the lake bottom stir up the
77 sediments (bottom-up control) (Scheffer and Van Nes, 2007). This seems to have been the
78 case of the formerly fishless Azorean lakes Furnas and Fogo (São Miguel island), which
79 were not only very sensitive to artificial nutrient loading, but also to trophic web controls after
80 the introduction of detritivorous fishes which promoted eutrophication (Skov et al. 2010;
81 Buchaca et al., 2011). As it has been addressed elsewhere, cultural eutrophication is
82 therefore the result of cumulative actions, distant in time and space, which make it difficult
83 to disentangle past and present causes from the legacy of past anthropogenic activities
84 (Thornton et al., 2013; Le Moal et al., 2019).

85 Besides human direct actions on freshwater ecosystems, it is also necessary to assess
86 the relative importance of natural processes which can also induce increases in productivity,
87 as climate-related or volcanic factors. Volcanism in particular could be a potential significant
88 source of nutrient enrichment in the highly active volcanic Azorean context. Ash deposition
89 after volcanic eruptions can prompt significant phytoplankton growth by nutrient enrichment
90 and attenuation of excessive light intensities (Modenutti et al., 2013), but it can also have
91 the opposite effect interfering with nutrient balances which in turn can strongly reduce
92 productivity (e. g., Barker et al., 2000). Although the amount of volcanic-derived nutrients is
93 at present negligible in terms of changes in trophic state of the Azorean lakes (Cruz et al.,
94 2006), this might not have been the case in the past, when volcanic activity was much more

95 common (Queiroz et al., 2008). Yet, the very short time spans covered by studies in lakes
96 Fogo (approx. 150 yr; Skov et al., 2010) and Furnas (approx. 50 yr; Buchaca et al., 2011)
97 does not allow the determination of the precise role played by tephra deposition in the trophic
98 status of lakes in the archipelago.

99 Finally, any eutrophication effect on a collection of different lake systems, natural- or
100 human-induced, must take into account that each lake has own characteristics which makes
101 it unique regarding resistance, resilience and trajectory (Thornton et al., 2013; Le Moal et
102 al., 2019). For instance, for assessing the effects of exotic fish introductions it is necessary
103 to consider a large array of trophic conditions, since understanding the coupling between
104 zooplankton and phytoplankton is dependent on nutrient levels (Esler and Goldman, 1991).
105 Such array of trophic conditions can be found in lakes of the Azores with studied
106 paleorecords. The mentioned lakes Furnas and Fogo constitute examples of systems with
107 distinct trophic status, eutrophic-hypereutrophic and mesotrophic respectively (Skov et al.,
108 2010; Buchaca et al., 2011). Yet, the paleoenvironmental reconstructions from these lakes
109 do not show periods of extended oligotrophy. By contrast, historical accounts (Barrois, 1896;
110 Bohlin, 1901) and fossil chironomid data (Raposeiro et al., 2017) point to past persistent
111 oligotrophy in Lake Azul (São Miguel island), the largest lake of the Azorean archipelago.
112 This lake constitutes an excellent candidate to understand changes in trophic status due to
113 anthropogenic and natural forcings acting in an insular lotic system from a former
114 oligotrophic condition, particularly as the chironomids (Raposeiro et al., 2017) and pollen
115 (Rull et al., 2017) have been analyzed from the same Lake Azul core.

116 In this study we reconstruct the environmental history of Lake Azul since early human
117 colonization, focussing on its response to both natural (volcanism and climate-related drivers)
118 and anthropogenically-induced perturbations (i. e., changes in land use, exotic species
119 introduction, and over-fertilization). We aim to understand the resilience of Lake Azul to
120 different long-term causes of eutrophication, contrasting it with analogous lake systems in

121 the Azorean archipelago and elsewhere which had a different trophic status in the past or
122 present. Such a study on the long-term combined effects of different types of nutrient loading,
123 biological invasions and natural forcings, a key issue in contemporary ecology (Ellis, 2011),
124 has barely been addressed in insular lake systems and/or those affected by catastrophic
125 volcanism. Understanding the long-term changes in the trophic condition of Lake Azul
126 provide a much better insight into the process of recent eutrophication affecting this lake.

127

128 **2. Geological, climate and limnological settings of Lake Azul**

129 Lake Azul is located in Sete Cidades caldera (37°51'N – 25°46'W), which occupies the
130 westernmost part of São Miguel Island (eastern sector of Azores archipelago) (Fig. 1). Three
131 major eruptive phases, at approximately 36, 29 and 16 kyr BP, conditioned the caldera
132 formation (Queiroz et al., 2008). The subsequent explosive Holocene eruptions formed
133 secondary volcanoes inside the caldera, generating ash and lapilli volcanoclastic deposits
134 (Queiroz et al., 2008). At present, the bottom of some of these secondary volcano craters
135 are occupied by perched lakes. Tephra deposits from Holocene eruptions of secondary
136 volcanoes accumulated both inside and in source areas of the lakes. The most significant
137 and recent eruptive episode which accumulated tephra in lakes of Sete Cidades was the
138 P17 eruption, which occurred in the Caldeira Seca volcano in the last millennium (Queiroz
139 et al., 2008, Shotton and Williams, 1971; Fig. 1) and which consisted in three different
140 phases of lapilli deposition (phases L1, L2 and L3 according to Cole et al., 2008).

141 Lake Azul is located approximately 260 m above sea level (Pereira et al., 2014) and has an
142 irregular bottom topography, resulting from faults affecting the substrate (Queiroz, 1997). It
143 can be divided into three main physiographic zones, from south to north, in an increasing
144 depth gradient (Figs. 1D and 2): (1) a shallow platform or ramp (0 to ~12 m depth), (2) a rise
145 (~12 to ~24 m depth) related to an extensional fault slope, and (3) a deep offshore plain

146 (~24 to 27 m depth). The deep plain receives water and sediments from ephemeral streams
147 located at the north of the inner caldera wall and from a main river forming a delta system
148 at the east, close to the locality of Cerrado das Freiras (Fig. 1). Lake Azul is a part of a more
149 complex lacustrine system inside the Sete Cidades caldera which includes a second large
150 waterbody located at its southern side, Lake Verde, to which it is connected hydrologically
151 by an inundated isthmus. Yet, historical accounts show that the two lakes were separate
152 water bodies in the past, as deduced by descriptions of the 16th century (Frutuoso, 1977) or
153 by the cartographic representation which still shows the two lakes in isolation in 1844 AD
154 (Vidal, 1850). Hydrologic connection occurred in 1877 AD, according to local accounts
155 (Andrade, 2003) and a preserved pictorial engraving (Reclus, 1830-1905). Both lakes
156 together constitute at present the largest lacustrine system in the island. A temperate
157 oceanic climate is characteristic of the archipelago, with mild temperatures, a rainfall regime
158 with a strong seasonal cycle and large interannual variability, high relative air humidity, and
159 frequent strong winds (Hernández et al., 2016). Those conditions are driven by oceanic
160 (strength and position of the Azores Current) and atmospheric (semi-permanent high-
161 pressure Azores Anticyclone) factors (Volkov and Fu, 2010). Thus, when the anticyclone
162 migrates northerly or is weaker, generally during the autumn-winter period, the archipelago
163 may be crossed by the North Atlantic storm tracks resulting in heavy rainfalls over it.
164 Conversely, in the spring-summer period, the strengthened anticyclone blocks the
165 storminess path (Santos et al., 2004). New insights, focused on the large-scale climate
166 variability modes of the North Atlantic, revealed that the North Atlantic Oscillation (NAO) and
167 the Atlantic Multidecadal Oscillation (AMO) exert a strong influence on the Azorean climate
168 variability. Thus, seasonal and interannual variability is mainly due to the NAO influence
169 (Andrade et al., 2008; Cropper and Hanna, 2014; Hernández et al., 2016), but at decadal
170 and longer time scales, the AMO also becomes relevant (Yamamoto and Palter, 2016;
171 Hernández et al., 2017).

172 The main physiographic and limnological variables of Lake Azul and Lake Verde are
173 summarized in Table 1. A generalized process of eutrophication has been observed in Lake
174 Azul since 1987 (Cruz et al., 2015). Primary productivity at present is governed by
175 cyanobacteria and, secondarily, by diatoms and cryptophytes. Diatoms reach maximum
176 abundances during autumn-winter and spring, with *Asterionella formosa* Hassal,
177 *Aulacoseira ambigua* (Grunow) Simonsen, *A. granulata* (Ehrenberg) Simonsen, *Fragilaria*
178 *crotonensis* Kitton, *F. cf. tenera*, *Ulnaria ulna* (Nitzsch) Compère and *U. delicatissima* var.
179 *angustissima* (Grunow) Aboal and P. C. Silva as the main dominant taxa (Gonçalves, 2008;
180 Pereira et al., 2014). At present, hydrophyte communities are mainly composed of invasive
181 species such as *Egeria densa* Planch., *Elodea canadensis* Michaux. and *Nymphaea alba*
182 Linnaeus (Gonçalves et al., 2013). The originally fishless condition of the Azorean lakes was
183 modified in the late 18th century, when different taxa of cyprinids and salmonids were
184 introduced and stocked (Valois-Silva, 1886; Vicente, 1956; Flor de Lima, 1993; Raposeiro
185 et al., 2017).

186

187 **3. Materials and methods**

188 In September 2011, fifteen sediment cores (AZ11) were recovered in Lake Azul (Fig. 1)
189 using a UWITEC[®] corer (Ø 60 mm) installed in a UWITEC[®] platform raft following two
190 transects: SW-NE direction (transect A) and W-E direction (transect B). Cores were split
191 longitudinally into two halves and imaged using a high-resolution digital photographic
192 camera installed in the Avaatec XRF core scanner (University of Barcelona). A detailed
193 description of colors, textures and sedimentary structures was performed. Smear slides
194 were also prepared for cores AZ11-02 (37°52'20.6" N – 25°46'26.1" W), AZ11-03
195 (37°52'21.5" N – 25°46'26.4" W) and AZ11-10 (37°52'33,3" N – 25°46'57,0" W) at 5 cm
196 intervals and examined to define facies and lithostratigraphic units. The cores were

197 correlated using the defined sedimentary facies and key beds.

198 The core AZ11-02 (133 cm long) from transect B, sampled at the deep offshore plain
199 (25.1 m of water depth), was selected as representative of the hemipelagic sedimentation
200 environment and used for the study of diatom assemblages. To ensure that the upper
201 sediments were recovered, we checked diatom analysis on a short gravity core taken in
202 2006 in a location very close to the deep offshore plain of Lake Azul (AZ06 (37°52'16.05" N-
203 25°46'30.68" W), 62 cm long, Fig. 1; Gonçalves, 2008). Because clear comparable changes
204 in diatom relative abundance data occur in both cores, tie-in levels could be defined,
205 especially using the trends in the relative abundances of *Aulacoseira* spp. and
206 *Psammothidium abundans* f. *rosenstockii* (Lange-Bertalot) Bukhtiyarova (see the diatom
207 diagram in the Results section). The resulting stratigraphic correlation allowed the
208 construction of a composite record referred in the text hereafter as the composite column.
209 This correlation showed a lack of correspondence between the diatom assemblages found
210 at the top of cores AZ06 and AZ011-02, allowing us to estimate that the first ~30 cm of AZ11-
211 02 were not recovered in the field.

212 Total carbon (TC), total nitrogen (TN), and isotopic composition of bulk organic matter
213 ($\delta^{13}\text{C}_{\text{org}}$ and $\delta^{15}\text{N}_{\text{org}}$) determinations were performed in core AZ11-02 using a Finnigan delta
214 Plus EA-CF-IRMS spectrometer at Center Científics i Tecnològics of the Universitat de
215 Barcelona (CCiTUB). Previous analyses by X-ray diffraction showed negligible amounts of
216 carbonates in the samples; consequently, TC was considered to be equal to total organic
217 carbon (TOC) (Raposeiro et al., 2017). TOC and TN results are expressed as percent values
218 of the sediment dry weight. The atomic ratio of TOC/TN was calculated and corrected
219 according to Talbot (2001) to discriminate inorganically bound nitrogen content from TN.
220 From here on, the TOC/TN ratio is therefore referred to as $\text{TOC}/\text{TN}_{\text{corr}}$. Fluxes of TOC into
221 the sediments have also been estimated in the form of mass accumulation rate (MAR, mg
222 $\text{cm}^{-2}\text{yr}^{-1}$) by multiplying their concentrations by the sediment dry densities and sedimentation

223 rates at each depth. For the calculation of dry bulk densities, the samples were dried to
224 remove free water. The isotopic composition of sediment organic matter was determined,
225 and isotopic values are reported in the conventional delta-notation in per mil (‰) relative to
226 the Pee Dee Belemnite (PDB) carbon and atmospheric nitrogen (N₂) standards.

227 Diatom analysis was performed following standardized procedures (Renberg, 1990). Slides
228 were mounted with Naphrax[®] mountant, and at least 400 valves per sample were counted
229 at X1000 using a Nikon Eclipse 600 microscope with Nomarski differential interference
230 contrast optics. Identifications of taxa were based on standard sources (e.g., Krammer and
231 Lange-Bertalot, 1986-1991; Lange-Bertalot, 2000-2013), and contrasted with previous
232 studies made on the Azores archipelago (Gonçalves et al., 2010). Taxa were grouped,
233 according to their habitat preferences, as allochthonous (aerophilic) or autochthonous
234 (euplanktonic, facultatively planktonic or tycho planktonic, and benthic). Raw valve counts
235 were converted to percentage abundance data. Statistical analyses were carried out on a
236 diatom relative abundance matrix of those taxa attaining an abundance of more than > 5%
237 in at least one sample. Samples which had sum abundances of allochthonous taxa reaching
238 at least 5% were excluded from the analyses (n = 37). Diatom abundances from the
239 remaining 77 samples were transformed by square-root transformation prior statistical
240 analysis. The definition of the main Diatom Assemblage Zones (DAZs) was performed using
241 stratigraphically constrained cluster analysis based on squared Euclidean dissimilarity
242 (CONISS, Grimm, 1987), as implemented in Psimpoll 4.10 (Bennett, 2002). Zonations with
243 variances that exceeded the values generated by a broken-stick model of the distribution of
244 variance were considered to be statistically significant (Bennett, 1996; Supplementary
245 Material). A detrended correspondence analysis (DCA) was performed to measure the
246 length of the main environmental gradient, which recommended the use of a linear model of
247 ordination (principal component analysis; PCA) to determine the environmental drivers in
248 the composition of the diatom assemblages. Both DCA and PCA were performed with the

249 CANOCO 4.5 software (ter Braak and Smilauer, 1998).

250 A new age-depth model was constructed for the composite column (cores AZ-06 + AZ11-
251 02), updating the previously available model which was restricted to core AZ11-02
252 (Raposeiro et al., 2017; Rull et al., 2017), and taking into account the non-recovery of the
253 upper sediments of this core. This new model is based on linear interpolation of the available
254 ^{210}Pb profile for the AZ06 core (Gonçalves, 2008), the radiocarbon data from the AZ11 cores
255 (Table 2), and several independent tie-in points. All ^{14}C ages were calibrated to calendar
256 years (cal AD) using the CALIB 7.1 software (Stuiver and Reimer, 1993), and the latest
257 INTCAL13 curve (Reimer et al., 2013).

258

259 **4. Results**

260 ***4.1. Lithological units and sedimentary facies***

261 Facies analysis from cores retrieved in 2011 resulted in the definition of eleven facies and
262 eight sedimentary units for the entire basin (Fig. 2; definition also followed by Raposeiro et
263 al., 2011 and Rull et al., 2011). These facies have been differentiated by lithology, texture,
264 color, lamination characteristics, and shards content. Offshore sedimentary facies of the
265 composite column have been grouped in 4 lithological units as follows:

266 Unit 1 (base–132 cm) is composed of gray tephra deposits (ash and lapilli) (Facies VS)
267 from the P17 eruptive episode (Queiroz et al., 2008). These volcanoclastic deposits are
268 usually interbedded by some thin layers of gray lacustrine muds in the deep plain. Cores
269 taken during the 2011 survey indicate that this unit extends to the entire lake bottom area.

270 Unit 2 (132–114 cm) is deposited above Unit 1 in the deep plain and rise zones of the
271 lake. This unit is made up of banded-to-laminated gray muds (Facies E). These deposits

272 were transported to the lake by runoff eroding volcanic ashes deposited in the catchment
273 from the same eruptive episode that deposited Unit 1.

274 Unit 3 (114–90 cm) is recorded above Unit 2 and is mainly composed of
275 greenish/yellowish brown laminated to banded muds (Facies C) deposited by decantation
276 of fine-grained particles forming plumes of the surface and/or subaquatic nepheloid layers
277 in the lake during short-term regular rains. These deposits intercalate some brown mud
278 horizons enriched in shard particles (Facies B) that could be added to the suspended
279 material by ash fallout from minor or distal eruptive episodes. Moreover, this unit intercalates
280 dark brown mud layers rich in terrestrial plant remains, but poor in diatoms (Facies D). The
281 composition and short lateral extent of layers of facies D indicate that they correspond to
282 subaquatic lobes deposited by flood events, likely during heavy rain episodes.

283 Unit 4 (90 cm–top) is deposited above Unit 3 and it is mainly composed of brown massive
284 to poor laminated mud (Facies A) transported and deposited in a process similar to facies
285 C. These muds also intercalate dark brown mud layers rich in terrestrial plant remains
286 corresponding to lobular deposits (Facies D).

287

288 **4.2. Chronology**

289 Available ^{210}Pb data from core AZ06 (Gonçalves, 2008) and non post-bomb radiocarbon
290 ages of the AZ11 cores (table 2, Fig. 3, Supplementary Materials) were used to construct
291 the age-depth model of the composite column which best fitted with events of independently
292 known age. The radiocarbon age at the bottom of the sequence was obtained immediately
293 above the basal tephra, yielding 690 ± 30 yr BP, almost exactly fitting with the age previously
294 estimated for the P17 eruptive episode of 663 ± 105 ^{14}C yr BP (Shotton and Williams, 1971).
295 By contrast, the basal flood layer of Unit 4 yielded a ca. 100 yr difference when dated in

296 cores AZ11-02 (c. 1770 AD) and AZ11-03 (c. 1870 AD) (Fig. 3, Supplementary Materials).
297 Comparison of the estimated and known dates for the first appearances in the pollen record
298 of AZ11-02 (Rull et al., 2017) of the exotic *Cryptomeria japonica* and *Pinus* spp., resulted in
299 a much closer fit of the flood event dated to 1870 AD in core AZ11-03 rather than 1770 AD
300 dated in core AZ11-02 (Fig. 3), so the former was preferred for the final age model.
301 Chronology for the upper sediments is based on the ^{210}Pb data from core AZ06 because of
302 the more reliable use of ^{137}Cs tie-in points (Gonçalves, 2008), instead of using a single post-
303 bomb radiocarbon age of core AZ11-02 (table 2).

304 In conclusion, the new age model therefore differs from the previously published
305 (Raposeiro et al., 2017; Rull et al., 2017) in a) the use of new ^{210}Pb dates of core AZ06 which
306 provide a chronology for the non-recovered history in core AZ11-02, and b) a reassessment
307 of the age of the basal flood event of Unit 4. Comparison of chironomid (Raposeiro et al.,
308 2017), pollen (Rull et al., 2017), and diatom (this work) zones using the old and definite age
309 models is shown in the Supplementary Materials.

310

311 **4.3. Diatom assemblages**

312 Diatom taxa with abundances higher than 5% in at least one sampling level were plotted
313 in stratigraphic order for the composite column (Fig. 4). Except for the lacustrine muds
314 corresponding to the facies VS at the base of the core (Unit 1), benthic diatoms dominated
315 the assemblages from approx. 140 to 40 cm. Above 40 cm planktonic diatoms (mainly
316 *Aulacoseira* spp. and also, higher up, *Asterionella formosa* and *F. crotonensis*) began their
317 dominance. Those levels close to or coincident with flood events (facies D) had a remarkably
318 lower total valve content due to the massive short-term deposition of terrestrial sediments.
319 Furthermore, these levels were characterized by high relative abundances of aerophilic
320 diatoms, mainly from the genera *Diadesmis* and *Diploneis* (Fig. 4), indicating that any

321 lacustrine signal given by the autochthonous taxa would be masked by the effects of both
322 the sedimentary dilution and by the incorporation of allochthonous valves during the flood
323 events. To avoid interferences in the lacustrine signal, data from all the volcanic levels in
324 Unit 1 (base–132 cm), as well as those with high TOC/TN_{corr} values (see geochemical results
325 below) and/or sum abundances of aerophilic diatoms >5%, were excluded from any further
326 statistical analyses.

327 The resulting broken-stick model of the distribution of variance allowed us to identify four
328 statistically significant DAZs (AZU-1 to AZU-4) based on CONISS (Table 3 and Fig. 4). DAZ
329 AZU-2 was also divided into two subzones.

330 DCA results indicated a linear response of the diatom assemblages to the environmental
331 gradients, since the longest gradient was 2.7 SD units (Leps and Smilauer, 2003), and a
332 PCA was therefore performed to interpret the underlying environmental variables explaining
333 the composition of the diatom assemblages.

334 The first two axes of the PCA explained 66.1% of the total variance (Fig. 5). The first axis
335 (PC1, 42.4% of the variance), places benthic diatoms (mostly epipellic and motile), such as
336 *Navicula notha* J. H. Wallace, *Eolimna* sp1, *Nitzschia* spp. aff. *pseudofonticola*, *N. lacuum*
337 Lange-Bertalot or *N. perminuta* (Grunow) M. Peragallo, on the positive side of the plot. The
338 negative side is occupied by some euplanktonic and eutrophic taxa as *A. ambigua*, *F.*
339 *crotonensis* and *Asterionella formosa*. The second axis (PC2, 23.7% of the variance), shows
340 the highest negative values for the euplanktonic. *A. ambigua*, *Asterionella formosa*, and *F.*
341 *crotonensis*, whereas periphytic diatoms, mainly *Stauroforma exiguiiformis* (Lange-Bertalot)
342 R.J. Flower, V.J. Jones & Round, *Encyonopsis* sp. aff. *cesatii*, *Adlafia minuscula* var. *muralis*
343 (Grunow) Lange-Bertalot, *Pseudostaurosira brevistriata* (Grunow) D.M. Williams & Round,
344 *P. abundans* f. *rosenstockii*, and the *Fragilaria capucina* group, exhibit positive scores. The
345 resulting biplot of PC1 vs. PC2 shows three main groups of samples corresponding to the

346 DAZs a) AZU-1, b) AZU-2 and c) AZU-3 + AZU4 (Fig. 5).

347 Variations in the two first principal components through the sedimentary sequence were
348 plotted on the stratigraphic chart (Fig. 6). PC1 shows a progressive decrease from AZU-1
349 to AZU-4, stabilizing at approx. 27 cm until the top of the core. PC2 shows an increasing
350 trend from the immediately post-eruptive phase at approx. 140 cm until 70 cm, decreasing
351 thereafter.

352

353 **4.4. Geochemical proxy data**

354 Very low percentages of TOC and TN characterize Units 1 to 3, with values ranging
355 between 0.18 to 1.13% and 0.05 to 0.12%, respectively (Fig. 6). Both proxies exhibit a net
356 increase in Unit 4 from 90 to 40 cm with values ranging from 0.81 to 3.53% and 0.08 to
357 0.34% for TOC and TN, respectively. TOC MAR oscillate between 0.21 and 14.86 mg C cm⁻²
358 yr⁻¹ from the base to 29 cm, respectively. TOC and TOC MAR exhibit a similar pattern from
359 the base of the core to 64 cm depth.

360 TOC and TN percent values show a high linear correlation ($r = 0.94$, $p < 0.01$), and
361 because of this, the correction suggested by Talbot (2001) was used to discriminate the
362 fraction of TN not attributable to TOC. Thus, the TOC/TN_{corr} atomic ratio allowed us to
363 separate those levels with allochthonous organic matter (Facies D) more efficiently. Facies
364 A, B and C show values of TOC/TN_{corr} between 8 and 13, a range that is typical of organic
365 matter of mixed but mainly lacustrine origin (Meyers and Teranes, 2001). Facies D shows
366 values ranging between 14 and 25, characteristic of the larger influence of C3 land plants,
367 which is consistent with the flood event origin of these sediments.

368 The $\delta^{13}\text{C}_{\text{org}}$ curve shows, in general, an inverse correspondence with the TOC/TN_{corr}
369 curve (Fig. 6). This is more clearly manifested in facies D deposits, where TOC/TN_{corr} values

370 are always higher than 14. Units 1, 2, 3, and the bottom half of Unit 4, when the last flood
371 event was recorded between 69–75 cm, show $\delta^{13}\text{C}_{\text{org}}$ values ranging between -27.5 and -
372 22.5‰. A significant rise is observed between 68 and 40 cm, when values oscillate between
373 -26.4 and -22.4‰. From here to 29 cm, the range shortens from -25.9 to -23.2‰. Despite
374 the lack of correspondence between TOC and $\delta^{13}\text{C}_{\text{org}}$ throughout most of the core, trends
375 exhibited from 68 cm are quite similar, and remarkably decreasing in the uppermost values
376 in both proxies.

377 The $\delta^{15}\text{N}_{\text{org}}$ values range between -0.02‰ and 3.09‰, showing lower values (close to 0)
378 in Facies D terrestrial sediments or levels close to these facies. The lacustrine levels of Units
379 1, 2, 3, and the bottom half of Unit 4 to 68 cm are characterized by oscillating values ranging
380 from 0.21 to 2.84‰. A slight upwards decreasing trend to values close to 0 is recorded
381 towards the top of the core AZ11-02.

382

383 **5. Discussion**

384 **5.1. Environmental gradients explaining diatom assemblage composition**

385 Results of PCA indicate the two main environmental components driving the long-term
386 changes in diatom composition in Lake Azul. The negative scores exhibited along PC1 by
387 the eutrophic and euplanktonic species *A. ambigua*, *F. crotonensis* or *Asterionella formosa*
388 (e. g., Reynolds et al., 2002) versus the high positive values of benthic species such as *N.*
389 *notha*, *N. lacuum* or *N. perminuta*, of predominantly oligotrophic affinities (e. g. Krammer
390 and Lange-Bertalot, 1986-1991), suggest that this main axis is related with a trophic gradient
391 (Fig. 5). The plot of samples on the space defined by the PC1 vs. PC2 (Fig. 5) shows two
392 extremes represented by the oligotrophic conditions and exclusive benthic production of
393 DAZ AZU-1 (1290-1475 AD) vs. the meso- to eutrophy characteristic of the pelagic

394 production of DAZs AZU-3 and AZU-4 (1930-2006 AD).

395 The biplot of PC1 vs. PC2 (Fig. 5) also shows on the positive side of PC2 diatoms
396 performing a large array of life form strategies, ranging from purely euplanktonic (e. g., *A.*
397 *granulata*), tychoplanktonic (e. g., *Pseudostaurosira elliptica* (Schumann) Edlund, Morales
398 and Spaulding, *P. brevistriata*), epiphytic (e. g., *P. abundans* f. *rosenstockii*), to sediment
399 dwelling (e. g. *A. minuscula* var. *muralis*, *E. sp. aff. cesatii*). Most of the positive sample
400 scores correspond to DAZ AZU-2, an assemblage interpreted as related with an increase in
401 the relative extension of shallow littoral vs. deep lacustrine habitats (table 3). By contrast,
402 the negative side of the plot shows diatoms behaving only as euplanktonic (*A. ambigua*, *F.*
403 *crotonensis*, *Asterionella formosa*) or sediment dwelling (*Eolimna* sp1, *N. notha*, *N. lacuum*
404 and *N. perminuta*). PC2 is therefore understood as reflecting a gradient in microhabitat
405 availability, whose maximum would be reached in DAZ AZU-2 (1475-1930 AD).

406

407 **5.2. Main ecological phases in Lake Azul**

408 The multidisciplinary study of the recent sedimentary record of Lake Azul reveals the
409 complex overlapping of natural and anthropogenic forcings that drove the evolution of this
410 system in the last ca. 720 yr. According to the obtained multiproxy information the lake went
411 through six different environmental phases, as described below.

412 **5.2.1 Phase I. Basal zone – Eruptive phase (P-17 eruption)**

413 The recent history of Lake Azul begins with a volcanic catastrophic event indicated by the
414 deposition of a thick tephra layer (facies VS), recorded in Unit 1. This event corresponds to
415 the Caldeira Seca P17 volcano eruption, which accumulated tephra deposits in extensive
416 areas of the Sete Cidades caldera (Cole et al., 2008). Although some exceptional fallout of
417 diatoms transported into the volcanic eruption plume cannot completely be disregarded (Van

418 Eaton et al., 2013), high abundances of the euplanktonic and eutrophic *A. granulata* in
419 muddy lacustrine sediments interbedded between volcanic deposits (facies VS) (Fig. 4) are
420 more easily explained by sedimentation *in situ* around the time of the eruption. They would
421 correspond to the most recent phase of the eruption (phase L3 according to Cole et al.,
422 2008), which would have accumulated 4-20 m of lapilli in the lake's bottom surface. Diatoms
423 of the genus *Aulacoseira* are characteristic of well-mixed waters necessary to maintain their
424 buoyancy and relatively high nutrient conditions (Hall and Smol, 2010). The species *A.*
425 *granulata* is accompanied during this phase by *Nitzschia valdestriata* Aleem and Hustedt, a
426 benthic diatom which has been reported as aerophilic (e.g., Robinson, 2004); thus, its
427 presence in Unit 1 can indicate transport from the emerged zones in the margins to the
428 innermost areas of the lake. The diatom assemblage found in this unit (Fig. 4) would
429 therefore represent the existence of a moderately deep, well mixed, and meso to eutrophic
430 lake, approx. at the time of ash deposition, with a significant contribution of allochthonous
431 materials. This interpretation is reinforced by moderate TOC/TN_{corr} values of approximately
432 15, along with low values of $\delta^{13}\text{C}_{\text{org}}$, which are indicative of isotopically light terrestrial
433 organic matter (Meyers and Teranes, 2001). Whereas the dominance of *Aulacoseira* has
434 been found as typical of the mid-depth zone across lake water-depth gradients elsewhere
435 (e. g. Kingsbury et al., 2012), the study of pollen and non-pollen palynomorphs (NPPs) in
436 Lake Azul suggested shallower water conditions (Rull et al., 2017). This circumstance might
437 imply that the lake was subjected to short-term fluctuations in water levels at this time.

438 The main ecological consequence of the major phase of the P17 volcanic eruption was
439 the replacement of a diatom community that included *A. granulata* and *N. valdestriata* by a
440 new one controlled by benthic attached life forms, mainly *Achnanthydium minutissimum*
441 (Kützing) Czarnecki. Tephra deposition can involve a disruption in the internal recycling of
442 P, which is more significant in lakes with small catchment areas relative to the total lake area
443 (Barker et al., 2000; Telford et al., 2004), such as Lake Azul, with a total lake area of 3.59

444 km² vs. a lake drainage area of 15.35 km² (Fig. 1; table 1). This, plus a significant increase
445 in Si loading associated with the deposition of tephras, would have greatly altered the Si:P
446 ratio, prompting the replacement of the previous diatom communities by new opportunistic
447 species (Kilham et al., 1986). The species *A. minutissimum* has been documented as a
448 pioneering *r*-strategist on disturbed aquatic environments (Peterson, 1992; Stevenson, 1996;
449 Leira et al., 2015) with a strong affinity for waters with a high Si content and usually attaching
450 to unspecific substrates (Stenger-Kovács, 2006). Moreover, this taxon is referred as a good
451 indicator of low organic content in the water column (Potapova, 2007). High abundances of
452 *A. minutissimum* would therefore indicate that, after tephra fallout, the lapilli and ash sterile
453 materials which covered the lake bottom were colonized by a new diatom community that
454 restarted ecological succession. This situation was also accompanied by low values of TOC
455 and TN in the sediments, as well as of TOC MAR, which are maintained in the following
456 phase, suggesting an oligotrophication event.

457 5.2.2. Phase II: Moderately shallow oligotrophic lake (ca. 1290–1480 AD)

458 During this phase, which is coincident with DAZ AZU-1 (125-90 cm), coarse-grained
459 tephra sediments of Unit 1 were replaced by fine-grained muddy sediments from Units 2
460 (Facies E) and 3 (Facies B and C). The reduction in grain size induced a change to an
461 epipellic-dominated diatom assemblage characterized by high abundances of *Eolimna* sp1,
462 together with *Navicula* s. l. and *Nitzschia* spp. (AZU-1, Fig. 4). Extensive growth of epipellic
463 diatom communities after tephra deposition, when the sediment grain-size of the lake bottom
464 surface is adequate, has also been reported elsewhere (e. g., Harper et al., 1986; Telford et
465 al., 2004), indicating the progression of the ecological succession. The referred taxa are
466 also typical of both shallow and mid-depth zones of lakes where light can reach the bottom
467 (Wang et al., 2012). These characteristics, and the minor role of euplanktonic and
468 tychoplanktonic taxa during this phase, would be indicative of a moderately shallow water
469 environment (Wolin and Stone, 2010), which according to the pollen and NPPs-based water

470 level reconstruction (Rull et al., 2017) should be below 15 m. Maximum PC1 values are
471 recorded during this phase, suggesting that oligotrophic conditions were maintained over
472 the approximately 200 yr of this phase, according also with the low values of TOC and TOC
473 MAR. Maximum percent abundances of *Nitzschia* spp. are also recorded during this phase,
474 almost disappearing thereafter. This genus is reported to be good at growing at low P supply
475 (Kilham et al., 1986), and many species are facultative or obligate nitrogen heterotrophs
476 (Werner, 1977; Kilham et al., 1986). This observation suggests that although tephra
477 deposition inhibited complete P recycling the lake was probably not N-limited.

478

479 5.2.3. Phase III: Deep oligotrophic lake (ca. 1480-1870 AD)

480 The most significant feature of this phase, corresponding to sedimentation of the lower
481 part of Unit 4 (DAZ AZU-2a, 90-75 cm), is the flooding of the platform ramp associated with
482 a water level increase, which allowed a large relative increase in littoral vs. pelagic
483 environments (Fig. 1). Chronostratigraphical, historical and diatom data support this
484 hypothesis. The stratigraphical chart shows the first appearance of lacustrine sediments in
485 the ramp environment radiocarbon dated in core AZ11-07 to ca. 1545 AD (Fig. 2). This
486 position is located at approximately 500 m from the limit between the ramp and the slope
487 (Fig. 2), pointing to an earlier flooding of the ramp. According to the available chronicles of
488 Gaspar Frutuoso (1522-1591), the lake had, at the time, a maximum depth of 7–8 fathoms
489 (Frutuoso, 1977), that would equal ~15–17 m. The lake bathymetric map shows an extensive
490 area of the ramp that would be subaereally exposed (Fig. 1), and this agrees with the
491 description of a large “beach” made up of “sterile sands” (Frutuoso, 1977). Flooding of the
492 ramp brought a sharp change in the diatom communities. Fragilarioid taxa (mainly *P.*
493 *brevistriata* and *P. elliptica*) became clearly dominant (DAZ AZU-2a, Fig. 4). These taxa are
494 early colonizers characteristic of the shallow-water littoral zone of a wide variety of water

495 bodies under conditions of environmental instability (Reed et al., 1999). Although their
496 appearance in Lake Azul could be related to a deeper water column due to their
497 tychoplanktonic character, increased availability of shallow littoral habitats when the flooding
498 occurred was probably a decisive contributing factor for their expansion (Stone and Fritz,
499 2004; Wigdhal et al., 2014). Their rise is also coincident with the increase of *Myriophyllum*
500 *alterniflorum* (Rull et al., 2017), a submerged macrophyte characterized by a high number
501 of thin leaves that largely increase the colonizable area for periphytic microalgae (Cattaneo
502 and Kalff, 1980). A complex permanent periphytic community was therefore established in
503 the lake littoral zone for the first time. (Fig. 6). Compared to Phase II, when both oligotrophy
504 and a steeper lake bottom resulted in a low diversification of the diatom assemblages, the
505 flooding of the platform ramp in Phase III resulted in an increased area of benthic vs.
506 planktonic habitats. As a result, life-form strategies adopted by diatoms diversified in Phase
507 III, as indicated by the high recorded values of PC2.

508 Both regular flood events from the lake catchment and the effects of deforestation during
509 this period (Rull et al., 2017), probably also brought episodic high nutrient concentrations
510 that allowed the short-term growth of eutrophic euplanktonic diatoms (*A. ambigua* and *A.*
511 *granulata*), which appear for the first time since the reset of the lake after the P17 volcanic
512 episode. Both the increase in the TOC/TN ratio and negative excursions of $\delta^{13}\text{C}_{\text{org}}$,
513 associated with the floods, point to a significant delivery of terrestrial organic matter to the
514 lake (Meyers and Teranes, 2001). The *Nitzschia* spp. sharp decline during this phase
515 suggests that this increased nutrient availability altered the dynamics of the P and N cycles
516 within the lake, decreasing the N:P ratio. Although TOC and TOC MAR values increased
517 compared to the previous phase, they still remained low, suggesting that oligotrophic
518 conditions persisted during this stage, as indicated also by the high values of PC1.

519

520 5.2.4. Phase IV: Deep oligotrophic lake and transition to a new trophic state (ca. 1870–
521 1940 AD)

522 During the sedimentation of mid-to-upper part of Unit 4 (DAZ AZU-2b, 75-41 cm), TOC
523 and TN follow the steady uprising trend since the ecological reset after the Caldeira Seca
524 P17 eruption, which suggests an increase in productivity. Most of the organic matter
525 produced has an algal origin, according to the TOC/TN_{corr} values (Meyers and Teranes,
526 2001). Moreover, the still low values of TOC and TOC MAR, suggests that the water column,
527 despite the increase in productivity, remained oligotrophic. This would be in accordance with
528 the large light availability at the time (19th century), indicated by the high abundances of the
529 charophytes *Chara fragilis* Desvaux and *Nitella tenuissima* (Desvaux) Kützing (Trelease,
530 1897; Cunha, 1939), the presence of the typical oligotrophic chrysophycean *Dinobryon*
531 *sertularia* Ehrenberg (Barrois, 1896), and the recorded high abundances of desmids (Bohlin,
532 1901).

533 Despite the lake still being oligotrophic, the proxy data suggest that during this phase, a
534 long-lasting ecological change commenced, indicated by heavier $\delta^{13}\text{C}_{\text{org}}$ values and the
535 reduction in TOC/TN_{corr} associated with a lesser flood events occurrence, with the exception
536 of the ca. 1870 AD event recorded at the start of this phase. Additionally, the
537 correspondence found during this phase between the TOC and $\delta^{13}\text{C}_{\text{org}}$ curves, which up to
538 this time were uncoupled, points to a change in carbon fractionation compared to the
539 previous phases. This change co-occurs with the remarkable landscape reconfiguration due
540 to the massive introduction of the exotic arboreal taxa *C. japonica* and *Pinus* spp. in the
541 catchment after 1850 AD (Rull et al., 2017). Restricted delivery of terrestrial organic matter
542 to the lake due to the increase in tree cover in the catchment would induce heavier $\delta^{13}\text{C}_{\text{org}}$
543 values and a reduction in the TOC/TN_{corr} ratio (Meyers and Teranes, 2001).

544 However, not only a more restricted delivery of terrestrial organic matter to the lake could

545 induce heavier $\delta^{13}\text{C}_{\text{org}}$ values but also the increase of in-lake productivity (Meyers and
546 Teranes, 2001), which is also indicated by the net rise in TOC values (Fig. 6) and by the
547 regular presence of the euplanktonic and meso- to eutrophic diatoms of the genus
548 *Aulacoseira* (Fig. 4). The necessary nutrient enrichment that triggered this increase in
549 productivity and the presence of *Aulacoseira* could not be due to the delivery of materials
550 from the catchment, as indicated by the decrease in the TOC/TN_{corr} ratio. Two alternative
551 mechanisms can be invoked to explain nutrient enrichment. First, fish introductions which
552 started in the late 18th century in this formerly fishless lake could intensify internal nutrient
553 release in the lake, especially the stockings of cyprinids, such as Goldfish *Carassius auratus*
554 Linnaeus introduced in 1792 AD (Valois-Silva, 1886), and Carp *Cyprinus carpio carpio*
555 Linnaeus, introduced in 1890 (Vicente, 1956). Their feeding activity is known to have a
556 strong effect on the release of nutrients to the water by sediment resuspension (e.g.,
557 Richardson et al., 1995). This concentration effect was probably enhanced by the
558 development at this time of an oxygen-depleted deep hypolimnion on a seasonal basis,
559 according to the chironomid data (Raposeiro et al., 2017), which would highly enrich the
560 bottom waters with P (Cohen, 2003). The primary role that internal nutrient recycling induced
561 by fish stockings could have played is in accordance with the known fact that the major
562 driver of eutrophication in this lake is, at present, internal P-loading (Cruz et al., 2015). A
563 second mechanism could be nutrient injection from Lake Verde overflow which probably
564 increased total nutrient concentration in Lake Azul after the connection between the two
565 lakes in 1877 AD (Andrade, 2003).

566 The multiproxy data suggest a long-term gradual process of eutrophication to a new trophic
567 state during this phase, mainly induced by sediment disturbance after fish introductions and
568 nutrient inputs from Lake Verde overflow after its connection in 1877 AD.

569 *5.2.5. Phase V: Deep mesotrophic lake (ca. 1940–1995 AD)*

570 In the upper part of Unit 4 (DAZ AZU-3, 41-11 cm), all proxies reveal a major and sudden
571 change in the ecosystem. From ca. 1940 to 1995 AD, there is a sharp shift in the diatom
572 assemblages, which now become dominated by the euplanktonic and eutrophic *A. ambigua*
573 (AZU-3, Fig. 4). Although tychoplanktonic diatoms subdominate the assemblages, benthic
574 taxa significantly decrease. Lighter values of $\delta^{13}\text{C}_{\text{org}}$, not related with flood events, also
575 support the hypothesis of a larger pelagic production compared to the previous phase, since
576 periphyton is usually enriched in ^{13}C compared to phytoplankton due to a higher CO_2
577 limitation of primary producers in the littoral zone (France, 1995). In addition, organic carbon
578 MARs attain maximum values, indicating increased productivity. The lack of correspondence
579 between the TOC MAR and TOC, which decrease during this phase, reflects the increased
580 relative importance of biogenic silica in the sediments associated with larger biosiliceous
581 productivity. The excess of nutrient loads from intensive fertilization and livestock manure,
582 especially since the 1960s (Gonçalves, 2008; Cruz et al., 2015), constitutes the main factor
583 responsible for the detected environmental change. They not only led to increased
584 eutrophication, but probably also prompted the shift from a benthic to pelagic-dominated
585 environment because of the shading effect of phytoplankton over benthic algae also
586 recorded in other Azorean lakes (Buchaca et al., 2011). This change is accompanied by the
587 significant decline in *Myriophyllum alterniflorum*, which already started in the previous phase
588 (Rull et al., 2017), a macrophyte sensitive to eutrophication and turbidity (Kohler and Labus,
589 1983).

590 5.2.6. Phase VI: Deep meso-eutrophic stratified lake (ca. 1995–2006 AD)

591 Although dominant pelagic production still characterizes this phase recognized at the
592 uppermost part of Unit 4 (DAZ AZU-4, 11-0 cm), there is an important reduction in *A.*
593 *ambigua*, which now co-dominates the diatom assemblages with *Asterionella formosa* and
594 *Fragilaria cf. tenera*. There is also a peak of the euplanktonic *F. crotonensis* during this
595 phase. This assemblage of *A. ambigua*, *Asterionella formosa* and *F. crotonensis* has been

596 reported elsewhere as typical of eutrophic light-limited conditions (Reynolds et al., 2002;
597 Saros and Anderson, 2015). Both *Asterionella formosa* and *F. crotonensis* have similar
598 resource requirements (Hobbs et al., 2011), being indicative of modest eutrophication by P
599 enrichment in temperate lakes (Saros et al., 2005). Changes in the TN:TP ratios can explain
600 the shifts in the diatom assemblages and the recent dominance of cyanobacteria in the lake
601 (Gonçalves, 2008; Cruz et al., 2015), but the response of phytoplankton communities to
602 changes in water chemistry are many times site-specific (e.g., Saros et al., 2005). Moreover,
603 both P and N enrichment have been demonstrated to favor the development of
604 cyanobacterial blooms in Lake Azul (Cruz et al., 2015). Alternatively, changes in thermal
605 structure rather than changes in stoichiometric ratios can be behind significant shifts in the
606 composition of phytoplankton in modern lakes (Mantzouki et al., 2018). Enhanced water
607 column stratification associated with warmer temperatures could explain the decline in
608 heavy diatom taxa such as *Aulacoseira*, which need well-mixed waters to thrive (Margalef,
609 1978). Water stratification would favor the development of *F. crotonensis* (Wolin and Stone,
610 2010), and the known dominance of cyanobacteria in the phytoplankton over diatoms for 10
611 months a year (Gonçalves, 2008) would put very fast-growing species such as *Asterionella*
612 *formosa* in the advantage (Reynolds, 2006). The data suggest that eutrophication increased
613 during this phase, transforming lake's condition into a meso-eutrophic state, and that
614 changes in the TN:TP ratio and/or enhanced stratification due to temperature increase were
615 the main factors responsible of this change.

616

617 **5.3. Main long-term drivers of trophic status changes**

618 Paleoenvironmental reconstruction of Lake Azul for the approx. last 700 yr allowed the
619 identification of different potential natural (volcanism and climate) and human-induced
620 drivers of change in its trophic status: a) eruptive volcanism, b) external nutrient loads from

621 the watershed, c) changes in morphometry associated to lake-level rise, d) bottom-up and
622 top-down trophic controls, e) changes in the water column mixing regime, and f) artificial
623 fertilization derived from agricultural and farming activities.

624 The recorded ca. 700 yr history of Lake Azul begins with the extreme Caldeira Seca P17
625 volcanic eruption of ca. 1290 AD (phase I) whose ashes deposited with a diatom
626 assemblage of meso to eutrophic affinities. Although this sin-eruptive process makes
627 unclear the existence of a pre-eruptive meso to eutrophic lake, the post-eruptive record
628 shows the abrupt replacement of this diatom assemblage by another characteristic of
629 oligotrophic conditions. This sharp shift in the diatom assemblages in Lake Azul points to a
630 likely reset of the lake ecosystem due to the sedimentation of thick tephra deposits. This
631 oligotrophication mediated by P limitation resembles that of Lake Massoko (Tanzania)
632 following the deposition of a few centimeters-thick tephra (Barker et al., 2000). Although the
633 magnitude of this event would be insignificant compared to the sedimentation of the several-
634 meters-thick tephra layer P17 in Lake Azul, both cases seem to have experienced a similar
635 process. Contrary to enhanced productivity after tephra deposition found elsewhere (e. g.
636 Modenutti et al., 2013), the catastrophic nature of the Caldeira Seca P17 eruption implied
637 settling of new pioneering biological communities which restarted ecological succession.
638 The dominant benthic algal community also played a prominent role in maintaining
639 oligotrophy in the following 200 yr (1290-1480 AD, phase II), irrespective of several flood
640 episodes (Facies D) that could potentially intensify allochthonous nutrient inputs. Despite
641 their similar requirements, planktonic algae obtain nutrients exclusively from water, while
642 periphytic algae, typical of the shallow water conditions during this period, can assimilate
643 nutrients from both water and the sediment pool (Hansson, 1992). The dominance of
644 periphytic communities during this phase would therefore have prevented the release of
645 nutrients to support euplanktonic diatoms, maintaining oligotrophy in the lake, more severe
646 in the pelagic environment. Moreover, the enhanced precipitation regime in São Miguel

647 Island for this period (Hernández et al., 2017) and the probable denudation of the watershed
648 by the eruption, which would favor large nutrient inputs to the lake, had no effect on aquatic
649 primary productivity at the studied temporal resolution.

650 The period 1480-1870 AD (phase III) encompasses the extractive and transformative
651 phases of human colonization which implied extensive deforestation in the archipelago
652 (Connor et al., 2012; Rull et al., 2017). Despite geochemical and diatom data which indicate
653 persistent allochthonous inputs due to forest clearance in the watershed, during approx. 400
654 yr the lake did not significantly alter its oligotrophic condition. Although precipitation events
655 might have contributed to very short-term flood events (Facies D, Figs. 3, 4 and 5), nutrient
656 delivery was not sufficient for a sustained development of the eutrophic *Aulacoseira* spp.
657 flora, which needs a more constant concentration of nutrients in the water column, as
658 reported by Hall and Smol (2010). It was also during this period when a net water level rise,
659 following regional more humid conditions (Hernández et al. 2017), flooded the platform ramp
660 (Fig. 2), increasing the area of the epilimnion sediments with respect to the total volume of
661 the epilimnion. Under these circumstances, recirculation of nutrients from the sediments to
662 the epilimnion should be increased (Fee, 1979), prompting eutrophication. Yet, this
663 ultimately natural eutrophication process did not significantly move Lake Azul from its
664 oligotrophic condition during 400 yr, acting at a much slower pace compared to meso- to
665 eutrophic paleo-lake systems, where significant changes in the area of the epilimnion
666 sediments with respect to the total volume of the epilimnion also occurred (e.g., Bao et al.,
667 2015). Oligotrophy was therefore maintained irrespective of the combined effect of man-
668 induced allochthonous nutrient inputs associated to deforestation and the natural infilling
669 with water which could have brought a situation of morphometric eutrophy as described by
670 Rawson (1955).

671 Another morphometric threshold would be represented by the connection between Lake
672 Azul and Lake Verde in 1877 AD, which is probably contemporary with the flood event of

673 1870 AD. It can be hypothesized that the much smaller water volume in Lake Verde would
674 have favored higher nutrient concentrations, as at present (table 1), and that connection of
675 both lakes could induce a significant nutrient transfer to Lake Azul. Exotic species
676 introduction in the lake is another factor which could have prompted any significant change
677 in trophic conditions via top-down and bottom-up controls of the food web (McQueen et al.,
678 1989). Data from Lake Azul indicate that the increase in productivity during the period 1870-
679 1940 AD (phase IV), coincident with local drier and colder conditions (Hernández et al., 2017)
680 that would diminish the delivery of nutrients from the catchment, as it is also indicated by
681 the TOC/TN data, was likely due to both nutrient delivery from Lake Verde after connection
682 took place and by internal nutrient recycling. Fish disturbance action favoring sediment
683 resuspension was the most probable cause for the latter. Additionally, grazing activity by
684 planktivore fishes, such as carp, imply an intensification of predation pressure on
685 zooplankton, whose reduction, besides the mentioned intensified nutrient release from the
686 bottom, results in increased phytoplankton biomass and productivity (Vanni, 2002). But
687 these bottom-up (by sediment resuspension) and top-down (predation over zooplankton)
688 effects by fish activity, as well as nutrient load from Lake Verde, had a quite limited action in
689 Lake Azul. Compared to the major role that fish introductions had on the long-term pelagic
690 nutrient enrichment of other Azorean lakes (Skov et al., 2010; Buchaca et al., 2011), the
691 effects in Lake Azul were quite attenuated. Paleoenvironmental data from Lake Azul suggest
692 that both fish introductions and Lake Verde overflow induced a gradual process of
693 transformation, instead of a sudden non-linear ecological change ascribable to an ecological
694 regime shift, as described by Lees et al. (2006). The oligotrophic inertia of the system was
695 maintained for another 70 yr because, either nutrient delivery from Lake Verde was low, or
696 fish introduction did not induce enough return of P from the sediments. This is in accordance
697 with the suggestion that in oligotrophic lakes productivity is more limited by nutrient supply
698 rather than by changes in trophic interactions (Schindler et al., 2001). It is not possible from

699 our data to disentangle the relative importance of increased nutrient inputs from Lake Verde
700 versus enhanced nutrient recycling by fish activity in this gradual process of eutrophication.

701 The most significant trophic event since the likely reset of the P17 eruption (ca. 1290 AD)
702 occurred after 1940 AD to the present (phases V and VI), when the oligotrophic inertia of
703 the lake was interrupted. The observed changes, mainly the sudden maximum increase of
704 euplanktonic eutrophic diatoms, the reduction of hydrophytes in the recent pollen record
705 (Rull et al., 2017), and, more recently, the dominance of cyanobacteria in the lake
706 (Gonçalves, 2008; Cruz et al., 2015), indicate that the present-day status as a meso-
707 eutrophic lake was reached during this period. Although eutrophication due to increased
708 artificial nutrient input from the watershed was the main responsible for this major
709 environmental change, other intervening factors need also be considered. It cannot be
710 completely disregarded that part of the N enrichment influencing present-day phytoplankton
711 composition in Lake Azul had an atmospheric origin (sensu Elser et al., 2009), but this is
712 difficult to disentangle from the confounding effect of N loading from the catchment by
713 human activities (as reported by Catalan et al., 2013). Likewise, increased thermal
714 stratification could explain the shifts in phytoplankton composition, such as the decline in
715 *Aulacoseira* species (e.g., Rühland et al., 2008), and the concurrent increase of other
716 components, such as cyanobacteria (e.g., Mantzouki et al., 2018). The synergetic effect of,
717 first, excess nutrient load and, second, reduced water turnover, could be behind the
718 exacerbation of the symptoms of eutrophication (Jeppesen et al., 2014; Le Moal et al., 2019).
719 This can be the reason why, despite some remediation measures such as surface runoff
720 diversion, both monitoring (Cruz et al., 2015) and the paleolimnological (this study) data
721 show that the lake is not experiencing at present a significant change in its trophic status.

722 Our results indicate that cataclysmic volcanism was the main driver in configuring Lake
723 Azul ecology in the last ca. 700 yr. Previous studies on the long-term effects of deposition
724 of thin distal tephra on biological communities have shown that these are usually short-lived

725 (100-150 yr, Telford et al., 2004). Recovery can sometimes be very rapid, such as the case
726 of oligotrophic Lake Galletué (Chile) after the deposition of a few cm thick tephra in 1957
727 AD which took just approx. 5 yr (Cruces et al., 2006) or the meso to eutrophic Lake Holzmaar
728 (Germany) which lasted 10-20 yr maximum after the deposition of approx. 8 cm thick tephra
729 (Lotter et al., 1995). Even catastrophic eruptions such as that of Mt. St. Helene (United
730 States) in 1980 AD, which brought the virtual elimination of algae population in Lake Spirit,
731 implied the quasi-recovery to the pre-eruptive conditions of this oligotrophic lake in approx.
732 30 yr (Larson et al., 2006; Gawel et al., 2018). Although it has been hypothesized that the
733 long-term disruption of lake ecosystems can occur when biogeochemical cycling is
734 interrupted after catastrophic volcanic events (Telford et al., 2004), few examples have been
735 demonstrated in the literature (e. g., Barker et al., 2000). Lake Azul constitutes an example
736 of such a disruption and of the gradual reestablishment of its pre-eruptive meso to eutrophic
737 condition throughout 650 yr only after artificial fertilization accelerated this process in the
738 last decades.

739 A consequence of this primary role of volcanism as a driver in the ecological trajectory of
740 Lake Azul is the potential ability or not of its diatom and bulk organic matter content to
741 reconstruct paleoclimates in the region. Comparison with the paleoclimate data obtained
742 from Lake Empadadas, located just 6 km away in São Miguel island (Hernández et al., 2017),
743 shows the minor role of changes in nutrient delivery associated to precipitation variability in
744 changing the trophic status in Lake Azul. Besides noteworthy differences in the size and
745 morphometric characteristics of both basins which make Lake Empadadas more sensitive
746 to any subtle precipitation regime change, the effects of the P17 eruption were irrelevant in
747 this lake compared to Lake Azul. Contrary to the effects of the deposition of thin tephra
748 layers which do not override the long-term changes due to climate change (e. g., Lotter et
749 al., 1995; Telford et al., 2004; Egan et al., 2019), any climatic signature on productivity in
750 Lake Azul has been largely obscured by the massive tephra deposition of 1290 AD. Any

751 paleoclimatic reconstruction based on the study of the diatom and bulk organic matter
752 records in Lake Azul would therefore be largely biased by the overprinting of the volcanic
753 signature after the cataclysmic eruptive episode of 1290 AD, so using alternative proxy data
754 should consequently be preferred instead.

755

756 **6. Conclusions**

757 Artificial fertilization and, secondarily, fish stockings and connectivity with Lake Verde,
758 were the main factors responsible of changes in trophic status in Lake Azul. A vast eruptive
759 episode which implied the deposition of several meters of tephra in the lake ca. 1290 AD
760 determined a state of oligotrophic inertia during approx. 650 yr. Since this event the lake
761 experienced a net long-term increase in productivity, but showed a high resilience to change
762 from an oligotrophic to a mesotrophic condition, the latter only being achieved when artificial
763 fertilization and livestock manure practices were intensively implemented in the island in the
764 period 1940-1995 AD. Bottom-up and top-down food web controls by fish stocking in this
765 formerly fishless lake, which started in the 18th century, or nutrient injection from Lake Verde
766 overflow in the late 19th century, had a secondary role in lake's trophism. Compared to the
767 mesotrophic Lake Fogo and the eutrophic Furnas, Lake Azul did not significantly change its
768 trophic condition, confirming that the volcanic-induced oligotrophy of the lake, and not
769 trophic interactions, was the main factor explaining the trophic status of the lake during most
770 of its recent history. Other processes, such as natural morphometric eutrophy, or increased
771 delivery of nutrients due to man-induced deforestation and climate variability had a negligible
772 role in reverting the oligotrophic inertia of the lake. By contrast, despite several interventions
773 to avoid the excess nutrient load which drove recent eutrophication, more persistent water
774 stratification seem to maintain or even exacerbate the effects of eutrophication. Lake Azul
775 constitutes an uncommon case in the literature of complete ecosystem restructuring and

776 long-term resilience to trophic change induced by a catastrophic volcanic eruption.

777

778 **Acknowledgments**

779 This research was funded by the Spanish Ministry of Economy and Competitiveness
780 projects PaleoNAO, RapidNAO and PaleoModes (CGL2010-15767, CGL2013-40608-R and
781 CGL2016-75281-C2, respectively) and by the Fundação para a Ciência e Tecnologia
782 (PTDC/CTA-AMB/28511/2017). David Vázquez-Loureiro, Armand Hernández, María Jesús
783 Rubio and Pedro Raposeiro benefited with grants from the Xunta de Galicia (I2C
784 Programme co-funded with the European Social Fund), Generalitat de Catalunya (Beatriu
785 de Pinós - Marie Curie cofund programme), Spanish Ministry of Economy and
786 Competitiveness (Programa de Formación de Personal Investigador, FPI), and Fundação
787 para a Ciência e Tecnologia (SFRH/BPD/99461/2014), respectively. We thank Olga
788 Margalef and Guiomar Sánchez-López for field assistance.

789

790 **References**

- 791 Andrade, C., Trigo, R.M., Freitas, M.C., Gallego, M.C., Borges, P., Ramos, A.M., 2008. Comparing historic
792 records of storm frequency and the North Atlantic Oscillation (NAO) chronology for the Azores region.
793 *Holocene* 18, 745-754.
- 794 Andrade, J. (2003). *Concelho de Ponta Delgada: 500 anos de história : cronologia de figuras e factos, 1499-*
795 *1999*. [Ponta Delgada, Azores]: Câmara Municipal, 648 pp.
- 796 Bao, R., Hernández, A., Sáez, A., Giral, S., Prego, R., Pueyo, J.J., Moreno, A., Valero-Garcés, B.L., 2015.
797 Climatic and lacustrine morphometric controls of diatom paleoproductivity in a tropical Andean lake.
798 *Quaternary Sci.Rev.* 129, 96-110. <http://dx.doi.org/10.1016/j.quascirev.2015.09.019>
- 799 Barker, P., Telford, R., Merdaci, O., Williamson, D., Taieb, M., Vincens, A., Gibert, E., 2000. The sensitivity
800 of a Tanzanian crater lake to catastrophic tephra input and four millennia of climate change. *Holocene*
801 10(3), 303 – 310. <http://dx.doi.org/10.1191/095968300672848582>

802 Barrois, T., 1896. Recherches sur la faune des eaux douces des Açores. Mémoires de la Société des
803 Sciences de l'Agriculture et des Artes de Lille, Série V, Fasc. 6. Société des Sciences de l'Agriculture et
804 des Artes de Lille, Paris.

805 Bennett, K.D., 1996. Determination of the number of zones in a biostratigraphical sequence. *New Phytol.*
806 132, 155-170. <http://dx.doi.org/10.1111/j.1469-8137.1996.tb04521.x>

807 Bennett, K.D., 2002. Documentation for Psimpoll 4.10 and Pscomb 1.03, C Programs for Plotting Pollen
808 Diagrams and Analysing Pollen Data. Uppsala University.

809 Bohlin, K., 1901. Étude sur la flore algologique d'eau douce des Açores. *Bihang till Kongl. Svenska*
810 *Vetenskaps-Akademiens* 27, 1-85.

811 Buchaca, T., Skov, T., Amsinck, S., Gonçalves, V., Azevedo, J., Andersen, T., Jeppesen, E., 2011. Rapid
812 Ecological Shift Following Piscivorous Fish Introduction to Increasingly Eutrophic and Warmer Lake
813 Furnas (Azores Archipelago, Portugal): A Paleoecological Approach. *Ecosystems* 1–20.
814 <https://doi.org/10.1007/s10021-011-9423-0>

815 Cañellas-Boltá, N., Rull, V., Sáez, A., Margalef, O., Bao, R., Pla-Rabes, S., Blaauw, M., Valero-Garcés, B.,
816 Giral, S., 2013. Vegetation changes and human settlement of Easter Island during the last millennia: a
817 multiproxy study of the Lake Raraku sediments. *Quaternary Sci. Rev.* 72, 36–48.
818 <http://dx.doi.org/10.1016/j.quascirev.2013.04.004>

819 Catalan, J., Pla-Rabés, S., Wolfe, A., Smol, J., Rühland, K., Anderson, N.J., Kopáček, J., Stuchlík, E.,
820 Schmidt, R., Koinig, K., Camarero, L., Flower, R., Heiri, O., Kamenik, C., Korhola, A., Leavitt, P.,
821 Psenner, R., Renberg, I., 2013. Global change revealed by palaeolimnological records from remote
822 lakes: a review. *J. Paleolimnol.* 49, 513-535. <https://doi.org/10.1007/s10933-013-9681-2>

823 Cattaneo, A., Kalff J., 1980. The relative contribution of aquatic macrophytes and their epiphytes to the
824 production of macrophyte beds. *Limnol. Oceanogr.* 25(2), 280-289.
825 <http://dx.doi.org/10.4319/lo.1980.25.2.0280>

826 Cohen, A.S., 2003. *Paleolimnology*. Oxford University Press, Oxford.

827 Cole, P.D., Pacheco, J.M., Gunasekera, R., Queiroz, G., Gonçalves, P., Gaspar, J.L., 2008. Contrasting
828 styles of explosive eruption at Sete Cidades, São Miguel, Azores, in the last 5000 years: Hazard
829 implications from modelling. *J. Volcanol. Geoth. Res.* 178 (3), 574-591.
830 <http://dx.doi.org/10.1016/j.jvolgeores.2008.01.008>

831 Connor, S.E., van Leeuwen, J.F.N., Rittenour, T.M., van der Knaap, W.O., Ammann, B., Björck, S., 2012.
832 The ecological impact of oceanic island colonization – a palaeoecological perspective from the Azores.
833 *J. Biogeogr.* 39, 1007–1023. <https://doi.org/10.1111/j.1365-2699.2011.02671.x>

834 Cropper, T.E., Hanna, E., 2014. An analysis of the climate of Macaronesia, 1865–2012. *Int. J. Climatol.* 34,
835 604–622. <http://dx.doi.org/10.1002/joc.3710>

836 Cruces, F., Urrutia, R., Parra, O., Araneda, A., Treutler, H., Bertrand, S., Fagel, N., Torres, L., Barra, R.,
837 Chirinos, L., 2006. Changes in diatom assemblages in an Andean lake in response to a recent volcanic
838 event. *Arch. für Hydrobiol.* 165, 23–35.

839 Cruz, J.V., Pacheco, D., Porteiro, J., Cymbron, R., Mendes, S., Malcata, A., Andrade, C., 2015. Sete
840 Cidades and Furnas lake eutrophication (São Miguel, Azores): Analysis of long-term monitoring data
841 and remediation measures. *Sci. Total Environ.* 520, 168-186.
842 <http://dx.doi.org/10.1016/j.scitotenv.2015.03.052>

843 Cunha, A. G. 1939. Sur la flore charologique des îles Açoréennes. *Bulletin de la Société Portugaise des*
844 *Sciences Naturelles* , 13 (13): 67-70

845 Dias, E., 2007. Açores e Madeira: A Floresta das Ilhas. Fundação Luso Americana, Lisboa.

846 Egan, J., Allott, T.E.H., Blackford, J.J., 2019. Diatom-inferred aquatic impacts of the mid-Holocene eruption
847 of Mount Mazama, Oregon, USA. *Quat. Res.* 91, 163–178. <https://doi.org/10.1017/qua.2018.73>

848 Ellis, B.K., Stanford, J.A., Goodman, D., Stafford, C.P., Gustafson, D.L., Beauchamp, D.A., Chess, D.W.,
849 Craft, J.A., Deleray, M.A., Hansen, B.S., 2011. Long-term effects of a trophic cascade in a large lake
850 ecosystem. *Proc. Natl. Acad. Sci.*, 108: 1070-1075. <https://doi.org/10.1073/pnas.1013006108>

851 Elser, J.J., Andersen, T., Baron, J.S., Bergstrom, A.-K., Jansson, M., Kyle, M., Nydick, K.R., Steger, L.,
852 Hessen, D.O., 2009. Shifts in Lake N:P Stoichiometry and Nutrient Limitation Driven by Atmospheric
853 Nitrogen Deposition. *Science* 326, 835-837. <http://dx.doi.org/10.1126/science.1176199>

854 Elser, J.J., Goldman, C.R., 1991. Zooplankton effects on phytoplankton in lakes of contrasting trophic status.
855 *Limnol. Oceanogr.* 36, 64–90. <https://doi.org/10.4319/lo.1991.36.1.0064>

856 Fee, E.J., 1979. A relation between lake morphometry and primary productivity and its use in interpreting
857 whole-lake eutrophication experiments. *Limnol. Oceanogr.* 24(3), 401-416.
858 <http://dx.doi.org/10.4319/lo.1979.24.3.0401>

859 Flor de Lima, H.M.Q., 1993. Contribuição para o estudo ictiológico das lagoas das Furnas e Sete Cidades.
860 *Estudos, Experimentação e Divulgação.* p. 99., Ponta Delgada.

861 France, R.L., 1995. Differentiation between littoral and pelagic food webs in lakes using stable carbon
862 isotopes. *Limnol. Oceanogr.* 40, 1310-1313. <http://dx.doi.org/10.4319/lo.1995.40.7.131>

863 Frutuoso, G., 1977. Livro Quarto das Saudades da Terra. Instituto Cultural de Ponta Delgada, Ponta Delgada,
864 1593 pp.

865 Gawel, J.E., Crisafulli, C.M., Miller, R., 2018. The New Spirit Lake: Changes to Hydrology, Nutrient Cycling,

866 and Biological Productivity, in: Crisafulli, C.M., Dale, V.H. (Eds.), *Ecological Responses at Mount St.*
867 *Helens: Revisited 35 Years after the 1980 Eruption*. Springer New York, New York, NY, pp. 71–95.
868 https://doi.org/10.1007/978-1-4939-7451-1_4

869 Gonçalves, V., 2008. *Contribuição para o estudo da qualidade ecológica das lagoas dos Açores.*
870 *Fitoplâncton e diatomáceas bentónicas*. PhD. Dissertation, Universidade dos Açores, Ponta Delgada,
871 343 pp.

872 Gonçalves, V., Marques, H., Fonseca, A., 2010. *Lista das Diatomáceas (Bacillariophyta)*, in: Borges, P.A.V.,
873 Bried, J., Costa, A., Cunha, R., Gabriel, R., Gonçalves, V., Martins, A.F., Melo, I., Parente, M.,
874 Raposeiro, P., Rodrigues, P., Santos, R.S., Silva, L., Vieira, P., Vieira, V. (Eds.), *Listagem dos*
875 *Organismos Terrestres e Marinhos dos Açores*. Príncipeia, Cascais, pp. 81-97.

876 Gonçalves V., Costa A.C., Raposeiro P.M., Marques H.S., Cunha A., Ramos J., Cruz A.M., Pereira C.L.,
877 Vilaverde J., 2013. *Monitorização das Massas de Água Interiores da Região Hidrográfica Açores.*
878 *Relatório Anual de 2012 (R5/2012)*. CIBIO Açores, Departamento de Biologia, Universidade dos
879 Açores, Ponta Delgada, 261 pp.

880 Grimm, E.C., 1987. CONISS: a Fortran 77 program for stratigraphically constrained cluster analysis by the
881 method of incremental sum of squares. *Comput. Geosci.* 13, 13-35. [http://dx.doi.org/10.1016/0098-](http://dx.doi.org/10.1016/0098-3004(87)90022-7)
882 [3004\(87\)90022-7](http://dx.doi.org/10.1016/0098-3004(87)90022-7)

883 Hall, R.I., Smol, J.P., 2010. Diatoms as indicators of lake eutrophication, in: Smol, J.P., Stoermer, E.F.
884 (Eds.), *The Diatoms: Applications for the Environmental and Earth Sciences*. Cambridge University
885 Press, Cambridge, pp. 122-151.

886 Harper, M.A., Howorth, R., McLeod, M., 1986. Late Holocene diatoms in Lake Poukawa: Effects of airfall
887 tephra and changes in depth. *New Zeal. J. Mar. Fres.* 20(1), 107-118.
888 <http://dx.doi.org/10.1080/00288330.1986.9516135>

889 Hansson, L. A., 1992. Factors regulating periphytic algal biomass. *Limnol. Oceanogr.* 37(2), 322-328.
890 <http://dx.doi.org/10.4319/lo.1992.37.2.0322>

891 Hernández, A., Kutiel, H., Trigo, R.M., Valente, M.A., Sigró, J., Cropper, T., Santo, F.E., 2016. New Azores
892 archipelago daily precipitation dataset and its links with large-scale modes of climate variability. *Int. J.*
893 *Climatol.* 36, 4439-4454. <http://dx.doi.org/10.1002/joc.4642>

894 Hernández, A., Sáez, A., Bao, R., Raposeiro, P.M., Trigo, R.M., Doolittle, S., Masqué, P., Rull, V.,
895 Gonçalves, V., Vázquez-Loureiro, D., Rubio-Inglés, M.J., Sánchez-López, G., Giral, S., 2017. The
896 influences of the AMO and NAO on the sedimentary infill in an Azores Archipelago lake since ca. 1350
897 CE. *Global Planet. Change* 154, 61-74. <https://doi.org/10.1016/j.gloplacha.2017.05.007>

898 Hobbs, W.O., Fritz, S.C., Stone, J.R., Donovan, J.J., Grimm, E.C., Almendinger, J.E., 2011. Environmental
899 history of a closed-basin lake in the US Great Plains: Diatom response to variations in groundwater flow
900 regimes over the last 8500 cal. yr BP. *Holocene* 21, 1203-1216.
901 <https://doi.org/10.1177/0959683611405242>

902 Hughes, S.J., Malmqvist, B., 2005. Atlantic Island freshwater ecosystems: challenges and considerations
903 following the EU Water Framework Directive. *Hydrobiologia* 544, 289–297.
904 <https://doi.org/10.1007/s10750-005-1695-y>

905 Jeppesen, E., Meerhoff, M., Davidson, T., Trolle, D., Søndergaard, M., Lauridsen, T., Beklioglu, M., Brucet,
906 S., Volta, P., González-Bergonzoni, I., Nielsen, A., 2014. Climate change impacts on lakes: An
907 integrated ecological perspective based on a multi-faceted approach, with special focus on shallow
908 lakes. *J. Limnol.* 73, 88–111. <https://doi.org/10.4081/jlimnol.2014.844>

909 Kilham P., Kilham S.S., Hecky R.E., 1986. Hypothesized resource relationships among African planktonic
910 diatoms. *Limnol. Oceanogr.* 6: 1169-181. <http://dx.doi.org/10.4319/lo.1986.31.6.1169>

911 Kingsbury, M. V, Laird, K.R., Cumming, B.F., 2012. Consistent patterns in diatom assemblages and diversity
912 measures across water-depth gradients from eight Boreal lakes from north-western Ontario (Canada).
913 *Freshw. Biol.* 57, 1151–1165. <https://doi.org/10.1111/j.1365-2427.2012.02781.x>

914 Kohler, A., Labus, B.C., 1983. Eutrophication processes and pollution of freshwater ecosystems including
915 waste heat, in: Lange, O.L., Nobel, P.S., Osmond, C.B., Ziegler, H. (Eds.), *Physiological plant ecology*
916 *IV. Ecosystem processes: mineral cycling, productivity and man's influence.* Springer, Berlin, pp. 413-
917 464.

918 Krammer, K., Lange-Bertalot, H., 1986-1991. *Bacillariophyceae. Volumes 1-4*, in: Ettl, H., Gerloff, J., Heynig,
919 H., Mollenhauer, D. (Eds.), *Süßwasserflora von Mitteleuropa.* Fischer-Verlag, Stuttgart.

920 Lange-Bertalot, H., 2000-2013. *Diatoms of the European Inland Waters and Comparable Habitats. Volumes*
921 *1-7.* A. R. G. Gantner Verlag, Ruggell, Liechtenstein.

922 Larson, D.W., Sweet, J., Petersen, R.R., Crisafulli, C.M., 2006. Posteruption Response of Phytoplankton and
923 Zooplankton Communities in Spirit Lake, Mount St. Helens, Washington. *Lake Reserv. Manag.* 22, 273–
924 292. <https://doi.org/10.1080/07438140609354362>

925 Le Moal, M., Gascuel-Oudou, C., Ménesguen, A., Souchon, Y., Étrillard, C., Levain, A., Moatar, F., Pannard,
926 A., Souchu, P., Lefebvre, A., Pinay, G., 2019. Eutrophication: A new wine in an old bottle?. *Sci. Total*
927 *Environ.* 651, 1–11. <https://doi.org/10.1016/j.scitotenv.2018.09.139>

928 Lees, K., Pitois, S., Scott, C., Frid, C., Mackinson, S., 2006. Characterizing regime shifts in the marine
929 environment. *Fish Fish.* 7, 104-127. <https://doi.org/10.1111/j.1467-2979.2006.00215.x>

930 Leira, M., Filippi, M.L., Cantonati, M., 2015. Diatom community response to extreme water-level fluctuations
931 in two Alpine lakes: a core case study. *J. Paleolimnol.* 53, 289-307. [http://dx.doi.org/10.1007/s10933-](http://dx.doi.org/10.1007/s10933-015-9825-7)
932 [015-9825-7](http://dx.doi.org/10.1007/s10933-015-9825-7)

933 Leps, J., Smilauer, P., 2003. *Multivariate analysis of ecological data using CANOCO*. Cambridge University
934 Press, Cambridge, 268 pp.

935 Lotter, A.F., Birks, H.J.B., Zolitschka, B., 1995. Late-glacial pollen and diatom changes in response to two
936 different environmental perturbations: volcanic eruption and Younger Dryas cooling. *J. Paleolimnol.* 14,
937 23–47.

938 Mantzouki, E., Lürling, M., Fastner, J., de Senerpont Domis, L., Wilk-Woźniak, E., et al., 2018. Temperature
939 Effects Explain Continental Scale Distribution of Cyanobacterial Toxins. *Toxins (Basel)*. 10, e156.

940 Margalef, R., 1978. Life forms of phytoplankton as survival alternatives in an unstable environment. *Oceanol.*
941 *Acta* 1(4), 493-509.

942 McQueen, D.J., Johannes, M.R.S., Post, J.R., Stewart, T.J., Lean, D.R.S., 1989. Bottom-Up and Top-Down
943 Impacts on Freshwater Pelagic Community Structure. *Ecol. Monogr.* 59, 289–309.
944 <https://doi.org/10.2307/1942603>

945 Meyers, P.A., Teranes, J.L., 2001. Sediment organic matter, in: Smol, J.P., Birks, H.J.B., Last, W.M. (Eds.),
946 *Tracking Environmental Change Using Lake Sediments. Volume 2: Physical and Geochemical Methods*.
947 Kluwer Academic Publishers, Dordrecht, pp. 239-269.

948 Modenutti, B.E., Balseiro, E.G., Elser, J.J., Navarro, M.B., Cuassolo, F., Laspoumaderes, C., Souza, M.S.,
949 Villanueva, V.D., 2013. Effect of volcanic eruption on nutrients, light, and phytoplankton in oligotrophic
950 lakes. *Limnol. Oceanogr.* 58, 1165–1175. <https://doi.org/10.4319/lo.2013.58.4.1165>

951 Pereira, C.L., Raposeiro, P.M., Costa, A.C., Bao, R., Giralto, S., Gonçalves, V., 2014. Biogeography and lake
952 morphometry drive diatom and chironomid assemblages' composition in lacustrine surface sediments of
953 oceanic islands. *Hydrobiologia* 730, 93-112. <http://dx.doi.org/10.1007/s10750-014-1824-6>

954 Peterson, C., Stevenson, R., 1992. Resistance and resilience of lotic algal communities: Importance of
955 disturbance timing and current. *Ecology* 73(4), 1445-1461. <http://dx.doi.org/10.2307/1940689>

956 Potapova, M., Hamilton, P.B., 2007. Morphological and ecological variation within the *Achnanthisidium*
957 *minutissimum* (Bacillariophyceae) species complex. *J. Phycol.* 43, 561-575.

958 Queiroz, G. 1997. *Vulcao das Sete Cidades (S. Miguel, Açores). Historia eruptiva e Avaliação do Hazrd.*
959 PhD Thesis. Azores University, 226 pp.

960 Queiroz, G., Pacheco, J.M., Gaspar, J.L., Aspinall, W.P., Guest, J.E., Ferreira, T., 2008. The last 5000 years
961 of activity at Sete Cidades volcano (São Miguel Island, Azores): Implications for hazard assessment. *J.*

962 Volcanol. Geoth. Res. 178: 562-573. <http://dx.doi.org/10.1016/j.jvolgeores.2008.03.001>

963 Raposeiro, P.M., Rubio, M.J., González, A., Hernández, A., Sánchez-López, G., Vázquez-Loureiro, D., Rull,
964 V., Bao, R., Costa, A.C., Gonçalves, V., Sáez, A., Giralt, S., 2017. Impact of the historical introduction of
965 exotic fishes on the chironomid community of Lake Azul (Azores Islands). *Palaeogeogr. Palaeocl.* 466,
966 77-88. <http://dx.doi.org/10.1016/j.palaeo.2016.11.015>

967 Rawson, D.S., 1955. Morphometry as a dominant factor in the productivity of large lakes. *Int. Vereinigung*
968 *fuer Theor. und Angew. Limnol. Verhandlungen* 12, 164–175.

969 Reclus, E., 1830-1905. *Africa and its inhabitants*. Volume 2. J. S. Virtue, London.

970 Reed, J., Roberts, N., Leng, M., 1999. An evaluation of the diatom response to Late Quaternary
971 environmental change in two lakes in the Konya Basin, Turkey, by comparison with stable isotope data.
972 *Quat. Sci. Rev.* 18, 631-646. [http://dx.doi.org/10.1016/S0277-3791\(98\)00101-2](http://dx.doi.org/10.1016/S0277-3791(98)00101-2)

973 Reimer, P.J., Bard, E., Bayliss, A., Beck, J.W., Blackwell, P.G., Ramsey, C.B., Buck, C.E., Cheng, H.,
974 Edwards, R.L., Friedrich, M., Grootes, P.M., Guilderson, T.P., Hafliðason, H., Hajdas, I., Hatté, C.,
975 Heaton, T.J., Hoffmann, D.L., Hogg, A.G., Hughen, K.A., Kaiser, K.F., Kromer, B., Manning, S.W., Niu,
976 M., Reimer, R.W., Richards, D.A., Scott, E.M., Southon, J.R., Staff, R.A., Turney, C.S.M., van der Plicht,
977 J., 2016. IntCal13 and Marine13 Radiocarbon Age Calibration Curves 0–50,000 Years cal BP.
978 *Radiocarbon* 55, 1869-1887. http://dx.doi.org/10.2458/azu_js_rc.55.16947

979 Renberg, I., 1990. A procedure for preparing large sets of diatom slides from sediment cores. *J. Paleolimnol.*
980 4, 87-90. <http://dx.doi.org/10.1007/BF00208301>

981 Reynolds, C.S., 2006. *The Ecology of Phytoplankton*. Cambridge University Press, Cambridge.

982 Reynolds, C.S., Huszar, V., Kruk, C., Naselli-Flores, L., Melo, S., 2002. Towards a functional classification of
983 the freshwater phytoplankton. *J. Plankton Res.* 24, 417-428. <https://doi.org/10.1093/plankt/24.5.417>

984 Richardson, M.J., Whoriskey, F.G., Roy, L.H., 1995. Turbidity generation and biological impacts of an exotic
985 fish *Carassius auratus*, introduced into shallow seasonally anoxic ponds. *J. Fish Biol.* 47:576–585.
986 <http://dx.doi.org/10.1111/j.1095-8649.1995.tb01924.x>

987 Robinson, M., 2004. A Late glacial and Holocene diatom record from Clettnadal, Shetland Islands, northern
988 Scotland. *J. Paleolimnol.* 31, 295-319. <http://dx.doi.org/10.1023/B:JOPL.0000021716.49552.da>

989 Rühland, K., Paterson, A.M., Smol, J.P., 2008. Hemispheric-scale patterns of climate-related shifts in
990 planktonic diatoms from North American and European lakes. *Glob. Change Biol.* 14, 2740-2754.
991 <http://dx.doi.org/10.1111/j.1365-2486.2008.01670.x>

992 Rull, V., Lara, A., Rubio-Inglés, M.J., Giralt, S., Gonçalves, V., Raposeiro, P., Hernández, A., Sánchez-
993 López, G., Vázquez-Loureiro, D., Bao, R., Masqué, P., Sáez, A., 2017. Vegetation and landscape

994 dynamics under natural and anthropogenic forcing on the Azores Islands: A 700-year pollen record from
995 the São Miguel Island. *Quat. Sci. Rev.* 159, 155-168. <https://doi.org/10.1016/j.quascirev.2017.01.021>

996 Santos, F.D., Valente, M.A., Miranda, P.M.A., Aguiar, A., Azevedo, E.B., Tome, A.R., Coelho, F., 2004.
997 Climate change scenarios in the Azores and Madeira Islands. *World Resour. Rev.* 16, 473–491.

998 Saros, J.E., Anderson, N.J., 2015. The ecology of the planktonic diatom *Cyclotella* and its implications for
999 global environmental change studies. *Biol. Rev.* 90, 522-541. <http://dx.doi.org/10.1111/brv.12120>

1000 Saros, J.E., Michel, T.J., Interlandi, S.J., Wolfe, A.P., 2005. Resource requirements of *Asterionella formosa*
1001 and *Fragilaria crotonensis* in oligotrophic alpine lakes: implications for recent phytoplankton community
1002 reorganizations. *Can. J. Fish. Aquat. Sci.* 62, 1681-1689. <https://doi.org/10.1139/f05-077>

1003 Sax, D.F., Gaines, S.D., 2008. Species invasions and extinction: The future of native biodiversity on islands.
1004 *Proc. Natl. Acad. Sci.* 105, 11490–11497. <https://doi.org/10.1073/pnas.0802290105>

1005 Scheffer, M., van Nes, E., 2007. Shallow lakes theory revisited: various alternative regimes driven by climate,
1006 nutrients, depth and lake size. *Hydrobiologia* 584, 455–466. <https://doi.org/10.1007/s10750-007-0616-7>

1007 Schindler, E.D., Knapp, A.R., Leavitt, R.P., 2001. Alteration of nutrient cycles and algal production resulting
1008 from fish introductions into mountain lakes. *Ecosystems* 4, 308-321. [http://dx.doi.org/10.1007/s10021-](http://dx.doi.org/10.1007/s10021-001-0013-4)
1009 [001-0013-4](http://dx.doi.org/10.1007/s10021-001-0013-4)

1010 Shotton, F.W., Williams, R.E.G., 1971. Birmingham University Radiocarbon dates V. *Radiocarbon* 11, 141-
1011 156. <https://doi.org/10.1017/S0033822200008419>

1012 Skov, T., Buchaca, T., Amsinck, S., Landkildehus, F., Odgaard, B., Azevedo, J., Gonçalves, V., Raposeiro,
1013 P., Andersen, T., Jeppesen, E., 2010. Using invertebrate remains and pigments in the sediment to infer
1014 changes in trophic structure after fish introduction in Lake Fogo: a crater lake in the Azores.
1015 *Hydrobiologia* 654, 13-25. <http://dx.doi.org/10.1007/s10750-010-0325-5>

1016 Stenger-Kovács, C., Padisák, J., Bíró, P., 2006. Temporal variability of *Achnanthydium minutissimum*
1017 (Kützing) Czarnecki and its relationships to chemical and hydrological features of the Torna-stream,
1018 Hungary. Program, abstracts & extended abstracts: 6th International Symposium on Use of Algae for
1019 monitoring Rivers. Magyar Algológiai Társaság, Göd, pp. 133-138. ISBN 963 06 0497 3

1020 Stevenson, R.J., Bothwell, M.L., Lowe, R.L., 1996. *Algal Ecology*. Academic Press, San Diego, p. 759.

1021 Stone, J.R., Fritz, S.C., 2004. Three-dimensional modeling of lacustrine diatom habitat areas: Improving
1022 paleolimnological interpretation of planktic : benthic ratios. *Limnol. Oceanogr.* 49, 1540-1548.
1023 <http://dx.doi.org/10.1371/journal.pone.0108936>

1024 Stuiver, M., Reimer, P.J., 1993. Extended ¹⁴C data base and revised CALIB 3.0 ¹⁴C age calibration
1025 program. *Radiocarbon* 35, 215-230. <https://doi.org/10.1017/S0033822200013904>

1026 Talbot, M.R., 2001. Nitrogen isotopes in paleolimnology, in: Smol, J.P., Birks, H.J.B., Last, W.M. (Eds.),
1027 Tracking Environmental Change Using Lake Sediments. Volume 2: Physical and Geochemical Methods.
1028 Kluwer Academic Publishers, Dordrecht, pp. 401-439.

1029 Telford, R.J., Barker, P., Metcalfe, S.E., Newton, A., 2004. Lacustrine responses to tephra deposition:
1030 examples from Mexico. *Quat. Sci. Rev.* 23, 2337-2353.
1031 <http://dx.doi.org/10.1016/j.quascirev.2004.03.014>

1032 ter Braak, C.J.F., Smilauer, P., 1998. CANOCO Reference Manual and User's Guide to CANOCO for
1033 Windows: Software for Canonical Community Ordination (Version 4). Microcomputer Power, Ithaca,
1034 New York.

1035 Thornton, J.A., Harding, W.R., Dent, M., Hart, R.C., Lin, H., Rast, C.L., Rast, W., Ryding, S.-O., Slawski,
1036 T.M., 2013. Eutrophication as a 'wicked' problem. *Lakes Reserv. Sci. Policy Manag. Sustain. Use* 18,
1037 298–316. <https://doi.org/10.1111/lre.12044>

1038 Trelease, W., 1897. Botanical Observations on the Azores. *Missouri Bot. Gard. Annu. Rep.* 1897, 77–220.
1039 <https://doi.org/10.2307/2992160>

1040 Valois-Silva, F., 1886. Descrição das águas minerais das Furnas na ilha de São Miguel, *Archivo dos Açores*.
1041 Vol. 8. Typografia do arquivo dos Açores. (Ponta Delgada). pp. 437–446.

1042 Van Eaton, A.R., Harper, M.A., Wilson, C.J.N., 2013. High-flying diatoms: Widespread dispersal of
1043 microorganisms in an explosive volcanic eruption. *Geology* 41, 1187-1190.
1044 <http://dx.doi.org/10.1130/G34829.1>

1045 Vanni, M., 2002. Nutrient Cycling by Animals in Freshwater Ecosystems. *Annu. Rev. Ecol. Syst.* 33, 341-370.
1046 <http://dx.doi.org/10.1146/annurev.ecolsys.33.010802.150519>

1047 Vicente, A., 1956. Introdução de peixes de água doce nas lagoas de S. Miguel. *Açoreana* 5.

1048 Vidal, A.T.E., Hydrographic Office, R.U., Walker, J.& C.C.N.-C.C. 166 A.. C.C. 166 A., 1850. San Miguel.
1049 Hydrographic Office, London.

1050 Volkov, D.L., Fu, L.-L., 2010. On the reasons for the formation and variability of the
1051 Azores current. *J. Phys. Oceanogr.* 40, 2197–2220. [http://dx.doi.org/10.1175/](http://dx.doi.org/10.1175/2010JPO4326.1)
1052 [2010JPO4326.1](http://dx.doi.org/10.1175/2010JPO4326.1).

1053 Wang, Q., Yang, X., Hamilton, P., Zhang, E., 2012. Linking spatial distributions of sediment diatom
1054 assemblages with hydrological depth profiles in a plateau deep-water lake system of subtropical China.
1055 *Fottea* 12, 59-73. <http://dx.doi.org/10.5507/fot.2012.005>

1056 Werner, D., 1977. *The Biology of Diatoms*. University of California Press, Berkely and Los Angeles, 498 pp.

1057 Wigdahl, C.R., Saros, J.E., Fritz, S.C., Stone, J.R., Engstrom, D.R., 2014. The influence of basin

1058 morphometry on the regional coherence of patterns of diatom-inferred salinity in lakes of the northern
1059 Great Plains (USA). *Holocene* 24, 603-613. <http://dx.doi.org/10.1177/0959683614523154>

1060 Wolin, J.A., Stone, J.R., 2010. Diatoms as indicators of water-level change in freshwater lakes, in: Smol,
1061 J.P., Stoermer, E.F. (Eds.), *The Diatoms: Applications for the Environmental and Earth Sciences*.
1062 Cambridge University Press, Cambridge, pp. 174-185.

1063 Wood, J.R., Alcover, J.A., Blackburn, T.I.M.M., Bover, P., Duncan, R.P., Hume, J.P., Louys, J., Meijer,
1064 H.J.M., Rando, J.C., Wilmhurst, J.M., 2017. Island extinctions: processes, patterns, and potential for
1065 ecosystem restoration. *Environ. Conserv.* 44, 348–358. <https://doi.org/10.1017/S037689291700039X>

1066 Yamamoto, A., Palter, J.B., 2016. The absence of an Atlantic imprint on the multidecadal
1067 variability of wintertime European temperature. *Nat. Commun.* 7. <http://dx.doi.org/10.1038/ncomms10930>

1068

1069

1070

1071 **Table captions**

1072

1073 **Table 1.** Environmental variables of Lake Azul and Verde, obtained from Pereira *et al.*
1074 (2014) and Gonçalves (2008).

1075 **Table 2.** Radiocarbon and calibrated dates from AZ11 core samples. (*) Used in the
1076 construction of the age model (see explanation in the text).

1077 **Table 3.** Summarized description of diatom assemblage zones from Lake Azul.

1078

1079 **Figure captions**

1080 **Figure 1.** A and B. Location of Azores archipelago and São Miguel island. C. Location of
1081 Sete Cidades crater caldera on São Miguel island with lakes Azul (rectangle) and
1082 Verde on caldera floor. D. Bathymetric map of Lake Azul showing transects A
1083 and B and cores recovered. Coring sites studied in this work (AZ06 and AZ11)
1084 are indicated with red circles.

1085 **Figure 2.** NE-SW cross section of Lake Azul showing lithological units, coring sites, and
1086 main sedimentary subenvironments. Thickness of lacustrine units not to scale.

1087 **Figure 3.-** Updated age-depth model (black line) based on the ^{210}Pb activity-depth profile of
1088 core AZ06 (Gonçalves, 2008) and the AMS ^{14}C dates of core AZ11-02. The
1089 expected age was calculated using linear interpolation and compared with
1090 palynological data studied in the same core (Rull *et al.*, 2017). Plot of the previous
1091 age model (grey line) for core AZ11-02 (Raposeiro *et al.*, 2017; Rull *et al.*, 2017)

1092 is also shown for comparison purposes. Corresponding sedimentary units are
1093 indicated.

1094 **Figure 4.-** Diatom percentage diagram for selected taxa ($\geq 5\%$ abundance in at least one
1095 sample) of Lake Azul cores: AZ11-02 (filled curves) and AZ06 (discontinued lines).
1096 Composite column on the left is based on the biostratigraphical correlation of both
1097 cores (see text). Notice comparison of the *Aulacoseira* spp. and *Psammothidium*
1098 *abundans* f. *rosenstockii*, among other taxa, percent abundance curves used for
1099 stratigraphic correlation of cores AZ11-02 and AZ06. Diatoms are grouped
1100 according to their habitat preferences. Diatom Assemblage Zones generated by a
1101 broken-stick model of the distribution of variance (Bennett, 1996) are represented
1102 by discontinued lines. Main lithological units and sedimentary facies are also
1103 shown.

1104 **Figure 5.-** Principal Component Analysis (PCA) ordination biplot of samples (numbers) and
1105 diatom taxa (acronyms) in Lake Azul. Achmin=*Achnantheidium minutissimum*,
1106 Adlmin=*Adlafia minuscula* var. *muralis*, Astfor=*Asterionella formosa*,
1107 Aulamb=*Aulacoseira ambigua*, Aulgra=*Aulacoseira granulata*, Diswol=*Discostella*
1108 *woltereckii*, Encces=*Encyonopsis* sp. aff. *cesatii*, Eolsp1=*Eolimna* sp1,
1109 Eolsp2=*Eolimna* sp2, Eunimp=*Eunotia implicata*, Fracap=*Fragilaria capucina*,
1110 Fracro=*Fragilaria crotonensis*, Fraten=*Fragilaria tenera* Navnot=*Navicula notha*,
1111 Nitgra=*Nitzschia gracilis*, Nitlac=*Nitzschia lacuum*, Nitper=*Nitzschia perminuta*,
1112 Nitpse=*Nitzschia* spp. aff. *pseudofonticola*, Pladau=*Planothidium dau*i, Psaros=
1113 *Psammnothidium abundans* f. *rosenstockii*, Psebre=*Pseudostaurosira brevistriata*,
1114 Pseell=*Pseudostaurosira elliptica*, Rospus=*Rosithidium pusillum*,
1115 Stfexi=*Stauroforma exiguiiformis*, Stamut=*Staurosira mutabilis*, Stapse=*Staurosira*
1116 *pseudoconstruens*, Tabflo=*Tabellaria flocculosa*. Shadings correspond to the two
1117 main groups of samples reflecting differences in trophic status.

1118 **Figure 6.-** Geochemical and diatom proxy data for Lake Azul. Proxies include: percent total
1119 organic carbon (%TOC), TOC mass accumulation rates (MARs), percent total
1120 nitrogen (%TN), TOC/TN (black line) and TOC/TN_{corr} (gray line) ratio (following
1121 Talbot, 2001), carbon and nitrogen isotopes of organic matter ($\delta^{13}\text{C}_{\text{org}}$, $\delta^{15}\text{N}_{\text{org}}$), and
1122 sample scores for axis 1 (PC1) and axis 2 (PC2) of Principal Component Analysis
1123 on the diatom assemblages. All data are plotted against age (cal yr AD).

1124

1125 **Supplementary material captions**

1126 Supplementary material I: Diatom abundance data

1127 Supplementary material II: Bulk organic matter elemental and isotopic composition

1128 Supplementary material III: Synthetic correlation diagram of chironomid biozones
1129 (core AZ11-02; Raposeiro et al., 2017), pollen zones (core AZ11-02; Rull et al.,
1130 2017), and diatom assemblage zones (composite column AZ06+AZ11-02; this
1131 work), showing the preliminary and updated age-depth models.

1132

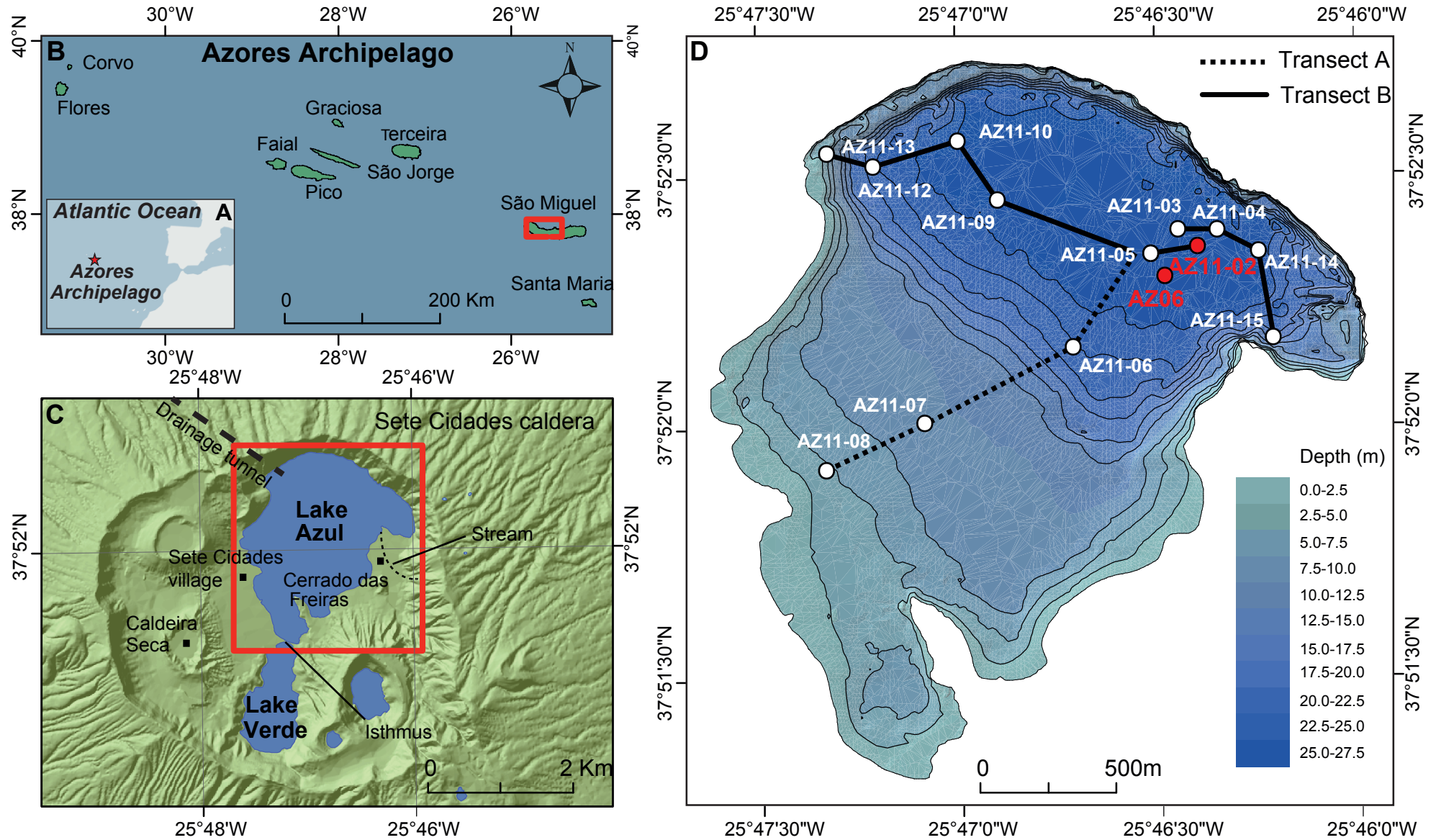


Figure 1

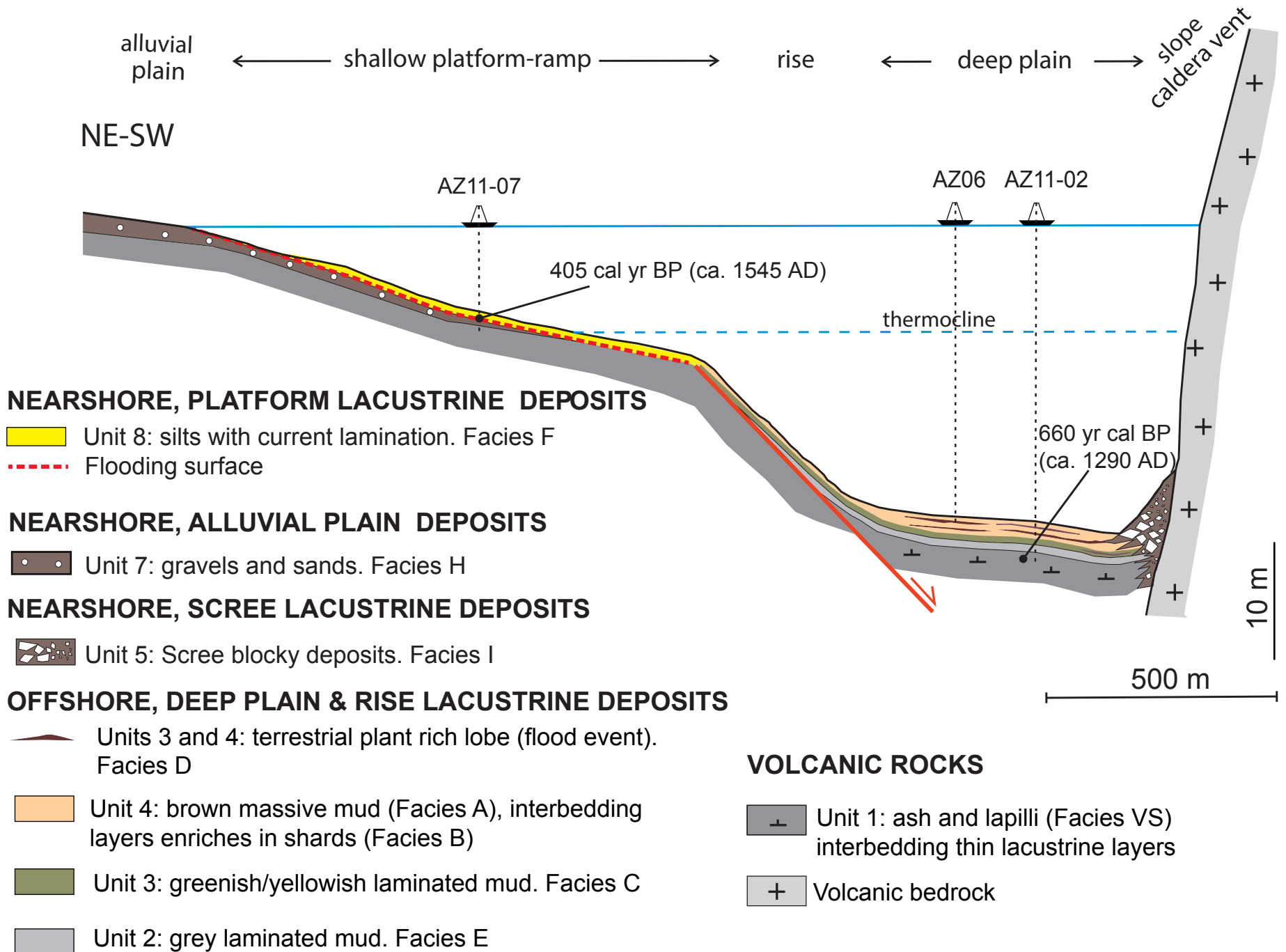


Figure 2

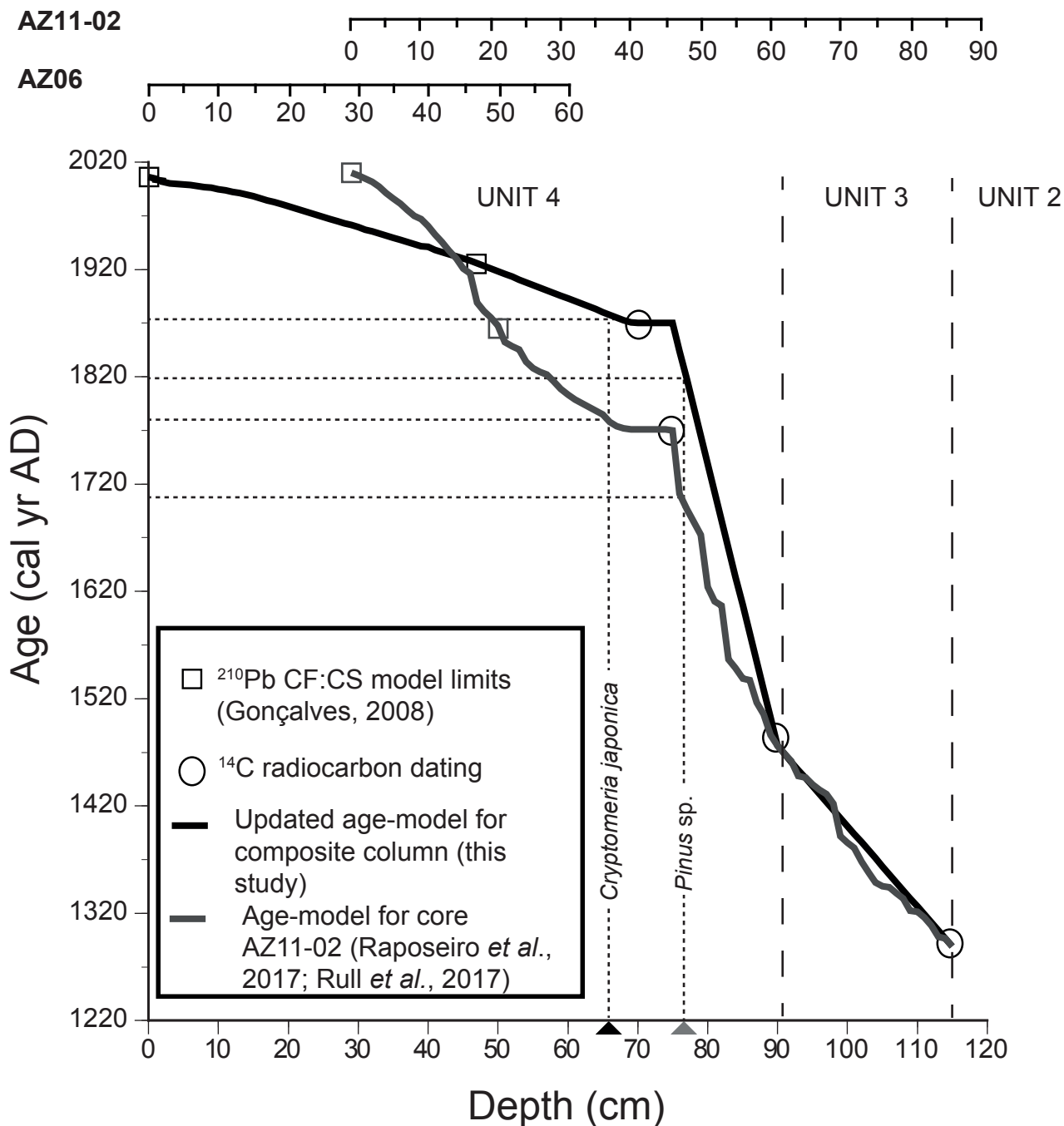


Figure 3

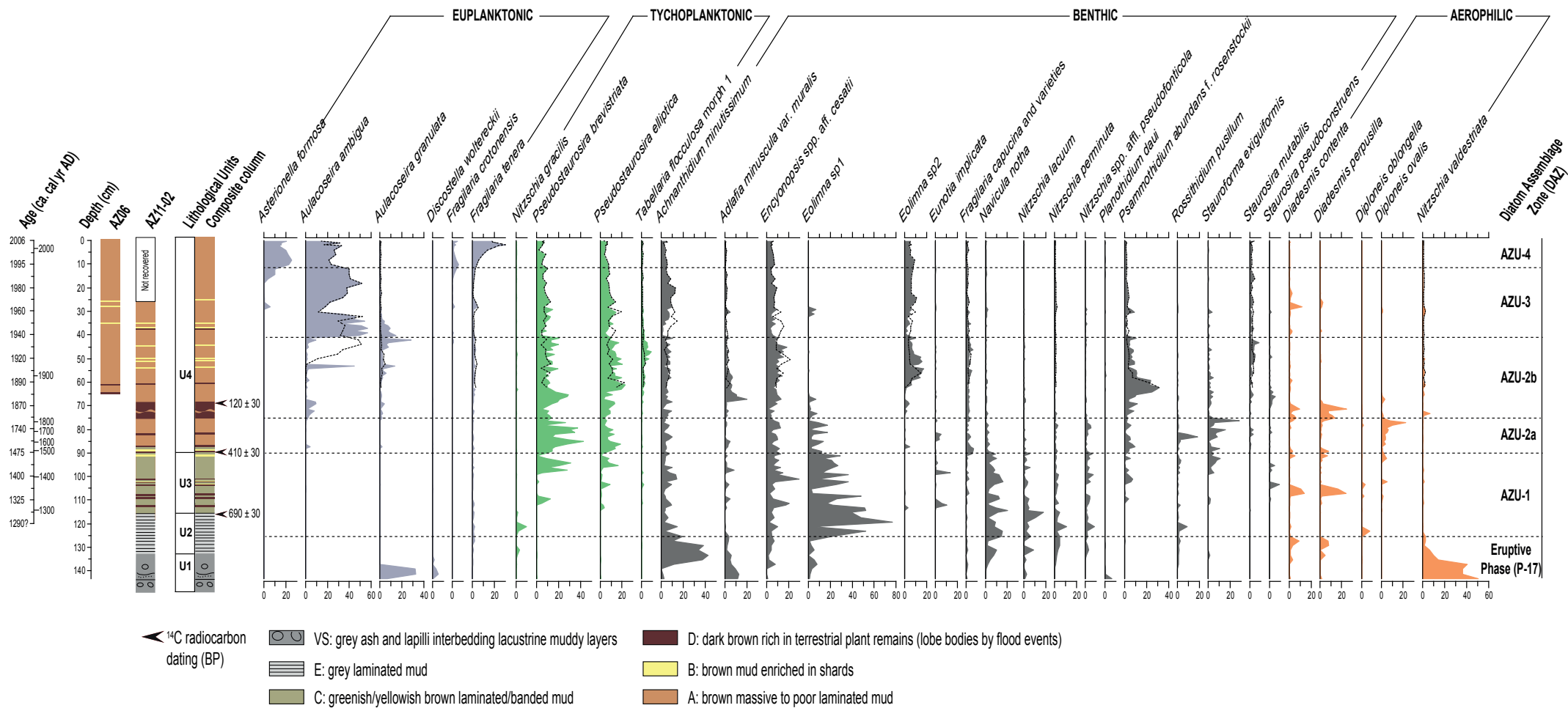


Figure 4

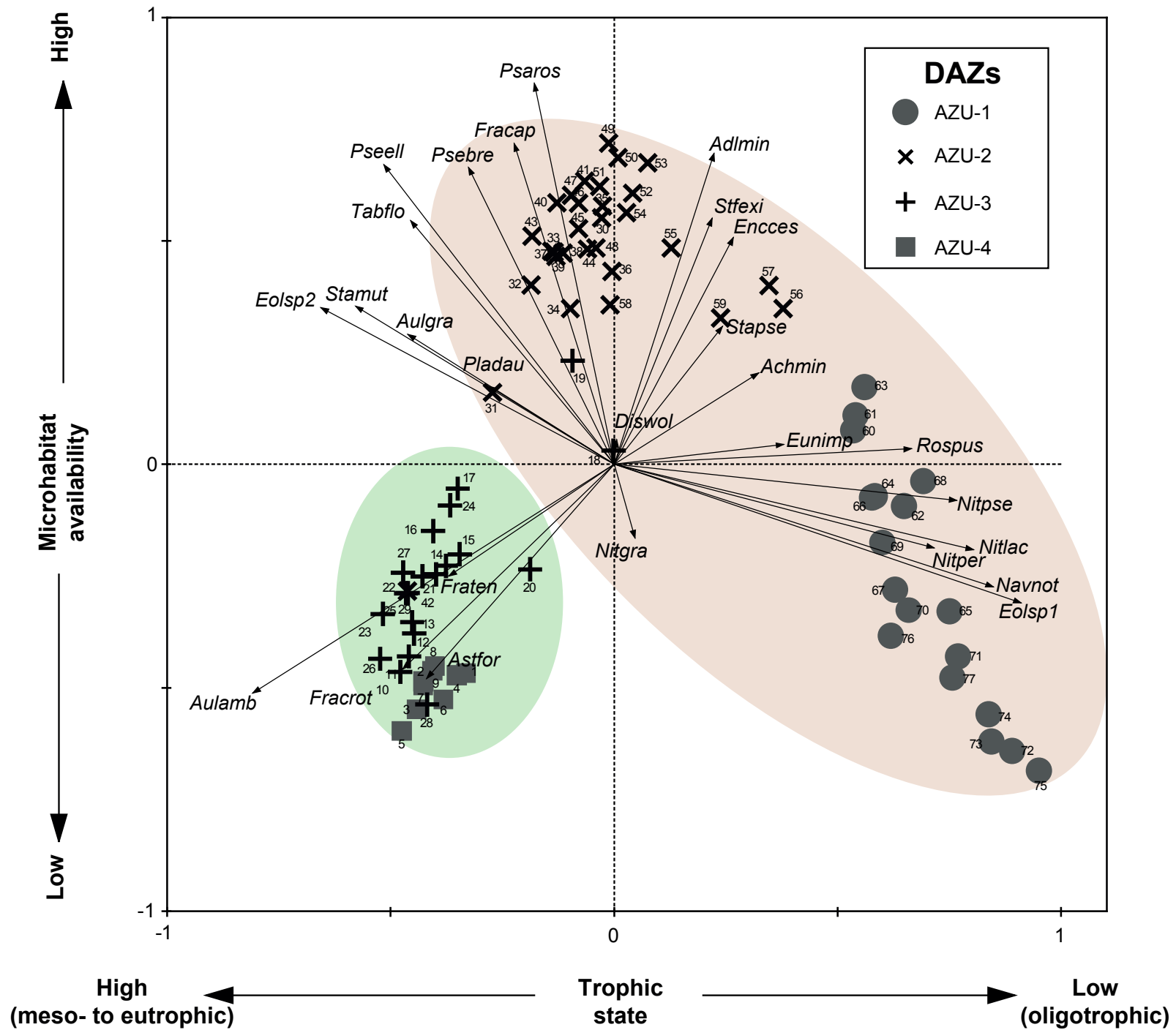


Figure 5

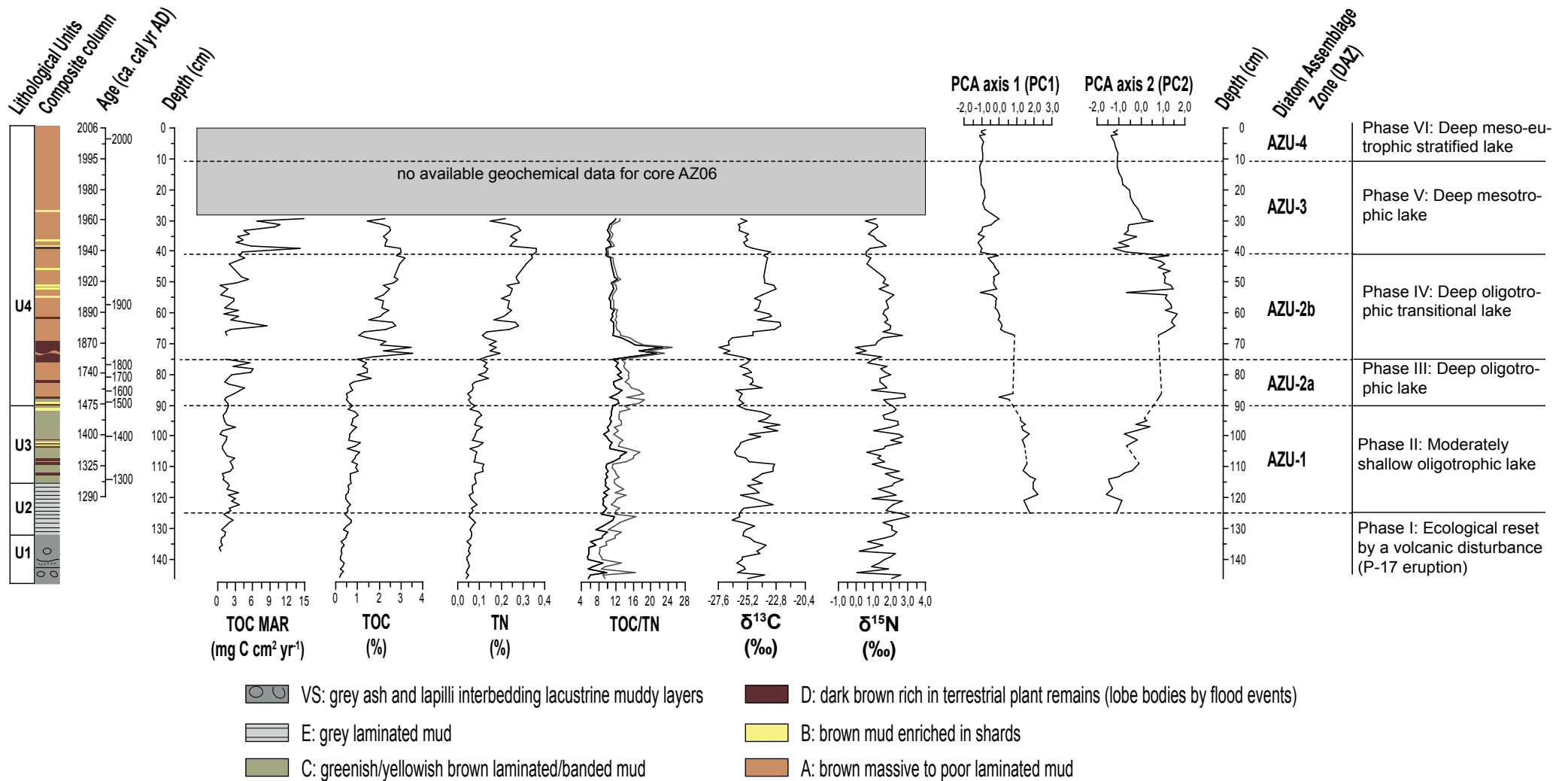


Figure 6

Variable	Values	
	Lake Azul	Lake Verde
Hydromorphological		
Hydromorphological		
Volume (10 ³ m ³)	39764	7696
Maximum depth (m)	25.35	23.50
Lake area (km ²)	3.59	0.86
Physicochemical		
Temperature (°C)	16.48	15.78
July temperature (°C)	18.70	19.20
pH	7.83	8.61
Conductivity (μS cm ⁻¹)	94.55	118.50
Total phosphorous (μg P l ⁻¹)	9.5	28.5
T nitrogen (mg N l ⁻¹)	0.19	0.43
Nitrate (mg NO ₃ l ⁻¹)	0.03	0.06
Silica (mg SiO ₂ l ⁻¹)	0.70	1.33
Transparency (m)	2.20	1.25
Chlorophyll a	5.35	26.19
Catchment variables		
Agricultural area (%)	42.34	18.09
Forestal area (%)	52.36	80.06
Other land uses (%)	7.56	2.04

Table 1: Environmental variables of Lakes Azul and Verde

Core	Core depth (mm)	Composite column depth (mm)	Material	Lab. Reference	Radiocarbon age (BP)	2 σ (cal yrs. AD)	$\delta^{13}\text{C}$ (‰)
AZ11-02	55	340	Plant macrorest	Beta-326594	154.4 \pm 0.4 pMC	1989-1991	-32.7
AZ11-03	650	700	Plant macrorest	Beta-316597	120 \pm 30	1801-1939*	-24.6
AZ11-02	460	750	Plant macrorest	Beta-316595	200 \pm 30	1634-1892	-28.6
AZ11-02	610	900	Pollen concentrate	Beta-331408	410 \pm 30	1431-1521*	-25.8
AZ11-02	860	1150	Pollen concentrate	Beta-331409	690 \pm 30	1266-1312*	-25.3

Table 2: Radiocarbon dates

**Diatom
assemblage
zone
Depth (cm)
Age (ca. AD)**

Main taxa

AZU-1 125-90 (1290-1475)	Biraphid diatoms, mainly benthic life forms (epipelagic), dominated by <i>Eolimna</i> sp1 and subdominated by <i>Navicula notha</i> , <i>Encyonopsis</i> spp. aff. <i>cesatii</i> , <i>Nitzschia perminuta</i> , <i>N. lacuum</i> and <i>Nitzschia</i> spp. aff. <i>pseudofonticola</i> . Aerophilic diatoms reach high abundances coinciding with Facies D, and tychoplanktonic life forms appear sporadically in low values.
AZU-2 90-41 (1475-1930)	Marked increase in periphyton, mainly tychoplanktonic and epiphytic taxa from littoral areas, such as <i>Peudostaurosira brevistriata</i> , <i>Staurosira elliptica</i> , <i>Fragilaria capucina</i> and varieties, <i>Staurosira mutabilis</i> and <i>Tabellaria flocculosa</i> (morph1). Decline of biraphid forms, except for <i>E. aff. cesatii</i> . Low abundances of <i>Rosithidium pusillum</i> and <i>Stauroforma exiguiformis</i> . Aerophilic taxa reach high abundances coinciding with Facies D (subzone AZU-2b). The euplanktonic <i>Aulacoseira</i> appears for the first time in the record, initially associated to this facies and with episodic peaks and uninterrupted low abundances thereafter, accompanied by epiphytic <i>Psammnothidium abundans</i> f. <i>rosenstockii</i> and benthic <i>Eolimna</i> sp2.
AZU-3 41-11 (1930-1985)	Sharp increase of the euplanktonic and eutrophic <i>Aulacoseira ambigua</i> , which dominates the assemblage, and <i>A. granulata</i> . Both taxa decline in the topmost levels. The tychoplanktonic <i>P. brevistriata</i> and <i>S. elliptica</i> are subdominant taxa.
AZU-4 11-0 (1985-2006)	Partial replacement of <i>Aulacoseira</i> spp. with other euplanktonic diatoms, mainly <i>Asterionella formosa</i> and <i>Fragilaria crotonensis</i> .

Table 3: Description of Diatom Assemblage Zones

Variable	Values	
	Lake Azul	Lake Verde
Hydromorphological		
Volume (10 ³ m ³)	39764	7696
Maximum depth (m)	25.35	23.50
Lake area (km ²)	3.59	0.86
Physicochemical		
Temperature (°C)	16.48	15.78
July temperature (°C)	18.70	19.20
pH	7.83	8.61
Conductivity (μS cm ⁻¹)	94.55	118.50
Total phosphorous (μg P l ⁻¹)	9.5	28.5
T nitrogen (mg N l ⁻¹)	0.19	0.43
Nitrate (mg NO ₃ l ⁻¹)	0.03	0.06
Silica (mg SiO ₂ l ⁻¹)	0.70	1.33
Transparency (m)	2.20	1.25
Chlorophyll a	5.35	26.19
Catchment variables		
Agricultural area (%)	42.34	18.09
Forestal area (%)	52.36	80.06
Other land uses (%)	7.56	2.04

Table 1: Environmental variables of Lakes Azul and Verde

Core	Core depth (mm)	Composite column depth (mm)	Material	Lab. Reference	Radiocarbon age (BP)	2 σ (cal yrs. AD)	$\delta^{13}\text{C}$ (‰)
AZ11-02	55	340	Plant macrorest	Beta-326594	154.4 \pm 0.4 pMC	1989-1991	-32.7
AZ11-03	650	700	Plant macrorest	Beta-316597	120 \pm 30	1801-1939*	-24.6
AZ11-02	460	750	Plant macrorest	Beta-316595	200 \pm 30	1634-1892	-28.6
AZ11-02	610	900	Pollen concentrate	Beta-331408	410 \pm 30	1431-1521*	-25.8
AZ11-02	860	1150	Pollen concentrate	Beta-331409	690 \pm 30	1266-1312*	-25.3

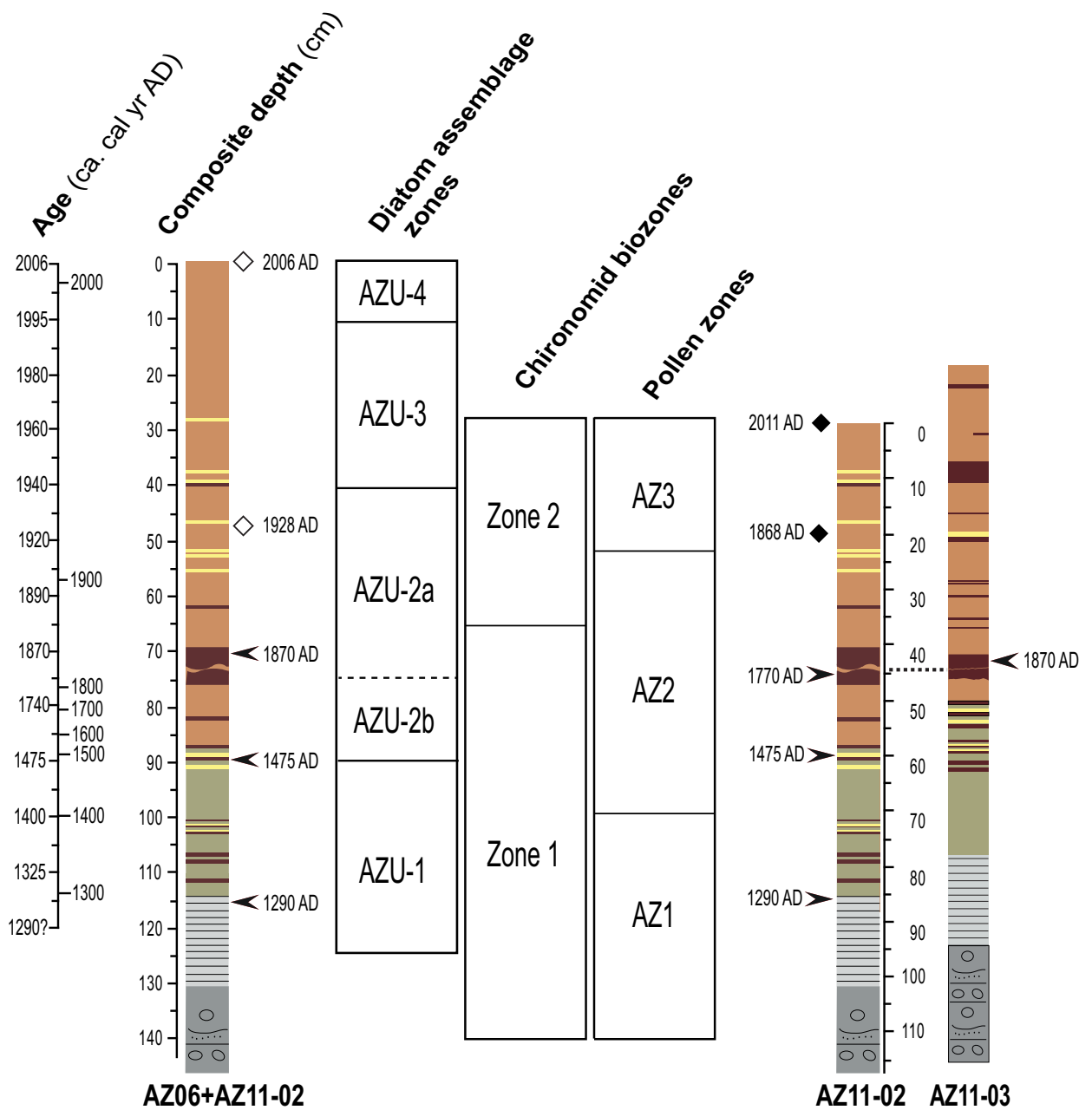
Table 2: Radiocarbon dates

**Diatom
assemblage
zone
Depth (cm)
Age (ca. AD)**

Main taxa

AZU-1 125-90 (1290-1475)	Biraphid diatoms, mainly benthic life forms (epipelagic), dominated by <i>Eolimna</i> sp1 and subdominated by <i>Navicula notha</i> , <i>Encyonopsis</i> spp. aff. <i>cesatii</i> , <i>Nitzschia perminuta</i> , <i>N. lacuum</i> and <i>Nitzschia</i> spp. aff. <i>pseudofonticola</i> . Aerophilic diatoms reach high abundances coinciding with Facies D, and tychoplanktonic life forms appear sporadically in low values.
AZU-2 90-41 (1475-1930)	Marked increase in periphyton, mainly tychoplanktonic and epiphytic taxa from littoral areas, such as <i>Peudostaurosira brevistriata</i> , <i>Staurosira elliptica</i> , <i>Fragilaria capucina</i> and varieties, <i>Staurosira mutabilis</i> and <i>Tabellaria flocculosa</i> (morph1). Decline of biraphid forms, except for <i>E. aff. cesatii</i> . Low abundances of <i>Rosithidium pusillum</i> and <i>Stauroforma exiguiformis</i> . Aerophilic taxa reach high abundances coinciding with Facies D (subzone AZU-2b). The euplanktonic <i>Aulacoseira</i> appears for the first time in the record, initially associated to this facies and with episodic peaks and uninterrupted low abundances thereafter, accompanied by epiphytic <i>Psammnothidium abundans</i> f. <i>rosenstockii</i> and benthic <i>Eolimna</i> sp2.
AZU-3 41-11 (1930-1985)	Sharp increase of the euplanktonic and eutrophic <i>Aulacoseira ambigua</i> , which dominates the assemblage, and <i>A. granulata</i> . Both taxa decline in the topmost levels. The tychoplanktonic <i>P. brevistriata</i> and <i>S. elliptica</i> are subdominant taxa.
AZU-4 11-0 (1985-2006)	Partial replacement of <i>Aulacoseira</i> spp. with other euplanktonic diatoms, mainly <i>Asterionella formosa</i> and <i>Fragilaria crotonensis</i> .

Table 3: Description of Diatom Assemblage Zones



◇ Pb²¹⁰ CF:CS model for AZ06 (Gonçalves, 2008) and composite column (this study)

◆ Pb²¹⁰ CF:CS model for AZ11-02 (Raposeiro *et al.*, 2017; Rull *et al.*, 2017)

◀ ¹⁴C (cal. yr AD)

VS: grey ash and lapilli interbedding lacustrine muddy layers

E: grey laminated mud

C: greenish/yellowish brown laminated/banded mud

D: dark brown rich in terrestrial plant remains (lobe bodies by flood events)

B: brown mud enriched in shards

A: brown massive to poor laminated mud

Supplementary Material